CHARACTERIZATION OF THE HUMAN CYTOMEGALOVIRUS TEGUMENT PROTEIN UL94 AND ITS INTERACTION WITH UL99

A DISSERTATION
SUBMITTED TO THE FACULTY OF THE GRADUATE SCHOOL
OF THE UNIVERSITY OF MINNESOTA
BY

Stacia L. Phillips

IN PARTIAL FULFILLMENT OF THE REQUIREMENTS
FOR THE DEGREE OF
DOCTOR OF PHILOSOPHY

Wade A. Bresnahan, Ph.D., Faculty Advisor

June 2012

Acknowledgements

I would like to thank my adviser Wade for his guidance and encouragement throughout my time in his lab. It is largely due to his mentorship that I have had such a positive graduate school experience and for that I am grateful.

I would also like to thank Steve Rice, Leslie Schiff, and Kathleen Conklin, each of who was an excellent source of advice and support during my graduate career.

Dedication

This dissertation is dedicated to OSM.

ABSTRACT

Human cytomegalovirus (HCMV) is a ubiquitous member of the betaherpesvirus family. Like all herpesviruses, HCMV establishes a lifelong latent infection that is characterized by periodic reactivation throughout the life of the host. While HCMV infection is predominantly asymptomatic in healthy individuals, it represents a significant cause of morbidity and mortality in those with compromised immune function. In addition, congenital HCMV infection is a leading cause of birth defects in the United States, with the potential to result in severe and permanent disability in infected children. HCMV is the largest and most complex of the human herpesviruses, both structurally and with respect to the coding capacity of the viral genome. HCMV particles are composed of a nucleocapsid core containing the double-stranded DNA genome, a surrounding layer of virally encoded proteins referred to as the tegument, and a host-derived lipid envelope studded with viral glycoproteins. Proteomic analysis of purified virions suggests that HCMV particles may be composed of as many as 71 virally encoded proteins. Despite intense investigation, the mechanisms by which HCMV particles are assembled in the cytoplasm of infected cells remain poorly understood. In an attempt to gain novel insight into the processes involved in virion assembly, we carried out a yeast two-hybrid screen designed to identify binary interactions among HCMV structural proteins. One interaction of particular interest that was identified in our screen was that between the herpesvirus-conserved tegument proteins UL94 and UL99. UL99 is essential for HCMV replication and functions at the stage of secondary envelopment in the cytoplasm. The function of UL94 is unknown. We hypothesize that the interaction between UL94 and UL99 is essential for HCMV replication. To investigate this hypothesis, we first sought to elucidate the function of UL94. Using a UL94-null mutant virus, we showed that UL94 is essential for HCMV replication. In the absence of UL94, early events such as viral gene expression and DNA replication proceeded at wild type levels. However, we observed a dramatic defect in the localization of UL99 to the viral assembly complex in the cytoplasm

of cells infected with the UL94-null mutant. In addition, ultrastructural analysis of cytoplasmic virus particles showed that in cells infected with the UL94-null mutant, there was a complete absence of enveloped virions, demonstrating that UL94, like UL99, is required for secondary envelopment. Finally, we used both yeast two-hybrid and co-immunoprecipitation approaches to map the domains of both UL94 and UL99 that are required for their interaction. We then incorporated mutations that abolish the interaction into the viral genome. We showed that when the interaction between UL94 and UL99 was abolished during HCMV infection, both proteins exhibited aberrant localization and the production of infectious virus progeny was completely blocked. Taken together, our results suggest that UL94 functions at least in part to direct the proper localization of UL99 to the assembly complex through their interaction and that this event is essential for HCMV replication. This work has implications for the development of novel antiviral therapies to treat HCMV infection.

TABLE OF CONTENTS

LIST OF TABLES

LIST OF FIGURES

CHAPTER 1

INTRODUCTION AND LITERATURE REVIEW

Human Cytomegalovirus Classification

Human cytomegalovirus (HCMV) or *human herpesvirus 5* is a member of the family *Herpesviridae* and is the prototypic member of the subfamily *Betaherpesvirinae.* Members of the β-herpesvirus subfamily are characterized by their strict species specificity and a long replication cycle. Inclusion of HCMV into the herpesvirus family is based on the structural features of the virion, which include an icosahedral nucleocapsid, surrounding tegument layer, and host-derived envelope studded with virally encoded glycoproteins (67). The classification of HCMV as a member of the herpesvirus family is also based on the organization of the double-stranded DNA genome, which contains both unique long and unique short segments flanked by inverted repeat sequences (67).

Epidemiology and Clinical Significance

Prevalence and Transmission

The prevalence of HCMV in a given population depends largely on socioeconomic factors but is widespread even in developed countries, where it is estimated that between 40 and 70 percent of the population is infected (73). After primary infection, virus is shed for weeks or months in bodily fluids including saliva, urine, tears, semen, and cervical secretions. Transmission of HCMV requires direct contact with infected fluids and frequently occurs by sexual contact or in the context of childcare. Another important route of HCMV exposure is vertical transmission from mother to fetus *in utero*, during birth, or through breast milk (73). HCMV infection in immunocompetent individuals is controlled by both innate and adaptive immunity and is generally asymptomatic. Like all herpesviruses, HCMV establishes lifelong latency after primary infection, and is

capable of periodic reactivation throughout the life of the host.

Rarely, HCMV infection can lead to mononucleosis of immunocompetent individuals, similar in presentation to the more common EBV-associated mononucleosis. HCMV infection does however represent a significant cause of morbidity and mortality in those with compromised immune function including patients undergoing bone marrow and solid organ transplant, those undergoing treatment for lymphoid cancers, and individuals with AIDS.

Congenital Infection

HCMV is the most common congenital viral infection and the leading viral cause of birth defects and brain damage in the United States (99). HCMV can be acquired *in utero* either from primary infection of the mother or reactivation of latent virus during pregnancy. Primary maternal infection is more likely to result in symptomatic congenital infection of the fetus and more severe sequelae. The most common manifestations of symptomatic congenital infection are sensorineural hearing loss, ophthalmologic defects, microencephaly, mental retardation, and cerebral palsy. Congenital HCMV infection affects between 1 and 3% of live births worldwide (27). Approximately 1 in 150 children are born with congenital HCMV infection annually in the United States and of those, 20% will develop permanent disability as a result of infection (124). Congenital HCMV infection accounts for approximately 30% of all childhood hearing loss, making it a leading cause of childhood deafness, second only to genetic defects. Hearing loss can occur even in children who are asymptomatic at birth and this delayed onset of hearing loss can occur up to 3 years of age, underscoring the importance of long-term follow up of congenitally infected infants (105).

Transplant Recipients

HCMV is among the most common infections to occur following organ transplantation and is a significant cause of morbidity and mortality in immunosuppressed transplant recipients. Primary infection following organ

transplant can be associated with transplant failure, multiorgan involvement, and life-threatening disease (99). The presence of a productive CMV infection is also associated with an increased risk of secondary opportunistic infections. Primary infection of a seronegative recipient after transplant from a seropositive donor can result in symptomatic disease in up to 66% of cases and is dependent on many factors including the type of transplant (48). Reactivation of latent virus under immunosuppression can also occur but is less likely to cause symptomatic disease.

Prevention and Treatment

HCMV Vaccine Status

Despite substantial efforts, there is currently no vaccine available for prevention or treatment of HCMV infection. Several vaccines, including live-attenuated, subunit, and DNA-based vaccines are in various stages of development and have been met with a range of success in human clinical trials (104). While live-attenuated vaccines based on lab-adapted AD169 and Towne strains were capable of eliciting humoral and cell-mediated immune responses, they proved ineffective at preventing subsequent infection (91). Subunit vaccines based on immunodominant viral proteins such as glycoprotein B, the major tegument protein pp65, and immediate early protein IE1 have also been developed and tested in animal models. Vaccination with gB subunit vaccine has shown promise in preventing CMV disease in both murine and guinea pig models of infection, and is currently being investigated for its efficacy in human clinical trials (91).

Antiviral Treatments and Limitations

Prevention of HCMV infection and the development of HCMV-related disease in transplant recipients is currently managed by prophylaxis or pre-emptive treatment. Prophylaxis by administration of antiviral drugs starting shortly after transplant and continuing for several weeks has shown success in

preventing HCMV infection and replication, however upon withdrawal of antiviral treatment, a significant number of patients will subsequently acquire HCMV infection (48). Another strategy for prevention is pre-emptive treatment, where the patient is monitored for the presence of HCMV replication on a weekly basis, and treatment is initiated upon viral replication attaining a threshold level, ideally prior to the onset of symptoms (48). The most commonly used antiviral drugs for preventing and treating HCMV infection are ganciclovir and its prodrug valganciclovir. The use of ganciclovir is complicated by the development of drug resistant virus, most often through the acquisition of mutations in the viral UL97 kinase (53). Foscarnet, cidofovir, and maribavir are alternative antivirals that may be used in the case of ganciclovir-resistance. However, all of the currently available antiviral drugs have the potential to cause complications due to toxicity and may have limited efficacy due to suboptimal bioavailability. As an alternative to antiviral drugs, immune-based therapies such as the administration of anti-CMV IgG and adoptive transfer of CMV-specific T-cells are undergoing investigation as treatment methods for post-transplant patients (48).

Virion Structure

Genome Structure

HCMV is the largest of the human herpesviruses with a genome composed of approximately 235 kilobasepairs of double-stranded DNA (67). The genome contains unique long (UL) and unique short (US) regions that are flanked by terminal (TRL) and internal (IRL) inverted repeat sequences (Fig. 1-1A). The HCMV genome has been estimated to encode between 192 and 252 open reading frames depending on the virus strain analyzed and the prediction method used (69, 70). There are approximately 26 genes conserved across all members of the herpesvirus family, referred to as the herpesvirus core genes (67). These core genes encode for proteins that function in gene regulation, DNA replication, and virion maturation and structure. While mutagenesis of the HCMV genome has shed light on the requirement of individual open reading frames for

replication in cultured fibroblasts, the specific function of the majority of HCMV genes remains unknown. Genetic mutagenesis indicates that ~70 of the predicted ORFs are dispensable for replication in culture, suggesting that a significant portion of the HCMV genome is dedicated to genes that function in tropism, immune evasion, and pathogenesis in the host (28, 125).

The HCMV virion is also large and complex compared to other members of the herpesvirus family. The virus particle is between 150 and 200 nm in diameter and has the basic structural features common to all herpesviruses (Fig. 1-1B). The genome is packaged inside an icosahedral nucleocapsid, surrounded by proteins composing the tegument layer, and enclosed in a host-derived lipid envelope into which viral glycoproteins are inserted. The most recent proteomic analysis of purified virus particles estimates that the HCMV virion may be composed of as many as 71 virally encoded proteins (113).

Capsid

The icosahedral nucleocapsid is formed by seven viral capsid proteins, five of which remain associated with the fully assembled infectious virion (31). The assembly of HCMV capsids occurs through a conserved mechanism that is homologous to the assembly of HSV capsids. Capsid pentamers and hexamers are formed by the major capsid protein (MCP) UL86, triplexes are formed by the less abundant minor capsid protein (mCP) UL85 and minor capsid-binding protein (mC-BP) UL46, and the small capsid protein UL48.5 is located at hexon tips (18). Finally, UL80 encodes for three additional proteins on co-terminal transcripts that are required for capsid assembly (60).

Glycoproteins

The HCMV genome encodes for as many as 60 predicted glycoproteins, however proteomic analysis by mass spectrometry of purified particles suggests that there are 19 glycoprotein species associated with virions (113). The major glycoprotein present in the viral envelope is UL55-encoded gB, one of the most

highly conserved proteins among the herpesvirus family (15). Also embedded in the envelope is the gO/gH/gL complex that is involved in entry of the virus into host cells (84). In addition to the major conserved glycoprotein species, there are several less abundant glycoproteins that are detected in association with purified virions. The individual functions of the majority of glycoproteins predicted to be encoded by the HCMV genome have not been defined.

Tegument

Tegument proteins are packaged into the virus particle in the space between the capsid and envelope (Fig. 1-1B), and are delivered directly to the cytoplasm of the host cell upon infection. Therefore, tegument proteins are available to function immediately after virus entry, prior to delivery of the viral genome to the nucleus and the onset of viral gene expression. Tegument proteins have been shown to function at various stages of the viral life cycle including capsid trafficking and delivery of the genome to the host cell nucleus, regulation of viral gene expression, modulation of the host immune response, and virion assembly and morphogenesis (3, 13, 14, 22, 49, 82, 98). Mutational analysis of the viral genome demonstrates that while some tegument proteins are essential for HCMV replication in culture, others enhance the efficiency of replication or are completely dispensable (28, 125). While the functions of many tegument proteins during HCMV infection have been well characterized, the roles of more than half of the known tegument proteins remain unknown.

Estimates of the exact protein composition of the tegument vary, however it is generally accepted that the HCMV tegument contains at least 25 virally encoded proteins (10, 32, 44, 113). Most if not all of the proteins present in the tegument layer of the virion are phosphorylated (indicated by the designation “pp”), however what role if any this phosphorylation plays in the function of tegument proteins is unknown. The most abundant tegument protein is UL83-encoded pp65, accounting for approximately 15% of the total protein content of infectious virions (113). Other abundant tegument proteins include UL32 (pp150),

UL82 (pp71), UL48, and UL99 (pp28). It was long thought that the tegument was an amorphous proteinaceous layer, however more recent ultrastructural analysis of virions suggests that the capsid-proximal portion of the tegument is in fact a highly ordered structure (112, 127). The overall structure of the tegument, if any, remains unknown, as does the mechanism by which tegument proteins become incorporated into virus particles during assembly. However, it is likely that the proper assembly of virus particles is mediated by protein-protein interactions between capsid, tegument, and glycoproteins.

Viral Replication

Entry

Attachment and entry of HCMV occurs through mechanisms that are not well understood. The initial attachment event is mediated by ubiquitous heparan sulfate proteoglycans on the cell surface (67). Subsequent to heparan sulfate-dependent attachment, events involving other poorly defined cell surface molecules mediate more stable attachment and penetration of the host cell. The epidermal growth factor receptor (EGFR) and annexin II have both been proposed to serve as receptors for HCMV, however their absence on the cell surface does not always correlate with a block in entry (24, 40, 77, 78, 115). These results and the fact that HCMV is capable of entering a vast variety of cell types suggest that the virus is capable of using multiple and/or ubiquitous host cell molecules to mediate attachment and entry.

The mechanism by which HCMV entry proceeds is cell type-dependent and occurs via fusion with the plasma membrane or by acid-mediated endocytosis. Both pathways require the viral gH/gL complex, however entry into fibroblasts is mediated by the gH/gL/gO while entry into endothelial and epithelial cells requires gH/gL in complex with UL128-131 (84). Entry ultimately leads to release of the virion contents, including the tegument and nucleocapsid, directly into the host cell cytoplasm (Fig. 1-2).

Viral Gene Expression

HCMV gene expression commences upon delivery of the viral genome to the nucleus and occurs in a tightly regulated temporal cascade (Fig. 1-2). The first viral genes to be transcribed are those of the immediate early (IE) kinetic class, defined by their ability to be transcribed in the absence of *de novo* protein synthesis. IE gene expression can be detected as early as 1 hour post-infection and reaches maximal expression levels between 4 and 8 hours (67). The majority of immediate early gene expression is driven from the viral major immediate early promoter. Functions of the IE genes include regulation of viral and cellular gene expression, inhibition of apoptosis, and down-modulation of MHC Class I expression on the host cell surface (23, 101).

Early and delayed early genes are defined as those that require the expression of immediate early genes but are not dependent on viral DNA synthesis. Early gene products function largely in the replication of viral DNA, for example the viral DNA polymerase and polymerase processivity factor encoded by UL54 and UL44 respectively. Other early genes function in continued immune-modulation and optimizing conditions for the replication of viral DNA (71).

The expression of late genes is restricted until the onset of viral DNA replication. Late genes largely encode for the viral structural proteins and those that are required for virion assembly and morphogenesis. Examples of late genes include the tegument proteins encoded by UL32, UL94, and UL99, all of which are essential for late events in virion assembly in the cytoplasm (4, 39, 76, 98, 118, 119).

Genome Synthesis and Packaging

Replication of viral DNA is facilitated by several herpesvirus-conserved DNA replication proteins including the viral DNA polymerase (UL54), processivity factor (UL44), single-stranded DNA binding protein (UL57), primase (UL70), helicase (UL105), and the primase-associated factor (UL102) (71). In addition,

UL84 encodes for a multi-functional protein that is required for oriLyt-dependent DNA replication. The viral genome circularizes upon entry into the nucleus and is thought to be replicated by a rolling circle mechanism to form concatemers (Fig. 1-2). Replication of viral genomes is a tightly regulated process and does not occur until approximately 24 hours post-infection in cell culture. Head-to-tail concatemers are subsequently cleaved into unit length DNA and packaged into pre-formed B capsids in the nucleus (71).

Cytoplasmic Assembly and Egress

Nucleocapsids exit the nucleus through consecutive envelopment and de-envelopment by budding through both the inner and outer nuclear membranes. There are conflicting reports regarding whether any tegument proteins associate with nucleocapsids in the nucleus or if tegument acquisition occurs exclusively in the cytoplasm (39, 87, 88). Once in the cytoplasm, capsids traffic by unknown mechanisms to the site of final assembly, a compact juxtanuclear structure referred to as the assembly complex (Fig. 1-2). The events that occur at the assembly complex that lead to the formation of fully tegumented and enveloped virions have not been fully defined. Several groups have characterized the assembly complex with respect to both viral and cellular proteins that accumulate at this site during infection. Many viral structural proteins including gB, pp28, pp150, and pp65 localize to the assembly complex at late times during infection (88). In addition, many markers of the cellular secretory apparatus have been detected at the assembly complex, including markers of early and recycling endosomes, late endosomes, lysosomes, Golgi, and the ESCRT-III complex (25, 26, 106). However, despite intense investigation, the mechanisms of virion envelopment and the cellular membranes at which envelopment occurs remain poorly understood.

While the mechanisms of cytoplasmic assembly are not well understood, it is generally accepted that this process is mediated in part by interactions between viral proteins that are likely required for the proper localization of viral

structural proteins as well as for tegument acquisition and envelopment. This thesis work was initiated with the goal of identifying such protein-protein interactions. To this end, we performed a yeast two-hybrid analysis designed to identify binary interactions among HCMV virion proteins. One interaction of interest that was revealed in our yeast two-hybrid screen was that between the tegument proteins UL94 and UL99. UL99 is an essential membrane-associated protein that is required for secondary envelopment in the cytoplasm. UL94 was also thought to be essential for efficient viral replication however when this work was initiated, the function of UL94 during infection was unknown. Therefore, we hypothesized that the interaction between UL94 and UL99 is essential for HCMV replication. The rest of this thesis work details the results of our investigation of UL94 function and of the significance of the interaction between UL94 and UL99 during infection.

UL94 and UL99

UL94

UL94 is a core herpesvirus gene that is universally conserved among all members of the herpesvirus family. Although UL94 is highly conserved, prior to the work presented here, its function during infection was unknown. In fact, at the time this thesis work was initiated there was only one report in the literature characterizing UL94. That study showed that UL94 transcription is dependent on the synthesis of viral DNA, demonstrating that UL94 is expressed with true-late kinetics (119). In addition, Western blot analysis of fractionated cell lysates showed that UL94 partitions exclusively to the nuclear compartment of infected cells. These results were obtained using a monoclonal antibody raised against a peptide antigen corresponding to amino acids 26-40 of the UL94 protein (119).

The UL94 protein is 345 amino acids in length with a predicted molecular weight of 36 kDa. Alignment of the amino acid sequence of UL94 with that of UL94 homologs from other herpesviruses reveals that the sequence conservation is restricted to the C-terminal half of the protein (119). Notable

features of the UL94 protein include several conserved cysteine residues throughout the C-terminus that may be involved in disulfide bond formation. In addition, there is a putative Cys_2His_2 zinc finger, the most common DNA-binding domain in eukaryotic transcription factors. Two nuclear localization signals as well as a nuclear export signal in the N-terminal half of the protein have recently been described (Fig. 1-3A) (55).

The best characterized homolog of UL94 is its HSV-1 counterpart, UL16. UL16 is a 40 kDa protein that exhibits nuclear localization early in infection and perinuclear localization at later times. UL16 co-localizes with capsids in the infected cell nucleus and associates with capsids isolated from the cytoplasm (66). Unlike UL94, UL16 is dispensable for replication of HSV in culture. Deletion of UL16 results in a modest growth defect with viral titers reduced by approximately 1-log compared to that of wild type virus (7).

UL16 has been identified as a binding partner of UL11, the HSV-1 homolog of HCMV UL99 (58). The functional relevance of this interaction is not well understood, but a model has been proposed in which the interaction between UL11 and UL16 acts to bridge capsids with the membranes at which envelopment occurs (66, 123). The interaction between UL94 and UL99 homologs is also conserved among other herpesvirus family members including Epstein Barr and Varicella-Zoster viruses (29, 100). Due to this high degree of evolutionary conservation, we predict that this interaction plays an important functional role during herpesvirus replication.

UL99 (pp28)

The UL99-encoded tegument protein pp28 is a 190 amino acid 28 kDa tegument protein that is essential for HCMV replication. As a true-late gene, UL99 expression is completely dependent on the onset of viral genome replication and UL99 protein does not accumulate in the infected cell until late times after infection (>48 hours) (76, 98, 118). UL99 exhibits cytoplasmic localization both in transfected and HCMV infected cells and this localization is dependent on

myristoylation of glycine 2 at the N-terminus of the protein (89) (Fig. 1-3B). This myristoyl moiety presumably mediates insertion of UL99 into cytoplasmic membranes associated with the cellular secretory apparatus; mutation of the myristoylated glycine to alanine results in the trafficking to and retention of UL99 in the nucleus. During HCMV infection, UL99 localizes to the juxtanuclear assembly complex and this localization is required for the production of infectious virus (96).

Phenotypic characterization of UL99-mutant viruses demonstrates that UL99 is essential for virus replication at the step of secondary envelopment in the cytoplasm. In the absence of UL99, early events of viral replication, including entry, gene expression, and viral genome synthesis appear to occur normally. However, there is an accumulation of partially tegumented and unenveloped capsids in the cytoplasm at late times during infection, suggesting that UL99 is required for acquisition of the final envelope at host cell membranes (98).

Mutagenesis of UL99 demonstrates that the N-terminal 61 amino acids are sufficient for wild type virus replication (42, 96). The first 50 amino acids of UL99 are also capable of supporting viral replication, albeit to decreased levels and with delayed kinetics compared to wild type virus (96). This defect is attributed to inefficient retention of UL99 at the assembly complex, resulting in a defect in virion envelopment (93, 96). Analysis of the subcellular localization of GFP-fusion proteins and Western blot analysis of fractionated infected cell lysates suggests that truncated forms of UL99 smaller than the first 61 amino acids are capable of trafficking to the assembly complex but are not efficiently retained there (93, 95, 96). An acidic region of UL99 located between amino acids 44 and 59 has been shown to be involved in the proper localization of UL99 to the assembly complex (Fig. 1-3B). This domain functions in a context dependent manner; relocation of these amino acids to the C-terminus of the protein abolishes the ability of UL99 to localize to the assembly complex (96). An additional essential region of UL99 was identified as amino acids 34-43, however the localization of UL99 after deletion of these residues was not examined (94) (Fig. 1-3B). Importantly,

trafficking of UL99 to the assembly complex requires the expression of other viral late genes, suggesting that there is an additional viral factor that is essential for the proper localization of UL99 (96).

The most thoroughly characterized homolog of UL99 is HSV-1 UL11. UL11 is also a myristoylated tegument protein, however at 96 amino acids and approximately 12 kDa, it is much smaller than its HCMV counterpart UL99 (62). UL11 also contains an acidic domain, however it is smaller and lacks sequence homology to the acidic domain of UL99 (57). UL11 is associated with Golgi and trans-Golgi membranes and this association is mediated by both myristoyl and palmitoyl moieties. Interestingly, these modifications are not essential for UL11 function (9). Deletion of UL11 from the HSV-1 genome results in an accumulation of partially tegumented and unenveloped capsids in the cytoplasm of infected cells, similar to the phenotype observed for HCMV UL99-deletion mutants (8). However, importantly, UL11 is not essential for replication of HSV-1 in culture. UL11-deletion mutants exhibit defects ranging from modest (~1-log) to severe (~3-logs) reduction in titers compared to that of wild type virus (8, 63). This suggests that either UL99 has multiple functions that are not conserved in HSV UL11 or that HSV has redundant mechanisms encoded by other viral proteins, that complement the function of UL11 in the absence of UL11 expression.

Summary and Thesis Statement

HCMV is a ubiquitous member of the herpesvirus family that is a significant cause of morbidity and mortality in individuals with compromised immune function as well as in the context of congenital infection. Therapeutic options for the prevention and treatment of HCMV infection are limited, therefore the development of novel antiviral therapies is a high priority. Events that are essential for the production of infectious virus such as the assembly of virions represent potential targets for antiviral compounds. To date, the mechanisms by which infectious virions are assembled in infected cells, as well as the viral proteins that are required for this stage of the viral life cycle are poorly

understood. The goal of this thesis work was to identify interactions among viral proteins that may play an essential role in virus replication and to further characterize the functional significance of such interactions in the context of HCMV infection. To this end, we carried out a yeast two-hybrid screen designed to identify binary interactions among HCMV structural proteins. One interaction of particular interest that was identified in our screen was that between the herpesvirus-conserved tegument proteins UL94 and UL99. We hypothesized that the interaction between UL94 and UL99 is essential for HCMV replication. We showed that UL94 is essential for HCMV replication and that in the absence of UL94 during infection, there was a defect in the localization of UL99 to the assembly complex and a complete block in secondary virion envelopment. We also mapped the interaction between UL94 and UL99 and showed that when the interaction between UL94 and UL99 was abolished during HCMV infection, both proteins exhibited aberrant localization, resulting in a complete block to the production of infectious progeny virus. Taken together, our results suggest that UL94 functions at least in part to direct the proper localization of UL99 to the assembly complex through their direct interaction and that this event is essential for HCMV replication. This work contributes several novel findings to the field of HCMV assembly and has implications for the development of novel antiviral therapies to treat HCMV infection.

A. HCMV Genome Structure

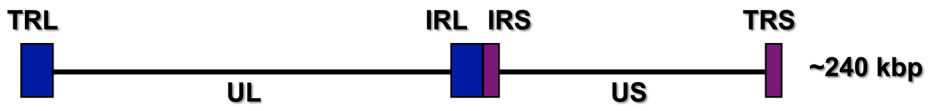

B. HCMV Virion Structure

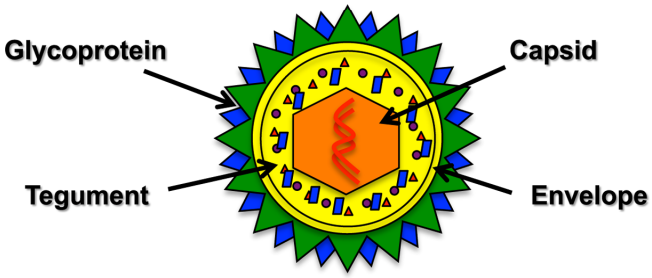

Figure 1-1. HCMV Structure. (A) HCMV genome structure depicting unique long (UL) and unique short (US) regions flanked by internal (IRS) and terminal (TRL) inverted repeat sequences. **(B)** HCMV virion structure. dsDNA genome is packaged in an icosahedral nucleocapsid, surrounded by the tegument layer, and enclosed in the host-derived lipid envelope studded with virally encoded glycoproteins.

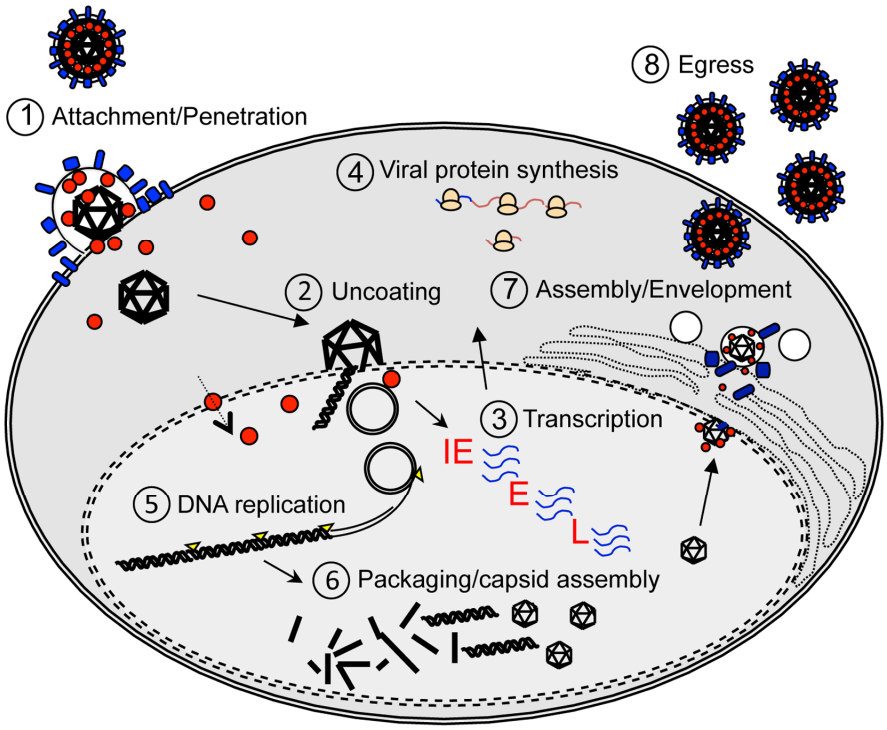

Figure 1-2. HCMV Life Cycle. (1) Attachment to the host cell is mediated by interactions between viral glycoproteins and molecules on the host cell surface. Penetration occurs via endocytosis or fusion at the plasma membrane. **(2)** Virion contents are released into the cytoplasm, the capsid docks at a nuclear pore, and the viral genome enters the nucleus. **(3)** Transcription of viral genes and **(4)** translation of viral proteins occurs. **(5)** The viral genome is replicated and **(6)** packaged into preassembled B-capsids in the nucleus. **(7)** Capsids exit the nucleus and tegumentation and envelopment occur at the cytoplasmic assembly complex. **(8)** Mature progeny virus exits the host cell.

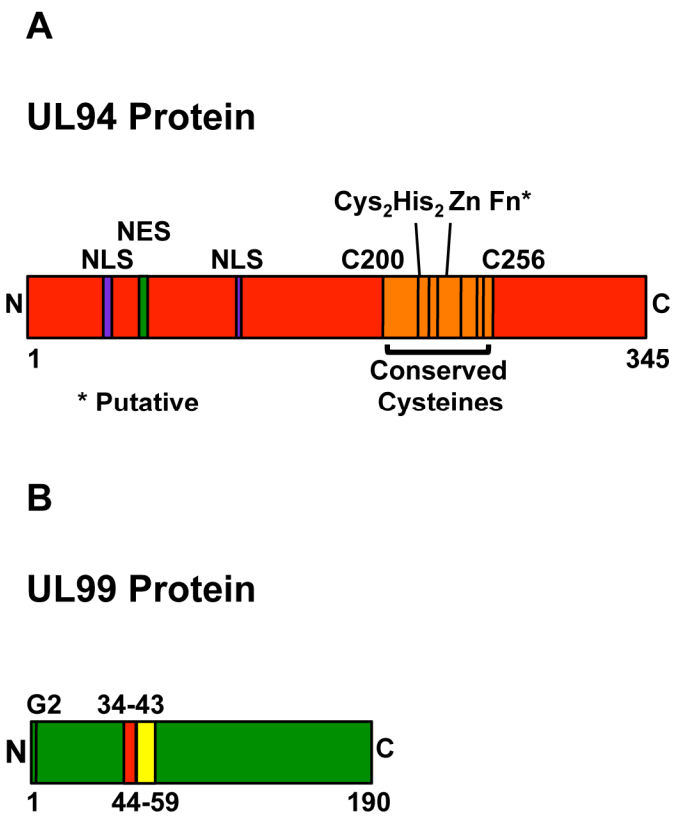

Figure 1-3. Schematic diagram of UL94 and UL99 proteins. (A) The 345 amino acid UL94 protein contains two nuclear localization signals, a nuclear export signal, and several cysteine residues that are conserved among UL94 homologs. A conserved putative Cys_2His_2 zinc finger binding domain is located between amino acids 219 and 233. **(B)** The 190 amino acid UL99 protein contains a myristoylation site at glycine 2. Amino acids 34-43 as well as an acidic domain located between amino acids 44-59 are both essential for UL99 function and for virus replication.

CHAPTER 2
MATERIALS AND METHODS

Cell culture and virus infections

Human foreskin fibroblast (HFF) cells and human embryonic kidney 293T cells were cultured in Dulbecco's modified Eagle's medium supplemented with 10% (vol/vol) fetal calf serum (HyClone), 100 units/ml penicillin, and 100 µg/ml streptomycin in an atmosphere of 5% CO_2 at 37℃. For HCMV infections, HFF cells were infected with the indicated strains of HCMV AD169 in complete growth medium. Following 2 hours incubation, the inoculum was removed and replaced with fresh complete medium. All HCMV AD169 viruses used were derived from either pADCRE (126) or pADCREGFP (19) bacterial artificial chromosomes as described. For protein inhibition experiments, cycloheximide was added to complete medium at a final concentration of 50 µg/ml. MG132 was used at a final concentration of 10 µM. For inhibition of viral DNA synthesis, phosphonoacetic acid was added to complete medium at a final concentration of 200 µg/ml.

Antibodies

Rabbit polyclonal α-FLAG (F-7425; Sigma) and goat polyclonal α-HA (Y-11; Santa Cruz Biotechnology) were used for immunoprecipitation. The following antibodies used for Western blot were obtained from commercial sources: Mouse α-HA (16B12; Covance), mouse α-FLAG (M2; Sigma), mouse α-UL94 (6J8; Santa Cruz Biotechnology), rabbit α-dsRed (632496; Clontech), mouse α-UL44 (1202S; Rumbaugh-Goodwin Institute), mouse αIE1/2 (1203; Rumbaugh-Goodwin Institute), mouse α-gB (1201; Rumbaugh-Goodwin Institute), mouse α-UL99 (1207; Rumbaugh-Goodwin Institute), mouse α-EEA1 (14; BD Transduction Labs), and mouse α-tubulin (TU-02; Santa Cruz Biotechnology). Mouse α-UL69 was kindly provided by T. Shenk (Princeton) and has been previously described (120). Rabbit polyclonal α-UL48 was kindly provided by W.

Gibson (Johns Hopkins) and has been previously described (46). Rabbit α-UL86 was kindly provided by W. Gibson (Johns Hopkins) and has been previously described (33). Mouse α-UL32 (36-14) was kindly provided by W. Britt (University of Alabama at Birmingham) and has been previously described (88). The following HRP-conjugated secondary antibodies were used for detection: goat α-mouse IgG (Santa Cruz Biotechnology), goat α-rabbit IgG (Zymed), and goat α-mouse IgM (Chemicon). Alexa546-conjugated Fab2 goat α-mouse (Molecular Probes) and alexa488-conjuated goat α-rat (Molecular Probes) were used for immunofluorescence analysis.

Yeast two-hybrid assay

Yeast two-hybrid analysis of protein-protein interactions was performed using the ProQuest Two-Hybrid System (Invitrogen) according to the manufacturer's instructions. Briefly, each HCMV ORF was transferred to both the pDEST22 (prey) and pDEST32 (bait) vectors using the LR Clonase II Enzyme Mix (Invitrogen) according to the manufacturer's protocol. All bait and prey vectors were then screened for proper recombination by restriction enzyme analysis.

The yeast two-hybrid screen was performed by co-transformation of bait and prey plasmids into *Saccharomyces cerevisiae* strain MaV203 using the Frozen-EZ Yeast Transformation II Kit (Zymo Research) according to the manufacturer's protocol. Transformants were selected on minimal synthetic agar medium containing dropout supplements lacking leucine and tryptophan (Leu-Trp-) (Clontech). Prior to screening for interactions, each bait vector was tested for auto-activation. Background levels of *HIS3* activation by the bait protein alone were tested on plates containing increasing concentrations of 3-amino-1,2,4-triazole (3AT). Each bait vector was then assayed on plates containing a concentration of 3AT that eliminated any auto-activation from the bait vector alone. Interactions were identified through activation of two independent reporter

genes. To assay for activation of the *HIS3* reporter gene, multiple colonies from each Leu-Trp- plate were resuspended in 0.9% NaCl and spotted onto synthetic complete agar medium containing dropout supplements lacking leucine, tryptophan, and histidine (Leu-Trp-His-) (Clontech). Plates were incubated for 3 days at 30°C and assessed for growth. Each plate included a set of interaction controls provided with the ProQuest Two-Hybrid System and a bait only control. Transformants that exhibited growth on Leu-Trp-His dropout medium were then assayed for activation of the *LacZ* reporter gene by filter lift assay. Briefly, cells were transferred to nitrocellulose filters and lysed by freeze/thaw in liquid nitrogen. Filters were incubated at 30°C for 24 hours on filter paper saturated with buffer containing 60 mM Na_2HPO_4, 40 mM NaH_2PO_4, 10 mM KCl, 1 mM $MgSO_4$, 1 mg/ml X-Gal, and 86 mM β-mercaptoethanol. Interactions were scored as positive when both the *HIS3* and *lacZ* reporter genes were activated.

Cloning of plasmid vectors

HCMV ORF entry vectors

Vectors containing the HCMV ORFs were constructed using the pENTR/D-TOPO Cloning Kit (Invitrogen) to generate Gateway compatible entry clones. All ORFs, with the exception of UL112, were PCR amplified using one primer that began at the start codon and a second primer that ended at the stop codon of each ORF using Advantage HD Polymerase (Clontech). Oligonucleotides used for the generation of HCMV entry clones are listed in Table 2-1. PCR products were subsequently gel purified and cloned into the pENTR/D-TOPO entry vector according to the manufacturer's instructions. For UL112, only the first exon (or 268 amino acids) was amplified and cloned into the entry vector and from here on is referred to as UL112e1. All ORFs except UL46, UL48 and UL86 were amplified using HCMV AD169 genomic DNA as template. Plasmids TA-MCP, UL48-pGEM, and UL86MH17 were kindly provided by W. Gibson (Johns Hopkins) and were used as template for UL46, UL48 and UL86

respectively. All entry clones were screened for proper insertion by restriction enzyme analysis and DNA sequencing.

HA and FLAG-tagged destination vectors

pcDNA3.1 (Invitrogen) and pCI-neo (Promega) were used as backbone vectors to generate Gateway compatible destination vectors containing an N-terminal FLAG or HA tag. The resulting vectors were named HA-Dest-pcDNA3.1, FLAG-Dest-pcDNA3.1, HA-Dest-pCI-neo, and FLAG-Dest-pCI-neo. To generate these vectors, the recombination cassette of pDEST22 containing the *att*R sites, chloramphenicol resistance marker, and *ccd*B counterselectable marker was amplified and cloned into the pcDNA3.1 or pCI-neo backbone. Oligonucleotides used to amplify the recombination cassettes from pDEST22 are listed in Table 2-2. Recombination cassettes were amplified and cloned into the *Hind*III and *Xho*I sites of pcDNA3.1 or the *Nhe*I and *Xho*I sites of pCI-neo. Due to the presence of the *ccd*B gene, these destination vectors were propagated in DB3.1 *E. coli* (Invitrogen). HCMV ORFs were then transferred to the FLAG and/or HA-tagged destination vectors using LR Clonase II Enzyme Mix (Invitrogen) according to the manufacturer's protocol.

Site-directed mutagenesis

UL94 mutant plasmids and the oligonucleotides used to generate them are listed in Table 2-3. Plasmids containing single amino acid substitutions were generated using the QuikChange Lightning Site-Directed Mutagenesis Kit (Stratagene) according to the manufacturer's protocol. Briefly, UL94pENTR/D-TOPO (75) was used as template for PCR-mutagenesis using complementary mutagenic oligonucleotides containing the desired nucleotide changes. Residual template was digested using *Dpn*I enzyme and mutagenized plasmids were transformed into electrocompetent *E. coli*. Plasmids were isolated and direct sequencing was employed to verify the presence of the desired mutations. Mutated ORFs were then transferred to pDEST22 or pDEST32 for yeast two-

hybrid analysis or HA-Dest-pcDNA3.1 or transfection experiments using LR Clonase II Enzyme Mix (Invitrogen) according to the manufacturer's protocol.

Internal deletion mutants

UL99 internal deletion mutant plasmids were generated by PCR amplification of FLAG-dest-pcDNA3.1 (75) using the oligonucleotides listed in Table 2-4. Linear amplification products were gel purified, phosphorylated with T4-PNK (NEB), and ligated with T4-DNA ligase (NEB). Resulting plasmids were transformed into electrocompetent *E. coli*. Plasmids were isolated and direct sequencing was employed to verify the presence of the desired mutations.

Immunoprecipitation and Western blot

Twenty-four hours prior to transfection, $5x10^6$ 293T cells were plated onto 100 mm dishes. The next day media was changed and the cells were transfected with 4μg each of the FLAG and HA-tagged expression constructs using the ProFection Mammalian Transfection System (Promega) according to the manufacturer's protocol. Total protein was harvested 48 hours post-transfection by trypsinization, centrifugation, and lysis in NP-40 lysis buffer (50 mM Tris, pH 7.4, 150 mM NaCl, 0.5% NP-40, 0.75% IPEGAL) containing protease inhibitor cocktail (Roche). Immunoprecipitations were performed with 200 μg of total protein incubated with 3 μg rabbit α-FLAG antibody or 600 ng goat α-HA antibody for 6 hours at 4°C. Protein complexes were precipitated with Protein A/G PLUS Agarose (Santa Cruz Biotechnology) for 2 hours at 4°C. Immunoprecipitates were washed 3 times with NP-40 lysis buffer and boiled in 2X SDS sample buffer (62.5 mM Tris-HCl, pH 6.8, 2.5% SDS, 20% glycerol, 1% ß-mercaptoethanol). Proteins were separated by SDS-PAGE and Western blotting was performed. Proteins were separated by electrophoresis on 8%-12% polyacrylamide gels and transferred to nitrocellulose membranes (Whatman Optitran). Membranes were blocked in 5% nonfat dry milk and probed with

primary and secondary antibodies. Immunoreactive proteins were detected by the ECL chemiluminescent system (Thermo).

Trypsin digestion of purified virions

HFF cells were infected at a multiplicity of 0.1 PFU/cell and supernatant was collected 14 days post-infection when 100% CPE was observed. Cellular debris was removed by centrifugation at 1500 rpm for 5 minutes. Supernatant was further cleared by centrifugation at 20K rpm for one hour on a 20% sucrose cushion. Supernatant was decanted and pelleted virus was resuspended in PBS. Equal aliquots of purified virus were subjected to treatment with 1% Triton-X100, 1 μg trypsin, or both at 37°C for one hour in digest buffer (50 mM Tris pH 7.5, 100 mM NaCl). Trypsin inhibitor was added to stop the reactions and an equal volume of 2X SDS sample buffer was added prior to Western blot analysis.

Recombinant virus generation

HAUL88 and UL94HA

pADCREGFP-HAUL88 and pADCREGFP-UL94HA BACs were generated using a two-step linear recombination protocol in SW102 *E. coli* as previously described (80, 116). The UL88 ORF overlaps with both UL87 at the 5' end and UL89 at the 3' end. The UL87 stop codon TGA is located at nucleotides 131178-131180 (RefSeq X17403.1), overlapping with the UL88 initiating ATG located at nucleotides 131177-131179. Therefore, to insert an HA epitope at the N-terminus of UL88, we inserted an ATT isoleucine codon immediately following the UL88 initiating ATG. This strategy allowed us to insert the HA tag in-frame with the N-terminus of UL88 while leaving the UL87 stop codon intact. The first step in generating pADCREGFP-HAUL88 was recombination between the HCMV wild type pADCREGFP BAC (19) and a linear PCR fragment containing a *GalK*/Kanamycin (*GalK*/Kan^R) marker cassette flanked by 50bp UL88 homology arms. The *GalK*/Kan^R linear fragment was obtained by PCR using the pYD-C255

plasmid (gift from D. Yu, Washington University) and the oligonucleotides UL88GalK 5' and UL88Kan 3' (Table 2-5). The first recombination step resulted in insertion of the *GalK*/Kan^R cassette at nucleotide 131181 of the AD169 genome (RefSeq X17403.1) directly downstream of the UL88 start codon to generate pADCREGFP*GalK*/KanUL88. Recombinants containing the *GalK*/Kan^R cassette were selected on LB kanamycin plates and screened by restriction enzyme analysis. A second recombination step was then carried out using double-stranded oligonucleotides containing an HA-tag to replace the *GalK*/Kan^R cassette. The oligonucleotides HAUL88 sense and HAUL88 antisense (Table 2-5) were annealed, purified, and transformed into competent SW102 *E. coli* cells containing pADCREGFP*GalK*/KanUL88. Recombinants were selected on 2-deoxy-galactose (DOG) minimal agar plates to counterselect for *GalK*. The resulting recombinant BACs were screened by restriction enzyme digest and PCR. The correct in-frame insertion of the HA tag at the 5' end of UL88 was verified by DNA sequencing.

The UL93 ORF overlaps with the 5' end of the UL94 ORF by 142 base pairs. Therefore, to generate pADCREGFP-UL94HA the stop codon of UL94 was removed and the HA epitope was fused to the C-terminus of UL94, leaving the coding sequence for UL93 intact. pADCREGFP-UL94HA was generated using the same protocol as described above. Briefly, The *GalK*/Kan^R linear fragment was amplified with the oligonucleotides UL94GalK 5' and UL94Kan 3' (Table 2-5). The first recombination step resulted in removal of the UL94 stop codon and insertion of the *GalK*/Kan^R cassette at nucleotide 137387 of the AD169 genome (RefSeq X17403.1) directly downstream of the UL94 ORF to generate pADCREGFP*GalK*/KanUL94. The second recombination step was carried out using double-stranded oligonucleotides UL94HA sense and UL94HA antisense (Table 2-5). Recombinant viruses were generated by transfecting ~1 μg BAC DNA and 5 μg pp71-pCGN expression plasmid into 5 x 10^6 HFF cells via electroporation (950μF, 260V). Cells were seeded into dishes and infectious virus

harvested when 100% cytopathic effect was observed. Infectious titers for all viruses were determined by plaque assay on HFF cells.

UL94stop and UL94stop Repair

pADCREGFP-UL94stop and pADCREGFP-UL94repair BACs were generated using a two-step linear recombination protocol in SW105 *E. coli* as previously described (80, 116). pADCREGFP-UL94stop was generated via a single nucleotide substitution to introduce a premature stop codon after the seventh codon in the UL94 open reading frame. The first step in generating pADCREGFP-UL94stop was recombination between the HCMV wild type pADCREGFP BAC (19) and a linear PCR fragment containing a *GalK* marker cassette flanked by 50bp UL94 homology arms. The *GalK* linear fragment was obtained by PCR using the pGalK plasmid (116) and the oligonucleotides UL94stopGalK5' and UL94stopGalK3' (Table 2-5). The first recombination step resulted in insertion of the *GalK* cassette after nucleotide 136375 of the AD169 genome (RefSeq X17403.1) downstream of the UL94 start codon to generate pADCREGFP*GalK*UL94. Recombinants containing the *GalK* cassette were selected on M63 minimal medium with galactose, leucine, biotin, and chloramphenicol followed by selection on MacConkey agar plates with galactose and chloramphenicol. Recombinant BACs were further screened by restriction enzyme analysis. A second recombination step to replace the *GalK* cassette was carried out using double-stranded oligonucleotides containing a C to A mutation at nucleotide 136376 of the genome (RefSeq X17403.1). The oligonucleotides UL94stop sense and UL94stop antisense (Table 2-5) were annealed, purified, and transformed into competent SW105 *E. coli* cells containing pADCREGFP*GalK*UL94. Recombinants were selected on 2-deoxy-galactose (DOG) minimal agar plates to counterselect for *GalK*. The resulting recombinant

BACs were screened by restriction enzyme digest and PCR. Insertion of the premature stop codon was verified by DNA sequencing.

pADCREGFP-UL94repair was generated as described above using pADCREGFP-UL94stop as the parental BAC. The *GalK* cassette was amplified with the oligonucleotides UL94GalK 5' and UL94GalK 3' (Table 2-5). Insertion of the *GalK* cassette by recombination with pADCREGFP-UL94stop resulted in generation of pADCREGFP-UL94repairGalK BAC. The *GalK* cassette was subsequently removed by recombination of pADCREGFPUL94repairGalK with double-stranded oligonucleotides UL94repair sense and UL94repair antisense (Table 2-5). The resulting recombinant BACs were screened by restriction enzyme digest and PCR. Insertion of the wild type UL94 sequence was verified by DNA sequencing. Recombinant viruses were generated by transfecting ~1 μg BAC DNA and 5 μg pCGN-pp71 expression plasmid into 5 x 10^6 HFF cells via electroporation (950μF, 260V). Cells were plated and infectious virus harvested when 100% cytopathic effect was observed. Infectious titers for all viruses were determined by plaque assay on HFF or UL94 complementing HFF cells.

UL94 C204A, C250A, C250A Repair, UL99 Δ37-39, UL99 Δ40-43, and UL99 Δ37-39 Repair

Recombinant BAC were generated using a two-step Red recombination protocol in GS1783 *E. coli* as previously described (110). Briefly, GS1783 cells containing parental ADCRE (126) or ADCREGFP BAC (19) were grown to mid-log phase and induced to express Red recombination proteins at 42° for 15 minutes. Induced cells were made competent and transformed with 100 ng purified PCR product composed of the Kan^R/I-*Sce*I cassette flanked by complementary viral DNA sequence containing the desired mutation. PCR products were generated using the oligonucleotides listed in Table 2-5 and pEPkan-S plasmid (110). Transformed cells were plated on LB agar plates containing chloramphenicol and kanamycin. Resulting colonies were screened

for proper insertion of the Kan^R/I-*Sce*I cassette by PCR. GS1783 cells containing the desired Kan^R/I-*Sce*I BAC were induced to express I-*Sce*I in media containing 1% L-arabinose and plated on LB agar plates containing 1% arabinose and chloramphenicol. Resulting colonies were replica plated to identify clones that were Kanamycin-sensitive, indicating removal of the Kan^R/I-*Sce*I cassette. Recombinant BACs were screened by restriction digest, PCR, and DNA-sequencing analysis to confirm the presence of the desired mutations. Recombinant viruses were generated by transfecting ~1 μg BAC DNA and 5 μg pp71-pCGN expression plasmid into 5 x 10^6 HFF cells via electroporation (950μF, 260V). Cells were seeded into dishes and infectious virus harvested when 100% cytopathic effect was observed. Infectious titers for all viruses were determined by plaque assay on HFF cells.

Complementation of UL94 mutant viruses

UL94 mutant viruses were propagated in cells transduced with LEX lentivirus (Open Biosystems) expressing HAUL94. HAUL94 was cloned into the *Bam*HI and *Xho*I sites of the LentiORF pLEX-MCS vector. The resulting HAUL94 pLEX plasmid was transfected into 293T cells with packaging mix using the Profection Mammalian Transfection System (Promega). Lentivirus was harvested at 48 and 72 hours post-transfection, passed through 0.45 μm filters, and used directly or stored at -80°C until transduction. To generate complementing cells, HFF were transduced with HAUL94-LEX in the presence of 8 μg/ml polybrene.

Analysis of viral DNA Replication

1 x 10^5 HFF cells were plated per well in 12-well culture dishes. Cells were infected with ADCREGFPUL94HA (UL94HA virus) or ADCREGFPUL94stop (UL94stop virus) at a multiplicity of 0.01 PFU/cell. Cells were harvested and lysed in Southern blot lysis buffer (0.5% SDS, 25 mM EDTA, 100 mM NaCl, 10 mM Tris pH 8, 100 μg/ml proteinase K) and spiked with 100 ng pGalK plasmid

(116). Lysates were incubated at 37°C for 2 hours followed by sequential phenol and chloroform:isoamyl alcohol extractions. DNA was precipitated with 100% ethanol and washed with 70% ethanol. Pellets were rehydrated in water and 100 ng was used for detection of viral genome by real-time PCR. Real-time PCR was performed with QuantiFast SYBR Green PCR mix (Qiagen) on the iQ5 Real-Time PCR Detection System (Bio-Rad). Viral genomes were detected by amplification of the UL44 ORF with the oligonucleotides 5'-CAGCTGCACGTTGATACGCATGTT-3' and 5'-TCCACCGGCCATCAAGTTTATCCT-3'. GalK plasmid was detected using the oligonucleotides 5'-TCTCATGCCTCTATGCGCGATGAT-3' and 5'-CACCTTTGTCGCCAATCACAGCTT-3'. Viral DNA present in each sample was calculated by comparison to a standard curve prepared from a viral DNA sample of a known concentration. Data was normalized to levels of GalK plasmid in each sample to account for variation in DNA yield during purification.

Immunofluorescence analysis

HFF cells on glass coverslips were washed in PBS and then fixed in 4% paraformaldehyde in PBS at room temperature for 20 minutes. Fixed cells were washed and permeabilized in PBS-T (PBS, 0.05% Tween 20, 0.1% Triton X-100). Cells were blocked with PBS-T + 0.5% BSA + 1% goat serum for 30 minutes followed by sequential incubation with primary and secondary antibodies in a humidified chamber at 37°C. Cells were incubated with Hoechst stain to visualize nuclei and mounted in 90% glycerol. Fluorescence was visualized on a Zeiss Axiovert 40 CFL microscope. Images were taken using a Jenoptik ProgRes C10 plus camera equipped with ProgRes CapturePro V.2.8.0 software.

Transmission electron microscopy

1×10^5 HFF cells were infected at a multiplicity of 0.05 PFU/cell and processed for TEM 120 hours post-infection. Briefly, cells were trypsinized, pelleted, and washed in PBS. Pellets were rinsed in 0.1 M cacodylate buffer and

fixed in 2.5% glutaraldehyde for 45 minutes at room temperature. Cells were washed and post-fixed in 1% osmium tetroxide for 30 minutes at room temperature. Samples were dehydrated with increasing concentrations of ethanol from 30-100% and then infiltrated with increasing concentrations of Poly/Bed 812 resin. Samples were embedded by curing at 40° for 24 hours followed by 60°C for 48 hours prior to sectioning for TEM. Embedded samples were cut into 65 nm thick sections and stained with uranyl acetate and lead citrate. Samples were imaged using a JEOL 1200-EXII transmission electron microscope and images were acquired using Olympus iTEM Imaging Platform software.

Oligonucleotides

Table 2-1

Oligonucleotides used for generation of entry vectors

CAPSID			
UL46 5'	CACCATGGACGCGCG	**UL46 3'**	TCAGACGAATTCTCGAAAGTCTCCC
UL48A 5'	CACCATGTCTAACACCGCGCCGGGAC	**UL48A 3'**	TCAGCGCCGGGTGCGCGA
UL80 5'	CACCATGACGATGGACGAGCAGCAGTC	**UL80 3'**	TTACTCGAGCTTATTGAGCGCAGCC
UL85 5'	CACCATGGCGGCCATGGAGG	**UL85 3'**	TCAGCCTTTAAATATGCAGGTCGC
UL86 5'	CACCATGGAGAACTGGTCGGCGCTCG	**UL86 3'**	TCACGAGTTAAATAACATGGATTGCTGC
TEGUMENT			
UL24 5'	CACCATGAGCGATCTGGCTAGCC	**UL24 3'**	TCAACGGTGCTGACGTCC
UL25 5'	CACCATGTCGTCGCGGCGTCGCA	**UL25 3'**	TCAGCAACAGTATTCCCCGCTGTC
UL26 5'	CACCATGACGAGTAGGCGCGCAC	**UL26 3'**	TTACGGCAACAGCGCTGATG
UL32 5'	CACCATGAGTTTGCAGTTTATCGGTCTAC	**UL32 3'**	CTATTCCTCCGTGTTCTTAATCTTC
UL35 5'	CACCATGGCCCAAGGATCGCGAG	**UL35 3'**	TCAGAGATGCCGTAGGTTTTCGGC
UL43 5'	CACCATGGAGAAAACGCCGGCGG	**UL43 3'**	TCACCTTCGAGCAAAGAGCCCC
UL44 5'	CACCATGGATCGCAAGACGCGCCT	**UL44 3'**	CTAGCCGCACTTTTGCTTCTTGGTG
UL45 5'	CACCATGAATCCGGCTGACGC	**UL45 3'**	CTAAGAGGCACAGTACTTATATACTC
UL47 5'	CACCATGATGGCGAGGCGCACGGTAG	**UL47 3'**	TCATGGCGAGGCCGGCG
UL48 5'	CACCATGAAAGTCACACAGGCCAGCTGCC	**UL48 3'**	TTACAAAAGATAGAGAAACCGCATG

UL69 5'	CACCATGGAGCTGCACTCACGCGG	**UL69 3'**	TTAGTCATCCATATCATCGCTGT
UL71 5'	CACCATGCAGCTGGCCCAGCGC	**UL71 3'**	TCACGCGCGGAACCCACAAAGG
UL82 5'	CACCATGTCTCAGGCATCGTCCTCG	**UL82 3'**	CTAGATGCGGGGTCGACTGC
UL83 5'	CACCATGGAGTCGCGCGGTCGCCGTTG	**UL83 3'**	TCAACCTCGGTGCTTTTTGGGCGTCG
UL84 5'	CACCATGCCACGCGTCGAC	**UL84 3'**	TTAGAGATCGCCGCAGACCATGGC
UL88 5'	CACCATGATGGAAGCCGCGGCCG	**UL88 3'**	TCAGCTAGGCACGCAGCAGAGC
UL94 5'	CACCATGGCTTGGCGCAGCGG	**UL94 3'**	TTAGTGCACTAGGTTCTTAAGCACCGG
UL96 5'	CACCATGACGTCGGTCAACAAAC	**UL96 3'**	TTAGACGGCGTCGTCGAC
UL97 5'	CACCATGTCCTCCGCACTTCGGTC	**UL97 3'**	TTACTCGGGGAACAGTTGGCG
UL99 5'	CACCATGGGTGCCGAACTCTGC	**UL99 3'**	TTAAAAGGGCAAGGAGGCGG
UL103 5'	CACCATGGAGGCCCTGATGATC	**UL103 3'**	TCACTCTTCCTCTCCTCGTTC
UL104 5'	CACCATGGAGCGAAACCACTGGAAC	**UL104 3'**	CTAGTGAAATCCGTATGGACCTCC
UL112 5'	CACCATGGATCTCCCTACTAC	**UL112 3'**	TTAATCGTCGAAAAACGCCG
US22 5'	CACCATGTCCCTACTCACCAAAGCC	**US22 3'**	TTAGGGACCCGGGTCTG
US24 5'	CACCATGATGGATCCGGCTGCGGGTTC	**US24 3'**	TCAAATCTGGATGTACTCGCGCACAC
IRS1 5'	CACCATGGCCCAGCGCAAC	**IRS1 3'**	TCAATGATGAACGTGGTGAGGG
TRS1 5'	CACCATGGCCCAGCGCAAC	**TRS1 3'**	TTATTGAGCATTGTAATGGTAGTGTG

GLYCOPROTEIN

RL10 5'	CACCATGTATCCGCGTGTAATGCACG	**RL10 3'**	TCAGACGTTGTCGTCCTCGTC
TRL14 5'	CACCATGCGACCGCAGTTACGAGG	**TRL14 3'**	TTAAGCCTTAGTCCAAAATTCATCTGG
UL5 5'	CACCATGTTTCTAGGCTACTCTGACTGTG	**UL5 3'**	CTACACGGTAGCGACGAGAC
UL22A 5'	CACCATGGCTCGGAGGCTATGG	**UL22A 3'**	TTACTGAATCTTCTTTTCATTTTC
UL33 5'	CACCATGGACACCATCATCCACAACTCGACCCGCAACAACACTCCTCCGCACATCAATG		

UL33 3'	TCATACCCCGCTGAGGTTATG		
UL38 5'	CACCATGACTACGACCACGCATAGCAC	**UL38 3'**	CTAGACCACGACCACCATCTG
UL41A 5'	CACCATGACACTCTTTTGCCGCAC	**UL41A 3'**	TTAAAAGTCTGTATCCGACTCCAT
UL50 5'	CACCATGGAGATGAACAAGGTTCTCC	**UL50 3'**	TCAGTCGCGGTGTGC
UL55 5'	CACCATGGAATCCAGGATCTGGTGCC	**UL55 3'**	TCAGACGTTCTCTTCTTCGTCGG
UL73 5'	CACCATGGAGTGGAACACACTAGTATT	**UL73 3'**	TCAATAGCCTTTGGTGGTGG
UL74 5'	CACCATGGGGAGAAAAGAGATGATGGTC	**UL74 3'**	TTACTGCAACCACCACCAAAGG
UL75 5'	CACCATGCGGCCCGGCCTC	**UL75 3'**	TCAGCATCTCTTGAGCATGCGGTAG
UL77 5'	CACCATGAGTCTGTTGCACACCTTTT	**UL77 3'**	TTACAACACCGCCACGCTC
UL93 5'	CACCATGGAAACGCACCTGTATTC	**UL93 3'**	CTAAAGATCGTCGAACGGC
UL100 5'	CACCATGGCCCCCTCGCCACG	**UL100 3'**	TTAAGCGTCCTCGAAGTCTCC
UL115 5'	CACCATGTGCCGCCGCCCGGATTG	**UL115 3'**	TTAGCGAGCATCCACTGCTTGAG
UL119 5'	CACCATGTGTTCCGTACTGGCGATC	**UL119 3'**	CTACCACTGCTTGAAGTAGGG
UL132 5'	CACCATGCCGGCCCCGCGGGGT	**UL132 3'**	CTAGTCGTACTCGGGATCTCTGAG
US27 5'	CACCATGACCACCTCTACAAATAATC	**US27 3'**	TTACAACAGAAATTCCTCCTC

Table 2-2

Oligonucleotides used for generation of destination vectors

FLAG-DEST-pcDNA3.1 5'

AAGCTTGTTTAAACATGGATTACAAGGATGACGACGATAAGTCTAGATCAACAAGTTTGTACAAAAAAGCTGAACGAG

HA-DEST pcDNA3.1 5'

AAGCTTGTTTAAACATGTATCCTTATGACGTGCCTGACTATGCCTCTAGATCAACAAGTTTGTACAAAAAAGCTGAACGAG

FLAG-DEST-pCI-neo 5'

GCTAGCGTTTAAACACCATGGCTGATTACAAGGATGACGACGATAAGTCTAGATCAACAAGTTTGTACAAAAAAGCTGAACGAG

HA-DEST-pCI-neo 5'

GCTAGCGTTTAAACACCATGGCTTATCCTTATGACGTGCCTGACTATGCCTCTAGATCAACAAGTTTGTACAAAAAAGCTGAACGAG

DEST conv 3'

CTCGAGGTTTAAACACCACTTTGTACAAGAAAG

Table 2-3

Oligonucleotides used for generation of UL94 point mutant plasmids

UL94 C200A S	TGTGTTACGACCTGTTTACCTCAGCCGGCAATCGGTG
UL94 C200A AS	CACCGATTGCCGGCTGAGGTAAACAGGTCGTAACACA
UL94 C204A S	CTCATGCGGCAATCGGGCCGATATCCCTTCCATG
UL94 C204A AS	CATGGAAGGGATATCGGCCCGATTGCCGCATGAG
UL94 C227A S	CAGGCGGGTTGCAGCTTTGCCACGGATCACG
UL94 C227A AS	CGTGATCCGTGGCAAAGCTGCAACCCGCCTG
UL94 C250A S	CCCGATATGGGCCGCGCTCTTTGTTACGTGCC
UL94 C250A AS	GGCACGTAACAAAGAGCGCGGCCCATATCGGG
UL94 C252A S	ATGGGCCGCTGTCTTGCTTACGTGCCCTGTGG
UL94 C252A AS	CCACAGGGCACGTAAGCAAGACAGCGGCCCAT
UL94 C256A S	CTTTGTTACGTGCCCGCTGGGCCCATGACGCA
UL94 C256A AS	TGCGTCATGGGCCCAGCGGGCACGTAACAAAG

Table 2-4

Oligonucleotides used for generation of UL99 internal deletion plasmids

UL99 Δ34-36 5' ATCCCTCCGACTTCCTCCTC	**UL99 Δ34-36 3'** GGAGCGTAGAGACACCTGGC
UL99 Δ37-39 5' ACTTCCTCCTCGGACGAAGG	**UL99 Δ37-39 3'** GTTGTCGTAGGAGCGTAGAG
UL99 Δ40-43 5' GACGAAGGGGAGGACGATGA	**UL99 Δ40-43 3'** CGGAGGGATGTTGTCGTAGG

Table 2-5

Oligonucleotides used for generation of recombinant BAC constructs

galK Positive/Counterselection

UL94stop and UL94stop repair

UL94stop GalK 5' TTGCCGTCTCTTCGCGCGTCACTCTTCATGGCTTGGCGCAGCGGGCTTTGCCTGTTGACAATTAATCATCGGCA

UL94stop GalK 3' AGCTTCCACATGCATTCCTCTTGCAAGAACTGCTTCAAAGTTCTGGAATCTCAGCACTGTCCTGCTCCTT

UL94stop sense

GCGGCTTTGCCGTCTCTTCGCGCGTCACTCTTCATGGCTTGGCGCAGCGGGCTTTGAGAGACCGATTCCAGAACTTTGAAGCAGTTCTTGCA
AGAGGAATGCATGTGGAAGCTGGTCGG

UL94stop antisense

CCGACCAGCTTCCACATGCATTCCTCTTGCAAGAACTGCTTCAAAGTTCTGGAATCGGTCTCTCAAAGCCCGCTGCGCCAAGCCATGAAGAGT
GACGCGCGAAGAGACGGCAAAGCCGC

UL94stop repair sense

GCGGCTTTGCCGTCTCTTCGCGCGTCACTCTTCATGGCTTGGCGCAGCGGGCTTTGCGAGACCGATTCCAGAACTTTGAAGCAGTTCTTGCA
AGAGGAATGCATGTGGAAGCTGGTC

UL94stop repair antisense

GACCAGCTTCCACATGCATTCCTCTTGCAAGAACTGCTTCAAAGTTCTGGAATCGGTCTCGCAAAGCCCGCTGCGCCAAGCCATGAAGAGTGA
CGCGCGAAGAGACGGCAAAGCCGC

galK/Kanamycin Positive/Counterselection

HAUL88

UL88GalK 5' ACGGCAGTTCTGAACCCACGTCGCCGCGAGCGCGGTTTGCATCACGATGACCTGTTGACAATTAATCATCG

UL88Kan 3' CGGACGCTCCTCCGGACGAAACGCCGCGGCGGCAGCGGCCGCGGCTTCCACTCAGCAAAAGTTCGATTTA

HAUL88 sense

ACGGCAGTTCTGAACCCACGTCGCCGCGAGCGCGGTTTGCATCACGATGATTTATCCTTATGACGTGCCTGACTATGCCAGCCTGGGAATGG
AAGCCGCGGCCGCTGCCGCCGCGGCGTTTCGTCCGGAGGAGCGTCCG

HAUL88 antisense

CGGACGCTCCTCCGGACGAAACGCCGCGGCGGCAGCGGCCGCGGCTTCCATTCCCAGGCTGGCATAGTCAGGCACGTCATAAGGATAAATC
ATCGTGATGCAAACCGCGCTCGCGGCGACGTGGGTTCAGAACTGCCGT

UL94HA

UL94 GalK 5' GTGTCACGTATGATAGTGTGTTCCTGTCCGGTGCTTAAGAACCTAGTGCACCCTGTTGACAATTAATCATCG

UL94 Kan 3' TCCTCCTTTTTTTTGTTATTTCTTGTTTCTTCTCCCCGTGAACTGTCAGACCCCGCTCAGCAAAAGTTCGATTTA

UL94HA sense

GTGTCACGTATGATAGTGTGTTCCTGTCCGGTGCTTAAGAACCTAGTGCACAGATCATATCCTTATGACGTGCCTGACTATGCCTAAGAATTCC
GGGGTCTGACAGTTCACGGGGAGAAGAAACAAGAAACAACAAAAAAAAGGAGGA

UL94HA antisense

TCCTCCTTTTTTTTGTTGTTTCTTGTTTCTTCTCCCCGTGAACTGTCAGACCCCGGAATTCTTAGGCATAGTCAGGCACGTCATAAGGATATCTT
GAGTGCACTAGGTTCTTAAGCACCGGACAGGAACACACTATCATACGTGACAC

Kanamycin/IsceI Positive Selection/Excision

UL94HA stop

UL94HA stop Kan/Iscel 5'

TCTTCGCGCGTCACTCTTCATGGCTTGGCGCAGCGGGCTTTGAGAGACCGATTCCAGAACTTTAGGATGACGACGATAAGTAGGG

UL94HA stop Kan/Iscel 3'

CCTCTTGCAAGAACTGCTTCAAAGTTCTGGAATCGGTCTCTCAAAGCCCGCTGCGCCAAGCCACAACCAATTAACCAATTCTGATTAG

UL94HA C204A

UL94 C204A Kan/IsceI 5'

CATTCTGTGTTACGACCTGTTTACCTCATGCGGCAATCGGGCCGATATCCCTTCCATGACGCGAGGATGACGACGATAAGTAGGG

UL94 C204A Kan/IsceI 3'

CCGTGGCCGCCGCCATGAGGCGCGTCATGGAAGGGATATCGGCCCGATTGCCGCATGAGGTAACAACCAATTAACCAATTCTGATTAG

UL94HA C250A

UL94 C250A Kan/IsceI 5'

CACTGGCAATTACGTGGGTTGCACCCCCGATATGGGCCGCGCTCTTTGTTACGTGCCCTGTGGAGGATGACGACGATAAGTAGGG

UL94 C250A Kan/IsceI 3'

TGAGCGACTGCGTCATGGGCCCACAGGGCACGTAACAAAGAGCGCGGCCCATATCGGGGGTGCCAACCAATTAACCAATTCTGATTAG

UL94HA C250A repair

UL94HA C250A repair Kan/IsceI 5'

ACTGGCAATTACGTGGGTTGCACCCCCGATATGGGCCGCTGTCTTTGTTACGTGCCCTGTAGGATGACGACGATAAGTAGGG

UL94HA C250A repair Kan/IsceI 3'

AGCGACTGCGTCATGGGCCCACAGGGCACGTAACAAAGACAGCGGCCCATATCGGGGGTGCAACCAATTAACCAATTCTGATTAG

UL94HA UL99 Δ40-43

UL99 Δ40-43 KanIsce 5'

TCGCCAGGTGTCTCTACGCTCCTACGACAACATCCCTCCGGACGAAGGGGAGGACGATGAAGGATGACGACGATAAGTAGGG

UL99 Δ40-43 KanIsce 3'

TATCGTCATCCTCCCCGTCGTCATCGTCCTCCCCTTCGTCCGGAGGGATGTTGTCGTAGGCAACCAATTAACCAATTCTGATTAG

UL94HA UL99 Δ37-39

UL99 Δ37-39 KanIsce 5'

ATGCTCTGGGTCGCCAGGTGTCTCTAGGCTCCTACGACAACACTTCCTCCTCGGACGAAGGGAGGATGACGACGATAAGTAGGG

UL99 Δ37-39 KanIsce 3'

TCCCCGTCGTCATCGTCCTCCCCTTCGTCCGAGGAGGAAGTGTTGTCGTAGGAGCGTAGAGACAACCAATTAACCAATTCTGATTAG

UL94HA UL99 Δ37-39 repair

UL99 Δ37-39 repair KanIsce 5'

CTGGGTCGCCAGGTGTCTCTACGCTCCTACGACAACATCCCTCCGACTTCCTCCTCGGACAGGATGACGACGATAAGTAGGG

UL99 Δ37-39 repair KanIsce 3'

TCGTCATCGTCCTCCCCTTCGTCCGAGGAGGAAGTCGGAGGGATGTTGTCGTAGGAGCGTCAACCAATTAACCAATTCTGATT

CHAPTER 3

IDENTIFICATION OF BINARY INTERACTIONS BETWEEN HCMV VIRION PROTEINS

Introduction

HCMV is the largest of the human herpesviruses with a >230 kbp genome composed of linear double-stranded DNA. The predicted coding capacity of the genome ranges from 160 to over 200 open reading frames (ORFs) (69, 70). HCMV particles are structurally complex and are composed of a DNA-containing nucleocapsid surrounded by a layer of virally encoded proteins referred to as the tegument. A host-derived envelope that is studded with virally encoded glycoproteins surrounds the nucleocapsid and tegument. As many as 71 viral proteins are predicted to be incorporated into HCMV particles (113).

The function of HCMV tegument proteins is a subject of intense interest. Although there may be as many as 35 proteins that are packaged in the tegument layer of the virion, less than half of these proteins have been ascribed a function (43, 113). Tegument proteins are released into the cytoplasm of the host cell upon viral entry, thus are able to function immediately upon infection, prior to the onset of viral gene expression. Tegument proteins function in various capacities throughout the course of infection including delivery of the viral genome, regulation of gene expression, modulation of host immune responses, nuclear egress, and virion envelopment (3, 13, 14, 22, 49, 82, 98).

The assembly of HCMV virions is poorly understood, especially with respect to acquisition of the tegument proteins. Several tegument proteins localize exclusively to the cytoplasm throughout the course of infection, suggesting that much of the tegument is acquired after nuclear egress of DNA-containing capsids (11, 89) This is supported by the observation that many tegument and glycoproteins localize to a unique perinuclear structure that is referred to as the assembly complex (AC) at late times during infection, where it is thought that final virion assembly and envelopment occur (88). However, it has also been shown that the abundant tegument protein UL32 (pp150) associates with capsids in the nucleus and remains bound to the capsid during nuclear egress and migration of the capsid to the AC (38, 86). While the formation of the

AC is a well documented phenomenon, the events that occur in the AC that result in the formation of mature virus particles have remained elusive.

Although the mechanisms of tegumentation and viral assembly are not well understood, these processes are generally thought to involve the stepwise addition of proteins through protein-protein interactions. In addition to the role played by protein-protein interactions in assembly of the virion, such interactions are also likely to be required for important functions of tegument proteins throughout the course of infection. Therefore, to identify protein-protein interactions among virion proteins, we carried out a yeast two-hybrid screen to identify binary interactions among HCMV capsid, tegument, and glycoproteins. Using this method we identified 24 interactions, including 13 novel interactions between tegument proteins and one novel interaction between capsid proteins. Co-immunoprecipitation experiments were used to confirm many of these interactions in both transfected and HCMV infected cells. Interactions identified in this screen will provide insight into virion assembly, tegumentation, and the function of tegument proteins in the HCMV life cycle.

Results

Interactions identified by yeast two-hybrid analysis. To identify protein-protein interactions between virion proteins we performed a yeast two-hybrid screen. Proteins selected for inclusion in the screen were previously identified as virion components by mass spectrometry (113). The selected proteins included 5 capsid, 28 tegument, and 19 glycoproteins (Table 3-1). Table 3-1 also lists the proposed function of each protein and whether the protein plays an essential, augmentive, or dispensable role in viral replication based on transposon mutagenesis studies (28, 125).

Each ORF was cloned into both the bait (pDEST32) and prey (pDEST22) vectors of the yeast two-hybrid system. This was done to account for the possibility that interactions may only occur in a single bait-prey orientation as has been previously reported (52, 83). Each protein was tested against itself and all

other proteins in a binary fashion by co-transformation of a single bait and prey vector for a total of 2704 pairwise combinations. Prior to screening, we tested each bait for auto-activation of the *HIS3* reporter. Yeast were transformed with an individual bait vector and the empty prey vector. Transformants were then tested for growth on plates containing increasing concentrations of 3-amino-1,2,4-triazole (3AT), which specifically inhibits the enzyme product of the *HIS3* gene. Subsequent screening was carried out using the lowest concentration of 3AT that inhibited growth of yeast cells containing each bait vector alone. UL32, UL69, UL71, and UL94 exhibited significant levels of auto-activation and were subsequently screened on plates containing 50 mM 3AT. The remaining 48 baits were screened on plates containing 12.5 mM 3AT. These stringent requirements were implemented to reduce the potential for false positives resulting from auto-activation by the bait protein.

Each bait and prey pair was tested for interaction by co-transformation into MaV203 yeast. Protein-protein interactions were first identified based on activation of the *HIS3* reporter gene as indicated by growth of transformants on His- minimal synthetic agar media. Colonies that grew on His- plates were then assayed for β-galactosidase activity to test for activation of *LacZ*, a second independent reporter gene. Each interaction identified in the initial screen was repeated at least twice and exhibited activation of both the *HIS3* and *LacZ* reporter genes. Each bait alone was analyzed as a negative control and was spotted to the left of each bait and prey combination.

The two-hybrid screen revealed 24 interactions among virion proteins. We identified 19 interactions between tegument proteins (Fig. 3-1) and 5 interactions between capsid proteins (Fig. 3-2). Of the 5 capsid-capsid interactions identified, only the interaction between the minor capsid binding protein UL46 and the major capsid protein UL86 has not been previously reported. Of the 19 interactions among tegument proteins, 13 are novel (Fig. 3-1, asterisks). The interactions between UL82-UL32 (90), UL82-UL35 (90), and UL94-UL99 (56) as well as self-interactions between UL44 (2), UL69 (54), and UL112e1 (72) have all been

previously demonstrated using either yeast two-hybrid analysis or co-immunoprecipitation. Of the 24 binding pairs identified, 7 are self-interactions and 17 are heterologous interactions. We identified interactions involving 21 of the 52 virion proteins tested. However, we did not identify any interactions involving glycoproteins or interactions between tegument and capsid proteins.

Of the 17 heterologous interactions identified, only the interaction between the tegument proteins UL25 and UL26 could be demonstrated in both bait/prey orientations (data not shown). This is consistent with the results of similar two-hybrid screens and validates our approach of testing each interaction in both orientations (52, 83).

Validation of interactions in transfected cells. To eliminate the possibility that the interactions identified in the yeast two-hybrid screen represent false positives, we sought to verify a subset of the interactions by co-immunoprecipitation of binding partners from transfected mammalian cells. Due to the unavailability of antibodies against specific viral proteins, we first generated epitope-tagged Gateway compatible expression plasmids using pcDNA3.1 and pCI-neo as backbone vectors. Each vector was designed to express the protein of interest fused in-frame with an N-terminal HA or FLAG tag.

293T HEK cells were co-transfected with vectors expressing HA and FLAG-tagged binding partners. Total protein was harvested 48 hours after transfection and immune complexes were precipitated with an antibody against the FLAG epitope. Precipitated proteins were subjected to SDS-PAGE followed by Western blot with an antibody against the HA epitope. Cell lysates were also analyzed to demonstrate the expression of each protein after transfection. Results of the co-immunoprecipitation analysis are shown in Fig. 3-3. For all eleven protein pairs tested, the HA-tagged protein immunoprecipitated with the FLAG-tagged binding partner as demonstrated by Western blot analysis of protein complexes (Fig. 3-3, top row). The self-interactions of UL69 (Fig. 3-3, panel 1) and UL112e1 (Fig. 3-3, panel 3) have been previously demonstrated

using co-immunoprecipitation analysis and were used as positive controls for validation of other interactions (54, 72). The interaction between UL99-UL94 (Fig. 3-3, panel 2) has been previously demonstrated using FRET and yeast two-hybrid analysis but has not been demonstrated using co-immunoprecipitation (56). The remaining eight interactions tested, UL25-UL25 (Fig. 3-3, panel 4), UL25-UL26 (Fig. 3-3, panel 5), UL45-UL25 (Fig. 3-3, panel 6), UL45-UL32 (Fig. 3-3, panel 7), UL45-UL69 (Fig. 3-3, panel 8), UL88-UL69 (Fig. 3-3, panel 9), UL94-UL82 (Fig. 3-3, panel 10), and UL94-US22 (Fig. 3-3, panel 11) are novel interactions between tegument proteins. These results confirm the results of the yeast two-hybrid screen and demonstrate that the interactions identified in the screen are not false positive results or artifacts of the two-hybrid system.

Generation of recombinant HA-tagged viruses. Yeast two-hybrid and co-immunoprecipitation from transfected cells are valid methods to demonstrate protein-protein interactions. However, these assays are carried out in the absence of other viral factors and may not necessarily reflect the interactions that occur during the course of infection. In addition, conditions of over-expression may result in an artificial association between proteins that would not otherwise interact. Therefore, we sought to verify a subset of interactions in infected cells to assess whether the interactions identified by yeast two-hybrid analysis could also be demonstrated in the context of HCMV infection.

We chose to examine the interactions between UL94-UL99, UL69-UL88, and UL48-UL88 during viral infection. Due to the unavailability of antibodies needed to directly test the interactions in the context of an infection, we generated recombinant viruses that express HA-tagged UL88 (ADCREGFP-HAUL88) or HA-tagged UL94 (ADCREGFP-UL94HA) proteins. The recombination strategy and characterization of ADCREGFP-HAUL88 and ADCREGFP-UL94HA are shown in Fig. 3-4A. We generated these recombinant viruses using a previously described two-step BAC recombineering protocol (80, 116) that involves site-specific insertion of a *GalK*/Kan marker cassette followed

by replacement of the marker cassette with the HA epitope tag. The UL93 ORF overlaps with the 5' end of the UL94 ORF by 142 base pairs. For this reason, the stop codon of UL94 was removed and the HA epitope was fused to the C-terminus of UL94, leaving the coding sequence for UL93 intact. The UL88 ORF overlaps with both UL87 at the 5' end and UL89 at the 3' end. The UL87 stop codon TGA is located at nucleotides 131178-131180 (RefSeq X17403.1), overlapping with the UL88 initiating ATG located at nucleotides 131177-131179. Therefore, to insert an HA epitope at the N-terminus of UL88, we inserted an ATT isoleucine codon immediately following the UL88 initiating ATG. This strategy allowed us to insert the HA tag in-frame with the N-terminus of UL88 while leaving the UL87 stop codon intact.

BAC constructs were analyzed by restriction enzyme digest for insertion and removal of the *GalK*/Kan^R cassette and the in-frame insertion of the HA tag was verified by DNA sequencing (data not shown). pADCREGFP-UL94HA and pADCREGFP-HAUL88 BAC DNA were transfected into HFF cells to generate virus stocks. The addition of the HA tag did not result in any observable change in the replication kinetics of either virus compared to wild type ADCREGFP virus (data not shown). To confirm expression of the tagged proteins during infection, HFF cells were infected at a multiplicity of 3 PFU/cell and total protein was harvested 96 hours post-infection. Cell lysates were analyzed by Western blot using an antibody directed against the HA epitope. As shown in Fig. 3-4B, we detected proteins at the predicted sizes of 36 kD (UL94) and 48 kD (UL88) following infection with the respective recombinant viruses.

Validation of interactions in HCMV infected cells. To validate the interactions between UL48-UL88, UL69-UL88, and UL99-UL94 in the context of infection, HFF cells were infected with the indicated viruses at a multiplicity of 3PFU/cell and total protein was harvested 120 hours post-infection. This time point was chosen because with the exception of UL69, each of the proteins involved in these interactions is expressed with true late kinetics and does not accumulate to

appreciable levels until late time-points during infection (46, 81, 119). Immunoprecipitation was carried out with polyclonal α-HA antibody. Immunoprecipitates were separated by SDS-PAGE and Western blot was performed with antibodies against UL48, UL69, or UL99. Cell lysates were also analyzed for expression of each protein (Fig. 3-5, bottom 3 rows). Fig. 3-5 shows that for each interaction tested, we were able to demonstrate co-immunoprecipitation of each set of binding partners (Fig. 3-5, top row). These results show that UL48-UL88 (Fig. 3-5, panel 3), UL69-UL88 (Fig. 3-5, panel, 2), and UL99-UL94 (Fig. 3-5, panel 1) are physically associated with each other at late times during HCMV infection of HFF cells.

Discussion

The goal of this study was to gain insight into the structure and organization of the HCMV virus particle by identifying interactions between virion proteins. To this end, we employed the yeast two-hybrid assay to identify binary interactions among HCMV tegument, capsid, and glycoproteins.

Our yeast two-hybrid screen identified 24 interactions among HCMV virion proteins. Of these 24 protein-protein interactions, 10 have been previously reported in the literature. These include UL44-UL44 (2) , UL69-UL69 (54), UL82-UL32 (40), UL82-UL35 (90), UL99-UL94 (56), UL112e1-UL112e1 (72), UL46-UL85 (33), UL48a-UL86 (51), UL80-UL80 (59, 121), and UL85-UL85 (33). Our screen also revealed 14 novel interactions including UL25-UL25, UL25-UL26, UL32-UL35, UL43-UL83, UL45-UL25, UL45-UL45, UL45-UL69, UL48-UL45, UL48-UL88, UL69-UL88, UL82-UL94, UL94-US22 (Fig. 3-1) and UL46-UL86 (Fig. 3-2). Several of these interactions were subsequently confirmed in co-immunoprecipitation experiments following co-expression in transient over-expression studies (UL25-UL25, UL25-UL26, UL32-UL45, UL45-UL25, UL45-UL69, UL69-UL88, UL82-UL94, and UL94-US22 (Fig. 3-3). Three of the interactions identified in the yeast two-hybrid screen were also confirmed in the context of HCMV infection (UL99-UL94, UL88-UL69, and UL48-UL88) (Fig. 3-5).

These co-immunoprecipitation studies validate the yeast two-hybrid results and suggest the importance of these interactions during HCMV infection.

We detected 19 tegument-tegument interactions and 5 capsid-capsid interactions. However, we did not identify any interactions involving glycoproteins. This was not entirely unexpected due to the use of full-length glycoproteins containing transmembrane domains, which may prevent these proteins from localizing to the yeast cell nucleus to activate reporter genes. While interactions involving full-length glycoproteins have been identified in previously reported yeast two-hybrid studies, the use of truncated versions of each glycoprotein consisting of only the cytoplasmic tail may be better suited for this type of screen.

Our screen also did not reveal any interactions between HCMV tegument and capsid proteins. These results were initially surprising considering the results of similar screens carried out for other herpesvirus family members. Analysis of interactions between HSV-1 and KSHV virion proteins revealed five and seven interactions, respectively, between capsid and tegument proteins (52, 83). Interestingly, a comprehensive yeast two-hybrid screen performed for murine cytomegalovirus also failed to detect any binary interactions between tegument and capsid proteins (29). The only HCMV tegument protein that has been shown to interact with the capsid is pp150 (UL32), an abundant tegument protein that is unique to β-herpesviruses. Interestingly, pp150 has only been shown to bind intact capsids isolated from virions but does not bind individual capsid subunits in GST pull-down assays (12). Therefore, HCMV tegument proteins may only bind the capsid in its fully assembled conformation and not to individual capsid proteins. Taken together, these data suggest the possibility that the mechanism of β-herpesvirus assembly differs markedly from those of α- and γ-herpesviruses.

There are a number of previously reported interactions between HCMV virion proteins that were not detected in the current study. Several factors can contribute to false negative results using the yeast two-hybrid assay. Improper folding or masking of binding domains due to the fusion of the GAL4 activation

domain or DNA-binding domain to each protein may prevent an interaction from occurring. False negatives may also result from the absence of post-translational modifications that may be necessary for an interaction to occur. This may be especially relevant for viral proteins that are normally glycosylated or phosphorylated during infection. Another possible explanation for the failure to detect interactions that have been previously demonstrated using other methods is that some of these interactions may be indirect or require the presence of other viral factors to form a complex. Finally, it is possible that false negatives in our screen resulted from insufficient expression of bait or prey proteins. However, we were able to detect interactions with all five capsid proteins and 16 of the 28 tegument proteins tested, confirming that all of these proteins were expressed in our system.

Using the data from our screen and from previous literature reports of interactions between HCMV proteins, we have constructed an interactome map (Fig. 3-6). This map illustrates interactions involving the proteins that are predicted to be incorporated into the tegument layer of the virion and does not include interactions involving capsid or glycoproteins. Novel interactions identified in the current study are indicated by solid lines. Previously reported interactions are indicated by dashed lines (13, 21, 30, 45, 47, 65, 92, 94, 102, 103, 109). The interactome map shows that all of the known interactions involving the proteins that are likely packaged in the virion tegument form a network to which each protein has at least one other binding partner. This map can be used to make predictions about tegument architecture or the mechanisms by which the tegument is assembled. In addition to possible roles in the structure or assembly of virions, these interactions may also have regulatory functions such as in regulation of viral gene expression, modulation of host cell responses, or pathogenesis *in vivo*.

Several of the novel interactions identified in our screen involve the tegument protein UL45. We demonstrated that UL45 associates with itself as well as with the tegument proteins UL25, UL32, UL48, and UL69. It was originally

hypothesized that UL45 functions as a ribonucleotide reductase or as an inhibitor of apoptosis based on homology to other proteins. However, UL45 does not appear to function in either of these capacities during HCMV infection *in vitro* (36). One group predicted that UL45 plays a role in assembly or egress based on an apparent defect in plaque formation by a UL45-deletion mutant (74). Our data are consistent with a possible role for UL45 in assembly due to its interaction with several other tegument proteins that are expressed at late times in infection. These interactions may contribute to the proper acquisition of tegument proteins or maintenance of tegument structure within the virion. Analysis of the tegument composition of virions produced by a UL45-deletion mutant will help reveal whether UL45 is required for proper tegument incorporation of UL25, UL32, UL48, or UL69.

Previous yeast two-hybrid analysis identified UL32 and UL35 as viral binding partners of UL82. Subsequent characterization of a UL35-deletion mutant demonstrated that in the absence of UL35, UL82 is retained in the nucleus rather than localizing to the cytoplasm during virion assembly (40). The UL35-deletion mutant was also associated with an accumulation of unenveloped cytoplasmic particles and a decrease in particle infectivity (90). In the current study, we identified the previously reported interactions between UL32-UL82 and UL35-UL82. In addition, we also detected an interaction between UL32 and UL35. Therefore, it is possible that these three proteins form a complex in infected cells. These interactions may contribute to the functions of these three proteins during infection.

Finally, an interaction of particular interest is that between UL94 and UL99. Both of these tegument proteins are required for efficient HCMV replication (28, 98, 125). Both UL94 and UL99 are core herpesvirus proteins and the homologs of these conserved tegument proteins from several other herpesviruses have also been shown to interact (29, 58). It is tempting to speculate that the interaction between these proteins serves an essential function in the viral life cycle, making it an attractive target for antiviral

compounds. Whether this interaction plays a structural or regulatory role during infection is not yet known. We are currently investigating whether the interaction between UL94-UL99 is essential for viral replication or if other unrelated functions of each protein are responsible for the defective phenotype of UL94 and UL99-deletion mutants.

Further study of the kinetics, subcellular location, and functional significance of these interactions during infection will be necessary to characterize the potential contribution of each interaction to HCMV replication. The interactions identified in this study will likely shed light on the mechanisms of tegument assembly during virion maturation and also provide clues about the functions of as yet uncharacterized tegument proteins.

TABLE 3-1. HCMV Virion Proteins Analyzed in Yeast Two-Hybrid Assay

Protein Type	ORF	Function	Role in Infection
Capsid	UL46	Major capsid-binding protein	Essential
	UL48A	Smallest capsid protein	Essential
	UL80	Capsid assembly protein	Essential
	UL85	Minor capsid protein	Essential
	UL86	Major capsid protein	Essential
Tegument/	UL24	Unknown	Dispensable
Uncharacterized	UL25	Unknown	Dispensable
	UL26	Transcriptional regulation	Augmentive
	UL32	Late phase maturation	Essential
	UL35	Transcription/particle formation	Augmentive
	UL43	Unknown	Dispensable
	UL44	DNA replication	Essential
	UL45	Unknown	Dispensable
	UL47	Unknown	Augmentive
	UL48	Ubiquitin-specific protease	Essential
	UL69	Transcriptional regulation	Augmentive
	UL71	Unknown	Essential
	UL82	Transcriptional regulation	Augmentive
	UL83	Lower matrix protein	Dispensable
	UL84	DNA replication	Essential
	UL88	Unknown	Dispensable
	UL94	Unknown	Essential
	UL96	Unknown	Essential
	UL97	Protein kinase	Augmentive
	UL99	Late phase maturation	Essential
	UL103	Unknown	Augmentive
	UL104	DNA packaging/cleavage	Essential
	UL112	DNA replication	Augmentive
	US22	Unknown	Dispensable
	US23	Unknown	Augmentive
	US24	Unknown	Dispensable
	IRS1	Transcription	Dispensable
	TRS1	Transcription/Egress	Augmentive
Glycoprotein	RL10	Envelope Glycoprotein	Dispensable
	TRL14	Unknown	Dispensable
	UL5	Unknown	Dispensable
	UL22A	Immune Regulation	Dispensable
	UL33	GPCR	Dispensable
	UL38	Unknown	Augmentive
	UL41A	Unknown	Dispensable
	UL50	Egress	Essential
	UL55	Entry (gB)	Essential
	UL73	Entry (gN)	Essential
	UL74	Entry (gO)	Augmentive
	UL75	Entry (gH)	Essential
	UL77	DNA packaging/cleavage	Essential
	UL93	Unknown	Essential
	UL100	Attachment	Essential
	UL115	Entry (gL)	Essential
	UL119	Fcγ Receptor	Dispensable
	UL132	Unknown	Augmentive
	US27	GPCR	Dispensable

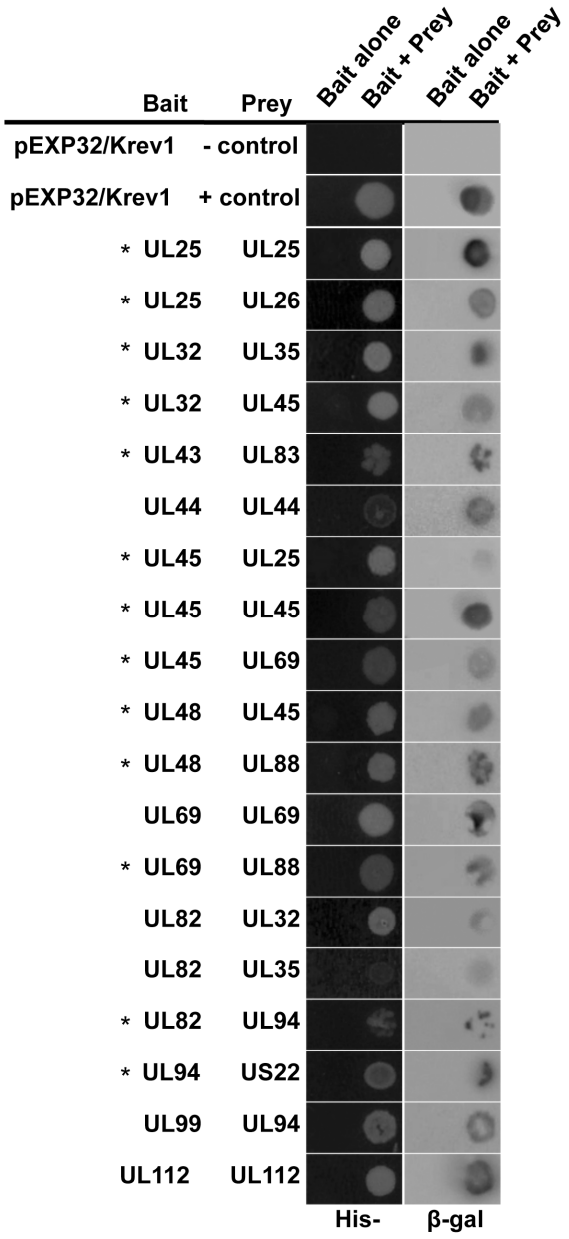

Figure 3-1. Interactions between HCMV tegument proteins. Yeast cells were co-transformed with bait and prey plasmids expressing the indicated tegument proteins. Interactions were scored as positive in the yeast two-hybrid assay based on activation of the *HIS3* reporter gene (left panels) and β-galactosidase activity (right panels). Novel interactions are indicated with an asterisk.

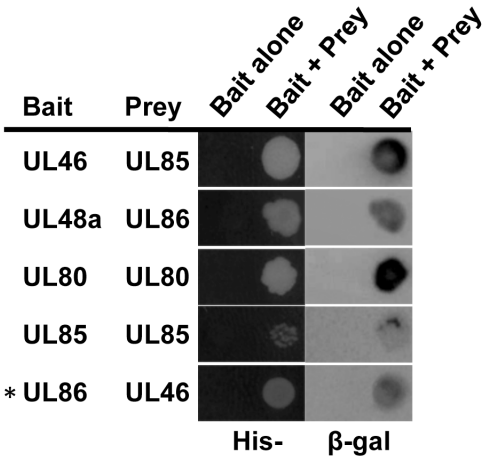

Figure 3-2. Interactions between HCMV capsid proteins. Yeast cells were co-transformed with bait and prey plasmids expressing the indicated capsid proteins. Interactions were scored as positive in the yeast two-hybrid assay based on activation of the *HIS3* reporter gene (left panels) and β-galactosidase activity (right panels). Novel interactions are indicated with an asterisk.

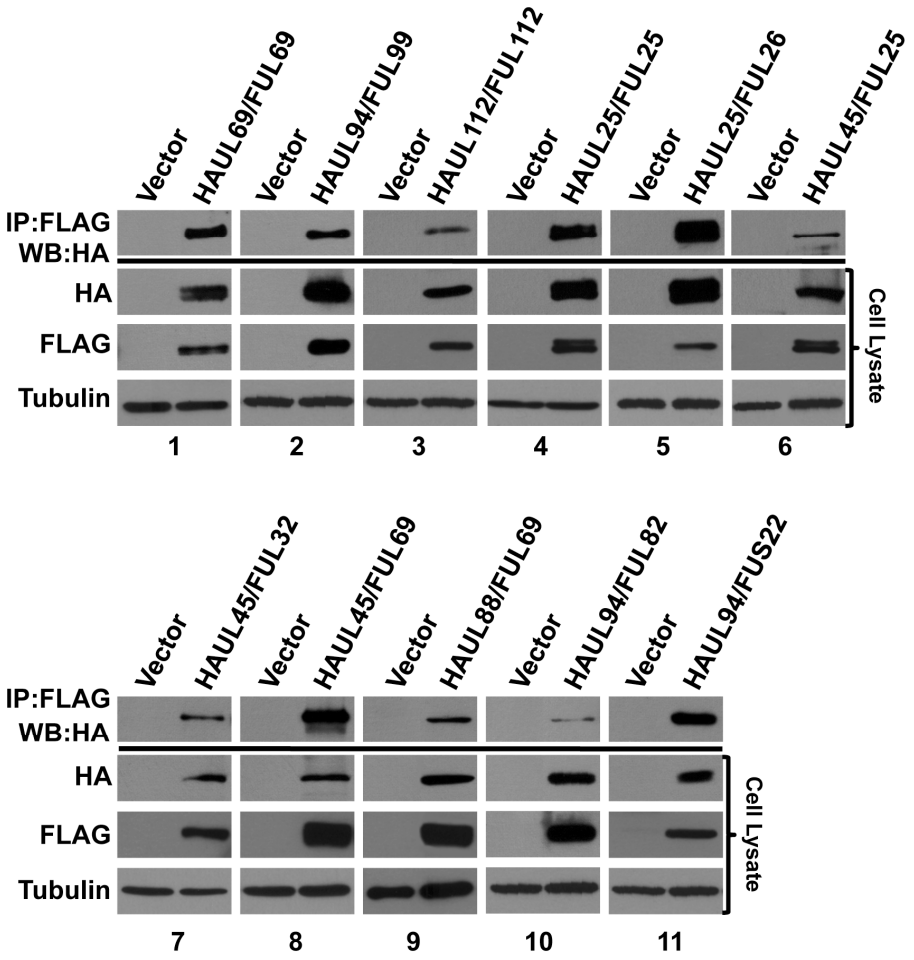

Figure 3-3. Validation of interactions by co-immunoprecipitation. 293T cells were transfected with HA and FLAG-tagged vectors expressing the indicated viral proteins. Total protein was harvested 48 hours post-transfection and protein complexes were immunoprecipitated with α-FLAG antibody. Precipitated proteins were separated by SDS-PAGE and HA-tagged protein detected by Western Blot with α-HA antibody. 20% of input was analyzed for expression of HA and FLAG-tagged proteins. Tubulin is shown as a loading control.

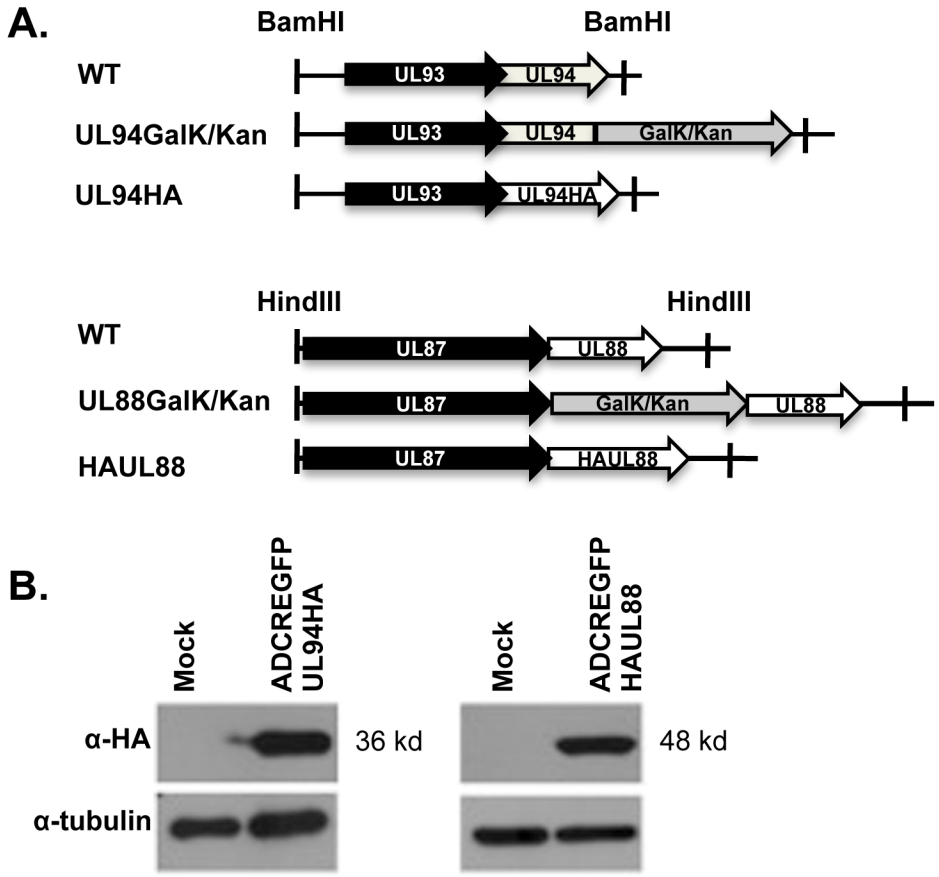

Figure 3-4. Generation of recombinant viruses expressing HA-tagged UL88 or UL94. (A) Schematic diagram of UL94 and UL88 genomic regions and the procedure used to generate recombinant BACs from wild type ADCREGFP BAC. In the first recombination step, the *GalK*/Kan^R selection cassette was inserted at either the 5' (UL88) or 3' (UL94) end of the ORF. The *GalK*/Kan^R cassette was then removed via recombination with a double-stranded oligonucleotide containing the HA tag and gene-specific flanking sequences. **(B)** HFF cells were either mock infected or infected with ADCREGFP-UL94HA or ADCREGFP-UL88HA at a multiplicity of 3 PFU/cell. Cell lysates were harvested 96 hours post-infection and assayed for UL94 or UL88 expression by Western blot analysis using α-HA antibody.

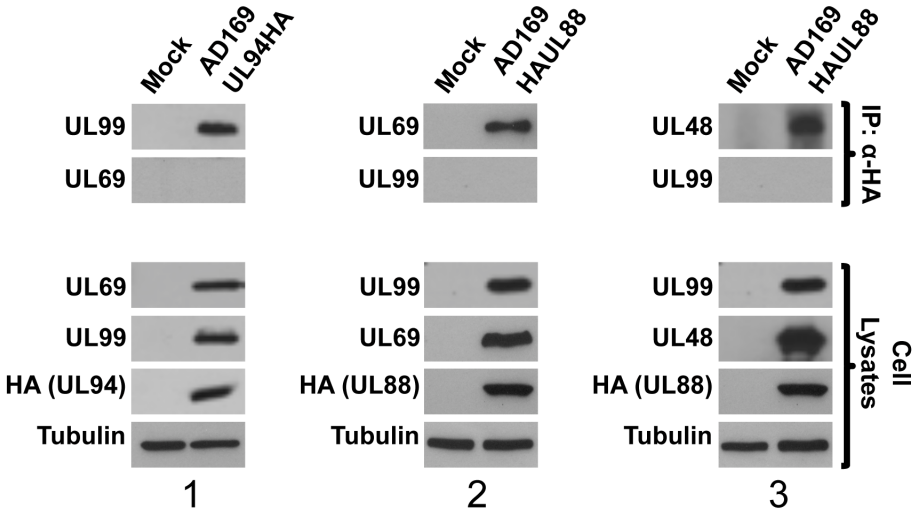

Figure 3-5. **Validation of interactions during HCMV infection**. HFF cells were mock infected or infected with either ADCREGFP-HAUL88 or ADCREGFP-UL94HA viruses at a multiplicity of 3 PFU/cell. Cell lysates were harvested 120 hours post-infection and subjected to immunoprecipitation with α-HA antibody. Precipitated proteins were separated by SDS-PAGE and Western blots were performed using the indicated antibodies to demonstrate co-immunoprecipitation of binding partners. Western blot of total cell lysates confirmed expression of each protein. Tubulin is shown as a loading control.

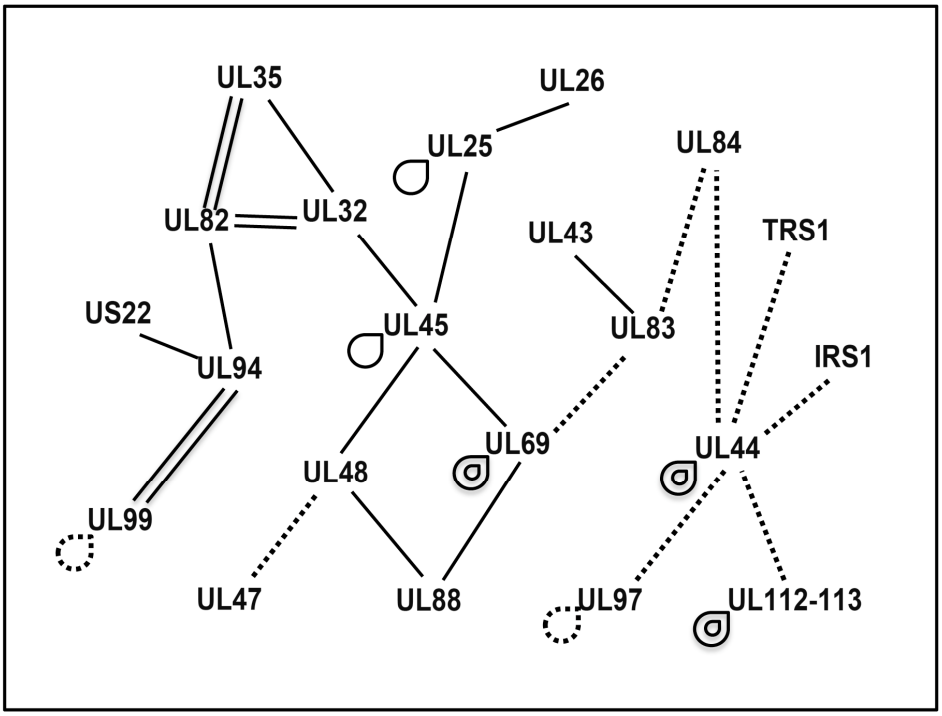

Figure 3-6. **Interactome map of HCMV tegument proteins**. Map illustrates novel interactions identified in this screen (solid lines), interactions identified in this screen that have been previously reported (double lines), and interactions that have been previously reported but were not identified in this screen (dashed lines). Self-interactions are indicated by loops. Map shows the relationship between 31 interactions involving 21 proteins. Proteins included in the map are known tegument proteins or virion proteins that have not yet been characterized.

CHAPTER 4

UL94 IS ESSENTIAL FOR SECONDARY ENVELOPMENT OF HCMV VIRIONS

Introduction

Many HCMV tegument and glycoproteins localize late in infection to a unique juxtanuclear structure that is referred to as the assembly complex (88). The assembly complex is formed through a dramatic relocalization of various components of the cellular secretory apparatus and is thought to be the site of final virion assembly and envelopment (25, 26, 88). While the formation of the assembly complex is a well-documented phenomenon, the subsequent events that result in the formation of mature virus particles remain elusive. Abundant viral structural proteins that are known to accumulate at the assembly complex include the tegument proteins UL32 (pp150) and UL99 (pp28) as well as the glycoproteins gB, gH, and gM:gN (50, 88, 89, 96). Phenotypic analysis of viral mutants lacking UL32 or UL99 demonstrate that the assembly complex forms normally in the absence of these proteins but that final particle maturation does not occur, indicating that these tegument proteins play essential roles in virion assembly (4, 98).

Although the mechanisms of tegumentation and viral assembly are not well understood, these processes are thought to be mediated at least in part by protein-protein interactions. Chapter 3 describes the identification of several interactions that may play an importnt role in virion assembly. We chose to further investigate the functional significance of the interaction between the tegument proteins UL94 and UL99 during HCMV infection. We and others have reported an interaction between UL94 and UL99 (29, 56, 75, 111). UL99 is essential for the acquisition of the viral envelope in the cytoplasm however the function of UL94 is unknown (93, 98). UL94 is a core herpesvirus gene that is conserved among all members of the herpesvirus family. UL94 was previously shown to be expressed with true-late kinetics and to partition exclusively to the nuclear fraction of infected cells, suggesting a potential role in the regulation of viral or cellular gene expression (119).

We sought to further characterize UL94 and investigate its function during HCMV infection. We confirmed that UL94 is expressed with true-late kinetics.

However, we found that UL94 localized almost exclusively to a juxtanuclear structure during infection that is consistent with the assembly complex. We also constructed a UL94-null mutant, designated UL94stop. The UL94stop mutant is completely defective for growth, demonstrating that UL94 is essential for HCMV replication. The UL94 mutant virus showed no defect in viral gene expression or genome synthesis, suggesting that UL94 functions during the late phase of infection, subsequent to DNA replication. Analysis of the subcellular localization of viral proteins to the assembly complex late in infection showed that while several structural proteins localize normally, UL99 displayed aberrant localization in the absence of UL94. Finally, we showed that there is an accumulation of non-enveloped capsids in the cytoplasm of cells infected with the UL94stop mutant. These data suggest that UL94 functions at least in part to direct the proper localization of UL99 to the assembly complex, a step that is necessary for secondary envelopment of virions.

Results

***Characterization of epitope tagged UL94 protein in infected cells*.** Several antibodies raised against UL94 are commercially available. All of these antibodies were raised against a peptide antigen corresponding to amino acids 26-40 of UL94. We tested three different UL94 antibody clones and found that none of them specifically recognized UL94 (Fig. 4-1C and data not shown). Therefore, to characterize the expression and localization of UL94 during infection, we generated recombinant viruses that express UL94 with a C-terminal HA tag, designated UL94HA virus (75) or UL94 fused to the fluorescent mCherry protein, designated UL94mCherry virus. To verify UL94 expression from these recombinant viruses, HFF cells were infected with wild type, UL94HA, or UL94mCherry virus. Cell lysates were harvested 72 hours post-infection and assayed for UL94 expression by Western blot using antibody directed against HA, dsRed (mCherry), or UL94 (Santa Cruz Biotechnology clone 6J8). We were able to detect UL94 with either the HA or dsRed antibody and these proteins

migrated at the expected molecular weights of 39 and 66 kDa respectively (Fig. 4-1A and B). In contrast, when an identical blot was incubated with an antibody raised against a peptide antigen corresponding to amino acids 26-40 of UL94, we were only able to detect a ~72 kDa band (Fig. 4-1C). Because we do not observe the expected size shift corresponding to the fusion of the HA tag or mCherry to the C-terminus of UL94, it is likely that the UL94 6J8 antibody is recognizing an infected cell protein other than UL94. Two other commercial antibodies raised against an identical peptide were also tested and neither antibody specifically detected UL94 (data not shown). The UL94HA virus replicates to wild type levels (Fig. 4-7). Therefore, we used the UL94HA virus as the wild type virus in all experiments designed to characterize UL94 during infection.

***UL94 is expressed with true-late kinetics and displays differential localization in transfected and infected cells*.** UL94 was previously reported to be expressed with true-late kinetics based on Northern blot analysis of UL94 transcript (119). We sought to confirm these results by analyzing the expression of UL94 protein. Therefore, we performed Western blot analysis of infected-cell lysates over a time-course of infection. HFF cells were infected with UL94HA virus at a multiplicity of 3 PFU/cell and total protein was harvested every 24 hours for five days. Infected cells were also incubated in the presence of phosphonoacetic acid (PAA) to inhibit viral DNA synthesis. Proteins were separated by SDS-PAGE and subjected to Western blot analysis for expression of representative immediate early (IE1/2), early (UL44), and late (UL99) genes as well as UL94 (HA). UL94 was first detected at 48 hours post-infection and its expression continued to increase over the next 48 hours (Fig. 4-2). In addition, the expression of UL94 was completely inhibited by the addition of PAA to the growth medium (Fig. 4-2, Lane 5). These data confirm that UL94 is a true-late gene and demonstrate that the addition of the HA-tag to the C-terminus of UL94 does not affect its expected expression kinetics.

UL94 is thought to be virion-associated based on proteomic analysis of HCMV particles. To establish whether UL94 is a tegument protein, HFF cells were infected with UL94HA virus and supernatant was collected when 100% CPE was observed. Virus particles were purified, incubated with trypsin and/or Triton X-100, and assayed by Western blot for the presence of UL94. As shown in Fig. 4-3, UL94 remains associated with the particle after treatment with Triton X-100 (Lane 1) or when particles are exposed to trypsin alone (Lane 3). However, when particles are treated with both detergent and protease, UL94 is readily degraded (Lane 2). The same results were observed when particles were assayed for the abundant tegument protein UL83 (pp65). Therefore, we conclude that UL94 is located within the tegument layer of the virion and that the addition of the HA-tag to the C-terminus of UL94 does not prevent its packaging into HCMV virions.

Previous reports analyzing the localization of UL94 in infected cells described conflicting results regarding whether UL94 localizes to the cytoplasm or nucleus of infected cells (56, 119). Therefore, we sought to determine the subcellular localization of UL94 in both transfected and HCMV infected cells. HFF cells were transfected with a plasmid expressing HA-tagged UL94 and immunofluorescence analysis with an α-HA antibody was performed 48 hours post-transfection. In the absence of other viral proteins, UL94 exhibits a diffuse pattern of localization that can be seen in both the nucleus and the cytoplasm of transfected cells (Fig. 4-4, left). To determine the localization of UL94 during infection, HFF cells were infected with UL94HA virus at a multiplicity of 3 PFU/cell and immunofluorescence analysis was performed 96 hours post-infection. In contrast to the pattern of localization observed in transfected cells, UL94 is detected predominantly in a juxtanuclear structure consistent with the viral assembly complex during infection (Fig. 4-4, right). An identical pattern of localization was observed with the UL94mCherry fusion protein during infection (data not shown). These results suggest that UL94 localizes to the assembly

complex late in infection and that this localization requires other infected-cell proteins.

***UL94 is essential for HCMV replication*.** To investigate the function of UL94 during infection, we generated a UL94-null mutant which we have designated UL94stop. This mutant was generated through a single point mutation that introduces a premature stop codon after the seventh codon of the UL94 ORF. Fig. 4-5A shows the region of the viral genome surrounding the UL94 ORF and the recombination strategy used to generate the UL94stop mutant. The UL93 ORF overlaps the 5' end of UL94 by 142 nucleotides. Due to this overlap, we generated the UL94stop mutant with a single C to A point mutation that introduces a premature stop codon in UL94 without altering the amino acid sequence of UL93. Fig. 4-5B shows verification of the desired recombination events by restriction digest analysis. The shifts in restriction fragment sizes based on the proper recombination events are indicated with arrows. Insertion of the *GalK* cassette results in a 1333 bp increase in the size of the *Eco*RI fragment containing the UL94 ORF. The *GalK* cassette was then removed by recombination with double-stranded oligonucleotides containing the desired mutation. The restriction pattern of the resulting UL94stop BAC is identical to that of the parental ADCREGFP BAC. The entire UL94 ORF in the UL94stop BAC was sequenced to confirm the presence of the C to A point mutation and to verify that no other mutations were incorporated into the UL94 gene. UL94stop BAC DNA was co-transfected into HFF cells with a pp71 expression plasmid to determine whether UL94 is essential for viral replication. The spread of infection was then monitored by GFP expression from the ADCREGFP viral genome (19). Fig. 4-5C shows GFP expression in cell cultures 21 days post-transfection of either wild type or UL94stop BAC DNA. Cells transfected with the wild type BAC displayed significant CPE and greater than 95% of the cells were GFP positive by 21 days post-transfection due to the production of infectious virus. In contrast, we were only able to detect single GFP-positive cells in cultures transfected with

the UL94stop BAC. These individual GFP positive cells represent those that were initially transfected with BAC DNA, however there was no subsequent spread of infection indicating that no infectious virus is produced from the UL94stop BAC. This result suggests that UL94 is essential for HCMV replication.

***Complementation of the UL94stop mutant*.** Because UL94 is likely essential for viral replication, we developed a complementation system that would allow us to propagate the UL94stop mutant. To do this, we used a lentiviral system that allows for transduction of quiescent HFF cells. UL94 complementing HFF cells were generated by transduction with lentivirus expressing HA-tagged UL94. Expression of UL94 from transduced HFF cells was verified by Western blot analysis with an α-HA antibody and compared to the expression of UL94 from cells infected with the UL94HA virus. The level of UL94 expressed from the UL94 complementing HFF cells was significantly lower than the level of UL94 present after infection with UL94HA virus (Fig. 4-6A, compare lanes 2 and 3). However, upon infection of UL94 complementing HFF cells with wild type HCMV we observed an induction in HAUL94 expression (Fig. 4-6A, compare lanes 3 and 4). This effect is likely due to the action of viral proteins on the CMV immediate-early promoter that is used to drive expression of UL94 from the lentivirus. However, even after induction, the levels of UL94 observed in the complementing cells were still less than the levels of UL94 observed during infection (compare lanes 2 and 4).

To generate a stock of the UL94stop virus, HFF cells were first transfected with the UL94stop BAC. Cells were then transduced with lentivirus expressing HA-tagged UL94 the day following BAC transfection. Virus produced after BAC transfection was harvested when cells exhibited advanced CPE and then used to infect a fresh culture of UL94 complementing HFF cells. The resulting UL94stop virus was titered by plaque assay on UL94 complementing HFF cells. Although we were able to generate a stock of the UL94stop virus, the complementation was inefficient. The UL94stop virus spread very slowly compared to wild type

virus and only produced titers of ~5 x 10^3 PFU/ml, approximately 3-logs lower than the titers routinely obtained with wild type virus. In addition, the UL94stop mutant formed plaques that were significantly smaller in size than those produced by UL94HA virus by 14 days after infection (Fig. 4-6B).

Once a stock of the UL94stop virus was obtained, we performed a growth curve analysis (Fig. 4-7). HFF cells were infected with wild type, UL94HA, UL94stop, or UL94repair viruses at a multiplicity of 0.01 PFU/cell. Total virus was harvested at the indicated times post-infection and viral titers were determined by plaque assay on UL94 complementing HFF cells. We were unable to detect any infectious virus from cells infected with the UL94stop mutant at any time post-infection (Fig. 4-7, filled triangles), confirming that UL94 is essential for replication. However, when the UL94stop mutation is repaired, the resulting UL94repair virus replicates to levels similar to wild type (Fig. 4-7, open triangles). This result demonstrates that the growth defect of the UL94stop mutant can be attributed specifically to the mutation in UL94 and is not due to a secondary mutation elsewhere in the viral genome. The UL94HA virus also replicates to wild type levels, demonstrating that the addition of the HA tag to the C-terminus of UL94 does not interfere with the essential function of UL94 (Fig. 4-7, open circles).

***UL94 is not required for viral gene expression or genome replication*.** We next sought to determine where the block in viral replication occurs following infection with the UL94stop virus. We first examined the kinetics of viral gene expression in cells infected with the UL94stop mutant. HFF cells were infected with UL94HA or UL94stop virus at a multiplicity of 0.01 PFU/cell and total protein was harvested at the indicated times following infection. Cell lysates were analyzed for expression of representative viral immediate-early (IE1/2), early (UL44) and late (UL86) proteins by Western blot. We observed no defect in the kinetics of immediate early, early, or late gene expression in cells infected with the UL94stop mutant when compared to the UL94HA virus (Fig. 4-8). We did

observe a modest increase in viral protein levels at late times in cells infected with the UL94HA virus when compared to the UL94stop mutant. However, this is likely due to viral spread in cells infected with the UL94HA virus whereas the UL94stop mutant is unable to produce infectious virus. These results suggest that the absolute growth defect of the UL94stop mutant is not due to a global defect in viral gene expression.

We also analyzed the kinetics and levels of viral genome replication in both UL94HA and UL94stop virus infected cells. HFF cells were infected at a multiplicity of 0.01 PFU/cell and total DNA was harvested at the indicated times post-infection. Purified DNA was subjected to real-time PCR analysis for levels of viral DNA. Results were normalized for both input DNA and variations in DNA recovery during purification. Picograms of viral DNA present in each sample were calculated from a standard curve prepared from purified viral DNA of a known concentration. The kinetics and levels of viral genome synthesis were nearly identical for both UL94HA and UL94stop virus infections (Fig. 4-9). This result suggests that UL94 does not play an essential role in viral DNA replication.

***UL94 directs the proper localization of UL99 to the assembly complex*.** Many viral tegument proteins function in assembly by directing proper tegumentation, capsid trafficking, and envelope acquisition at the assembly complex in the cytoplasm (4, 87, 93, 95, 98, 107, 108). We therefore sought to characterize the phenotype of the assembly complex with respect to the localization of viral proteins in cells infected with the UL94stop mutant. HFF cells were seeded on glass coverslips and infected at a multiplicity of 0.01 PFU/cell with either UL94HA or UL94stop virus. Cells were fixed and stained for immunofluorescence analysis of viral proteins 120 hours post-infection (Fig. 4-10). In cells infected with UL94HA virus we observed the expected localization pattern of UL94, UL32, gB, and UL99 to the juxtanuclear viral assembly complex (Fig. 4-10). We saw a similar localization of UL32 and gB to the assembly complex in cells infected with the UL94stop virus. Interestingly, we observed a

dramatic difference in the localization of UL99 following infection with the UL94stop mutant. In contrast to the juxtanuclear localization observed in cells infected with the UL94HA virus, UL99 remained predominantly diffuse throughout the cytoplasm in cells infected with the UL94stop mutant.

The assembly complex is composed of many components of the cellular secretory apparatus including early endosomes. To determine whether cellular components of the assembly complex localize properly in the absence of UL94, we determined the localization of the cellular early endosomal marker EEA1 in cells infected with the UL94stop mutant (Fig. 4-11). Infected cells are indicated by GFP expression from the viral genome. In cells infected with either UL94HA virus (top row) or UL94stop virus (bottom row), early endosomes become reoriented and accumulate at the juxtanuclear assembly complex as previously described (20, 25, 26). In contrast, early endosomes in uninfected cells are observed throughout the cytoplasm. These results show that the reorientation of early endosomes to the assembly complex does not require UL94. Taken together, these data suggest that the absence of UL94 does not result in a global defect in the formation of the assembly complex, but rather that UL94 is required specifically for the proper localization of UL99.

***UL94 is required for secondary envelopment in the cytoplasm*.** To determine the ultrastructural morphology of virus particles in the absence of UL94, we performed TEM analysis. HFF cells were infected with UL94HA or UL94stop virus at a multiplicity of 0.05 PFU/cell and cells were collected for TEM analysis 120 hours post-infection. Images of thin sections were collected at a final magnification of X20,000 (Fig. 4-12). We observed similar numbers of empty and DNA-containing capsids in the nuclei of both UL94HA and UL94stop virus infected cells, suggesting that there is no defect in capsid formation or DNA packaging in the absence of UL94 (Fig. 4-12A). The cytoplasm of cells infected with both UL94HA and UL94stop virus also contained both empty (Fig. 4-12B, black arrowheads) and DNA-containing capsids (Fig. 4-12B, white arrows). The

majority of cytoplasmic particles in both UL94HA and UL94stop virus infected cells appeared to be surrounded by a layer of tegument proteins based on their thickness compared to nuclear capsids, suggesting that the initial steps involved in tegument acquisition do not require UL94. We also observed a >3-fold increase in the total number of capsids in the cytoplasm of UL94stop infected cells compared to cells infected with UL94HA virus. Importantly, we were able to readily detect fully enveloped virions in cells infected with the UL94HA virus (Fig. 4-12B, black arrows). Approximately 10% of all cytoplasmic particles in UL94HA virus infected cells were surrounded by an envelope. However, we were unable to detect any enveloped virions in cells infected with the UL94stop mutant. Numerous infected cell sections were examined and after counting greater than 600 cytoplasmic capsids in cells infected with the UL94stop virus, we were unable to detect a single enveloped virion. We also observed large spherical electron-dense structures in the cytoplasm of cells infected with the UL94stop mutant that were enlarged compared to those found in the cytoplasm of cells infected with the UL94HA virus. Immature particles formed by the UL94stop mutant were often found on the periphery of these structures but did not acquire an envelope. These results suggest that there is a complete block in secondary envelopment in the absence of UL94.

Discussion

The mechanisms that facilitate the assembly of mature HCMV particles in the cytoplasm of infected cells remain poorly understood. While the events that result in virion maturation remain largely undefined, many reports have demonstrated a role for tegument proteins in virion assembly. Our lab and others have reported an interaction between the tegument proteins UL99 (pp28) and UL94 (29, 56, 75, 111). We demonstrated that this interaction occurs at late times in infection, when infectious progeny are being produced (Figure 3-5) (75). UL99 localizes to the viral assembly complex and is essential for secondary envelopment of virions in the cytoplasm (89, 93, 98). In the absence of UL99,

partially tegumented but non-enveloped capsids accumulate in the cytoplasm and no extracellular infectious virus is produced. Localization of UL99 to the cytoplasmic assembly complex is essential for virus replication and requires the expression of other late viral proteins (93, 96). In contrast, despite being a conserved herpesvirus core gene, little is known about UL94 and its function during infection has not been investigated. Mutagenesis of the HCMV genome has suggested that UL94 was either essential or augmenting depending on the mutagenesis strategy used (28, 125). Further, overlap of ORFs and the presence of co-terminal transcripts in the region of the viral genome in which UL94 is located complicate the interpretation of results obtained with these mutants. The role of UL94 for HCMV replication has never been tested by the generation of a specific UL94-null mutant. Therefore, we sought to characterize UL94 and determine whether it is required for HCMV replication.

To circumvent the lack of a specific UL94 antibody, we generated a recombinant virus that expresses UL94 with a C-terminal HA tag (75). This virus expresses a protein of the predicted molecular weight and replicates to wild type levels (Fig. 4-1A and 4-7). Using the UL94HA virus, we demonstrated that UL94 is a tegument protein that is expressed with true-late kinetics (Fig. 4-2 and 4-3). We also used this virus to determine the subcellular localization of UL94 in infected cells. Interestingly, we observed a dramatically different pattern of UL94 localization in transfected cells when compared to infected cells (Fig. 4-4). Whereas UL94 was found throughout both the nucleus and the cytoplasm of transfected cells, we found that UL94 localized almost exclusively to the viral assembly complex during infection. This demonstrates that the proper localization of UL94 in infected cells requires other infected-cell proteins.

To elucidate the function of UL94 during infection, we generated a UL94-null virus designated UL94stop. The UL94stop mutant is completely defective for replication, which necessitated the development of a complementation system for propagating the mutant virus. We utilized a UL94 lentivirus complementation system to generate HFF cells that stably express HA-tagged UL94. UL94stop

virus grown on complementing cells only replicated to titers of ~5 x10^3 PFU/ml. The reason for this poor complementation is unknown. Analysis of the localization of UL94 and UL99 in UL94 complementing cells infected with the UL94stop mutant indicates that both proteins localize properly to the assembly complex in these cells, suggesting that the low level of complementation achieved is not due to improper localization of UL94 or UL99 (data not shown). The most likely explanation is that it is due to the decreased level of UL94 protein expressed in the complementing cells when compared to the levels of UL94 achieved during infection (Fig. 4-6). Another possibility is that poor complementation results from constitutive expression of UL94 in the complementing cells. Viral gene expression is precisely controlled and many structural proteins are expressed with true-late kinetics, meaning that their expression is tightly suppressed until after the onset of viral DNA synthesis. Late viral proteins expressed constitutively in the host cell are therefore temporally dysregulated and may not complement properly or perhaps may even interfere with normal viral replication. Other groups have also reported difficulty in complementing HCMV mutants of essential viral structural proteins (4, 98). Interestingly, the levels of complementation for the UL94stop mutant were similar to those achieved for a UL99-deletion mutant (98).

Phenotypic analysis of the UL94stop mutant suggests that UL94 functions late in infection, subsequent to viral DNA replication. The early phases of viral replication such as immediate early and early viral gene expression as well as the synthesis of viral DNA occur at wild type levels in the absence of UL94 (Fig. 4-8 and 4-9). We also observed proper localization of the abundant viral proteins UL32 (tegument) and gB (envelope) to the assembly complex following infection with the UL94stop virus (Fig. 4-10). Proper formation of the assembly complex was further confirmed by demonstrating reorientation of the early endosomal marker EEA1 to the juxtanuclear site of virion assembly (Fig. 4-11). Interestingly, we observe a dramatic defect in the localization of UL99 following infection with the UL94stop mutant. In the absence of UL94, UL99 fails to accumulate at the

assembly complex and remains largely diffuse throughout the cytoplasm. These results suggest that UL94 functions at least in part to ensure the proper localization of UL99 to the assembly complex where final virion envelopment is thought to occur. These data are further supported by our ultrastructural analysis, which shows that in the absence of UL94 there is a block in secondary virion envelopment as indicated by the complete absence of enveloped virions in the cytoplasm of cells infected with the UL94stop virus (Fig. 4-12B). A very similar phenotype was previously reported for cells infected with a UL99-deletion mutant (98). Taken together, our results suggest that UL94 is required for the proper localization of UL99 to the assembly complex, a step that is necessary for secondary envelopment of virions.

While we cannot rule out the possibility that UL94 directly influences virion envelopment, we favor a model in which the accumulation of un-enveloped particles is secondary to the absence of sufficient amounts of UL99 at the assembly complex. It has been shown that the localization of UL99 to the assembly complex is essential for HCMV replication and that a mutant form of UL99 that traffics to but is not retained in the assembly complex shows a defect in envelopment and delayed growth kinetics (93, 96). Further, UL99 exhibits differential localization in transfected and infected cells, associating with different cellular membranes in the presence of other viral proteins (89, 96). These observations indicate that other viral factors are required for the proper localization of UL99 during infection. Based on the data presented here, we propose that UL94 is the late viral protein that is essential for trafficking of UL99 to the assembly complex.

UL94 and UL99 are both conserved across all members of the herpesvirus family. Although their interaction is also conserved (29, 52, 56, 64, 100, 114), its functional significance remains unclear. In the case of HSV-1, the interaction between the UL94 homolog (UL16) and the UL99 homolog (UL11) has been proposed to function in virion morphogenesis in the cytoplasm (58, 66, 123). However, neither UL16 nor UL11 is essential for HSV-1 replication,

whereas HCMV lacking UL94 or UL99 is completely defective for growth. Thus, it is likely that the mechanisms of cytoplasmic virion assembly are different for beta-herpesviruses compared to alpha-herpesviruses.

The data shown here represent the first report of a specific function of the essential UL94 tegument protein during HCMV infection. Our data suggests that UL94 is required for the proper localization of UL99 to the cytoplasmic assembly complex, an event ultimately necessary for final envelopment. Interestingly, the phenotype of the UL94-null virus characterized in this study is virtually identical to that of a previously characterized UL99-deletion mutant (98). Mutants lacking either UL94 or UL99 exhibit wild type replication until the phase of cytoplasmic assembly, during which immature particles accumulate in the cytoplasm without subsequent envelope acquisition. Based on the fact that UL94 and UL99 physically interact during infection, it is reasonable to hypothesize that their interaction is required for the proper localization of UL99 and thus for virus replication. However, we cannot rule out alternate mechanisms involving other viral or cellular proteins in this process. For example, it is possible that while the proper localization of UL99 requires UL94, the localization of UL94 may also be influenced by UL99. In addition, the localization of each protein to the assembly complex may also require one or more cellular proteins. We are currently investigating the functional significance of the interaction between UL94 and UL99 during HCMV replication.

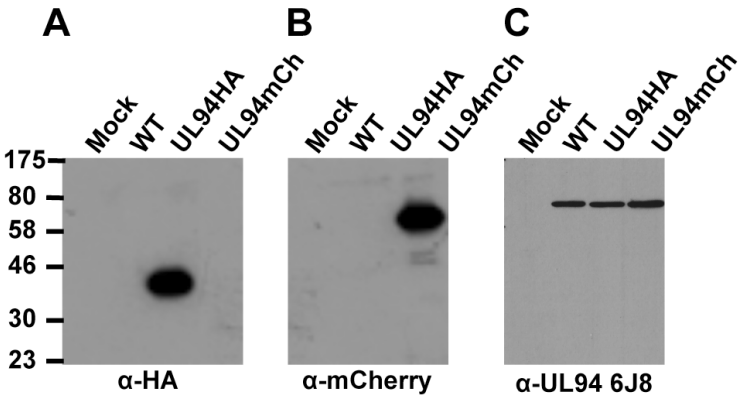

Figure 4-1. Detection of UL94 fusion proteins in infected-cell lysates. HFF cells were mock infected or infected at a multiplicity of 3 PFU/cell with wild type, UL94HA, or UL94mCherry virus. Total protein was harvested at 72 hours post-infection and lysates were analyzed for UL94 expression. **(A)** Western blot probed with α-HA antibody. **(B)** Western blot probed with α-dsRed antibody, which also recognizes mCherry. **(C)** Western blot probed with α-UL94 antibody clone 6J8.

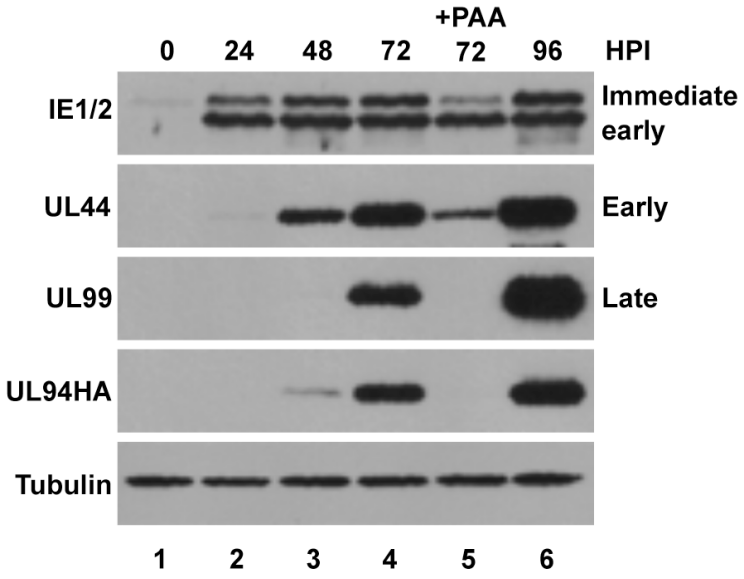

Figure 4-2. **UL94 is expressed with true-late kinetics.** HFF cells were infected with UL94HA virus at a multiplicity of 3 PFU/cell and total protein was harvested at the indicated times post-infection. Cell lysates were analyzed by Western blot with the indicated antibodies.

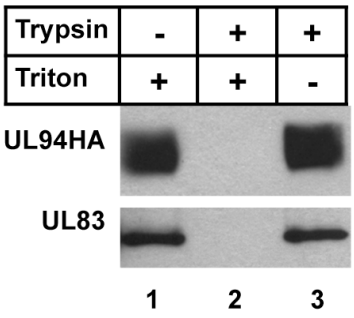

Figure 4-3. **UL94 is incorporated into the virion tegument.** Equal amounts of purified virions were subjected to treatment with trypsin and/or triton as indicated. Samples were analyzed for the presence of viral proteins by Western blot.

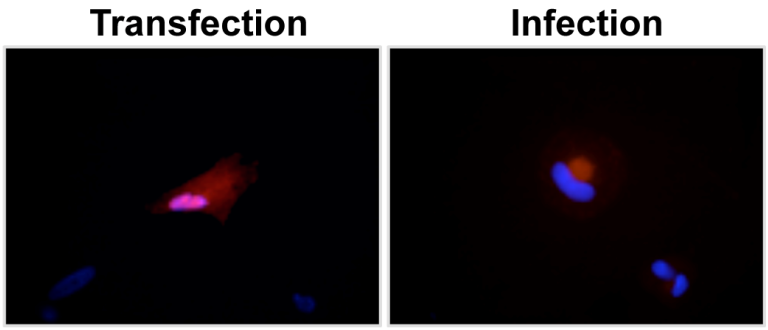

Figure 4-4. **UL94 localization in transfected and infected cells.** HFF cells were transfected with HAUL94-pcDNA3.1 expression plasmid (left), or infected at a multiplicity of 0.01 PFU/cell with UL94HA virus (right). UL94 protein was visualized by immunofluorescence staining with α-HA antibody 48 hours post-transfection or 120 hours post-infection. Alexa546-conjugated secondary was used to visualize UL94 (red). Nuclei are stained with Hoechst (blue).

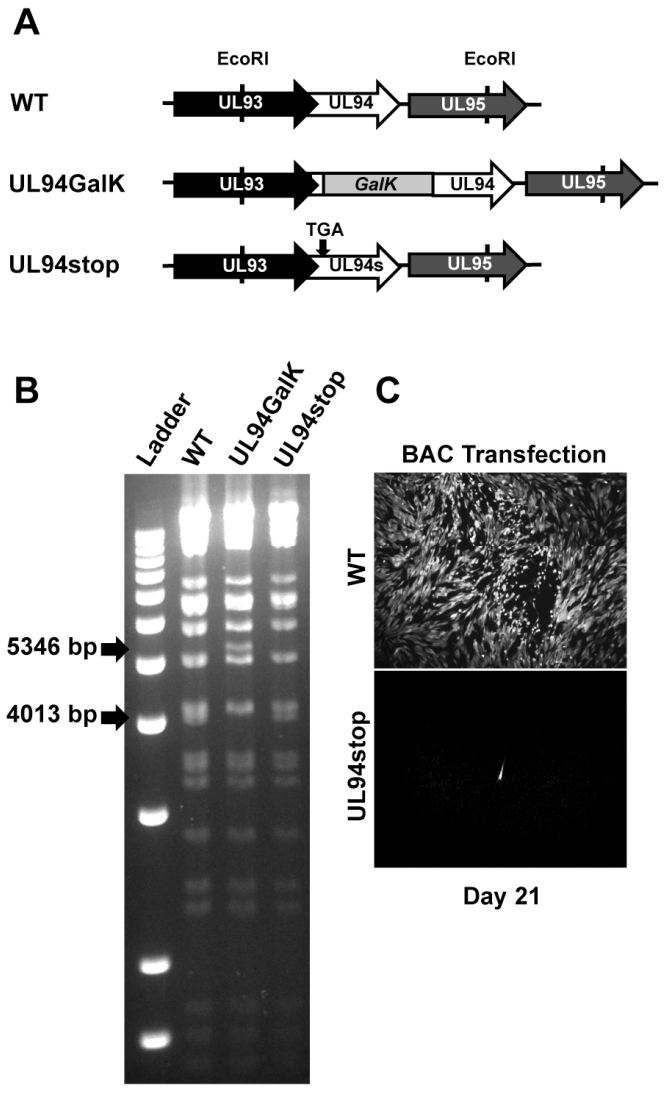

Figure 4-5. **Generation of UL94stop mutant BAC. (A)** Schematic diagram of genomic region containing UL94 and the strategy used to generate the UL94stop BAC containing a premature stop codon from wild type ADCREGFP. **(B)** BAC DNA was isolated and digested with *Eco*RI. Digested DNA fragments were separated by agarose gel electrophoresis. Arrows indicate predicted fragments generated as a result of the desired recombination events. **(C)** Wild type or UL94stop BAC DNA was transfected into HFF cells. Spread of infection was visualized 21 days post-infection by GFP expression from the viral genome.

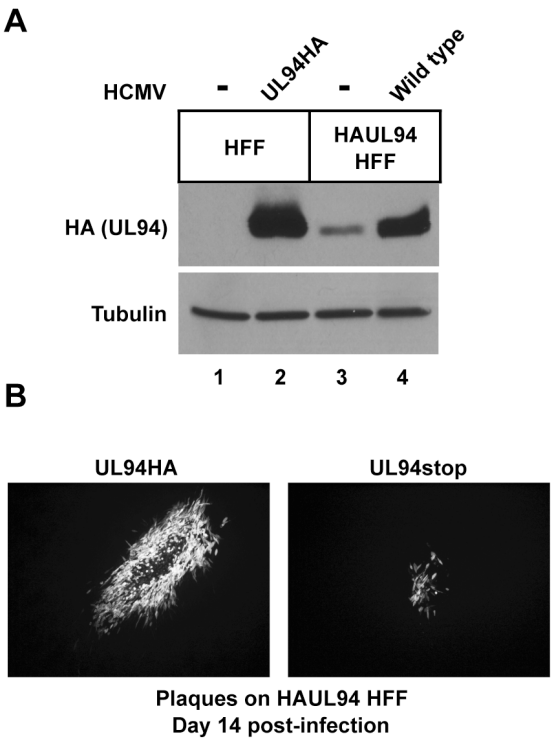

Figure 4-6. **Complementation of UL94stop mutant. (A)** Western blot analysis of HAUL94 expression in complementing cells. Normal HFF or complementing HAUL94 HFF cells were either mock infected (lanes 1 and 3) or infected at a multiplicity of 3 PFU/cell with UL94HA virus (lane 2) or wild type virus (lane 4). Total protein was harvested 72 hours post-infection and analyzed for expression of HA-tagged UL94. **(B)** Plaques formed 14 days post-infection by UL94HA virus (left) or UL94stop virus (right) on complementing HAUL94 HFF.

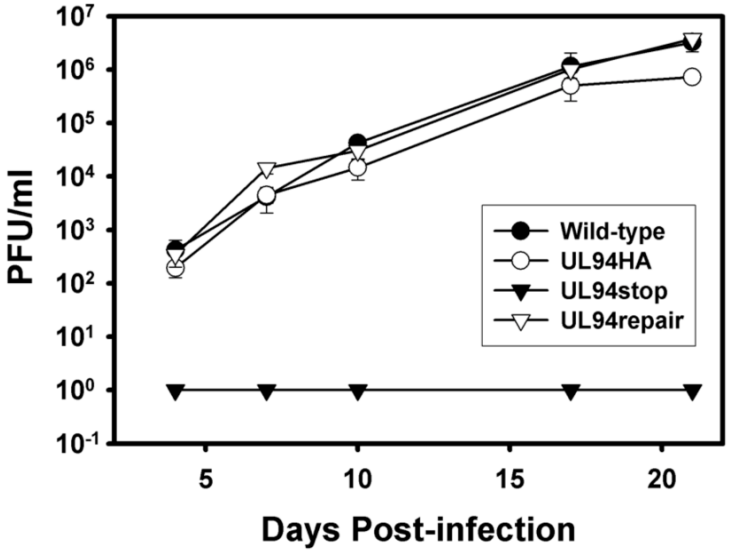

Figure 4-7. **The UL94stop mutant is completely defective for replication.** HFF cells were infected with the indicated viruses at a multiplicity of 0.01 PFU/cell. Total virus (cells and supernatant) was harvested on the indicated days post-infection. Harvested virus was titered by plaque assay on HAUL94 complementing cells.

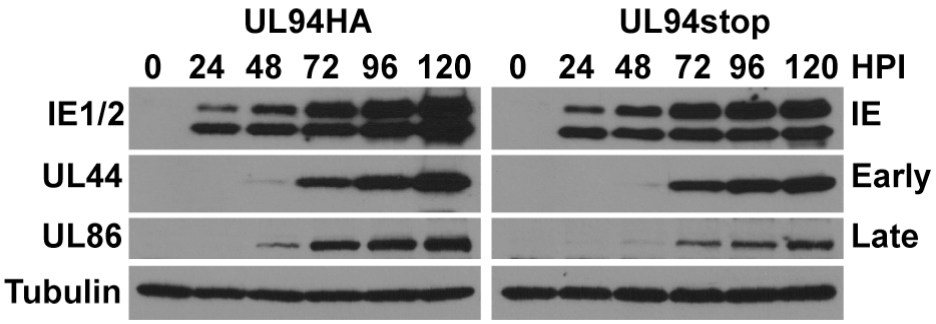

Figure 4-8. **UL94 is not required for viral gene expression.** HFF cells were infected with UL94HA virus or UL94stop virus at a multiplicity of 0.01 PFU/cell and total protein was harvested at the indicated times post-infection. Viral proteins were analyzed by Western blot with the indicated antibodies.

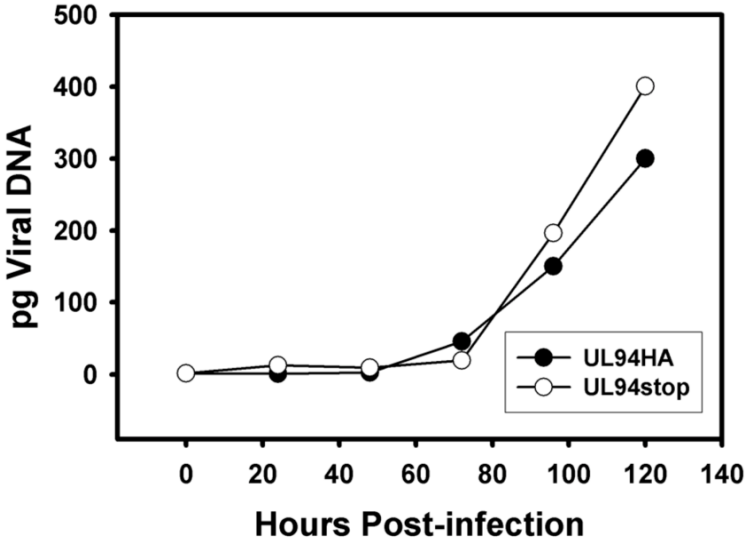

Figure 4-9. **UL94 is not required for viral genome replication.** HFF cells were infected with UL94HA virus or UL94stop virus at a multiplicity of 0.01 PFU/cell and total DNA was harvested at the indicated times post-infection. Accumulation of viral DNA was analyzed by qPCR. Results were normalized for both input DNA and variations in DNA levels introduced during the purification process. Picograms of viral DNA present in each sample were calculated from a standard curve prepared from purified viral DNA of a known concentration.

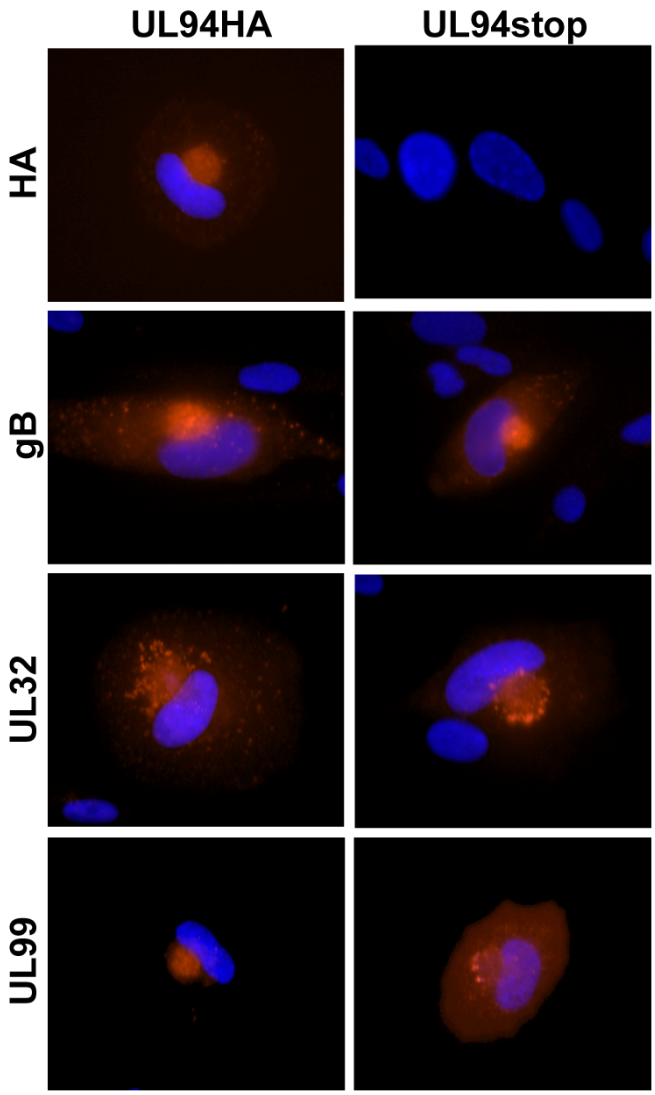

Figure 4-10. **UL94 directs the proper localization of UL94 to the assembly complex.** HFF cells were infected with UL94HA virus or UL94stop virus at a multiplicity of 0.01 PFU/cell. Cells were fixed 120 hours post-infection and immunofluorescence analysis was performed with the indicated antibodies to visualize viral proteins. Proteins were visualized using an Alexa546-conjugated secondary antibody (red). Nuclei are stained with Hoechst (blue).

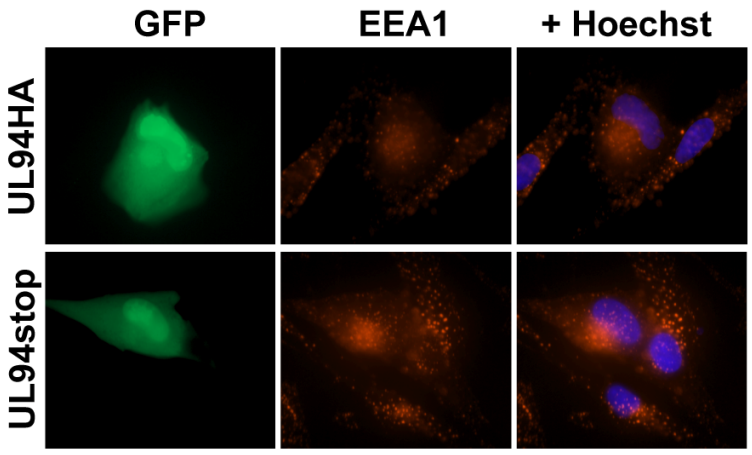

Figure 4-11. **UL94 is not required for the reorganization of EEA1.** HFF cells were infected with UL94HA virus or UL94stop virus at a multiplicity of 0.01 PFU/cell. Cells were fixed 120 hours post-infection and immunofluorescence analysis was performed with the indicated antibodies to visualize cellular EEA1, a marker of early endosomes. EEA1 was visualized using an Alexa546-conjugated secondary antibody (red). Nuclei are stained with Hoechst (blue). Infected cells are indicated by GFP expression from viral genome.

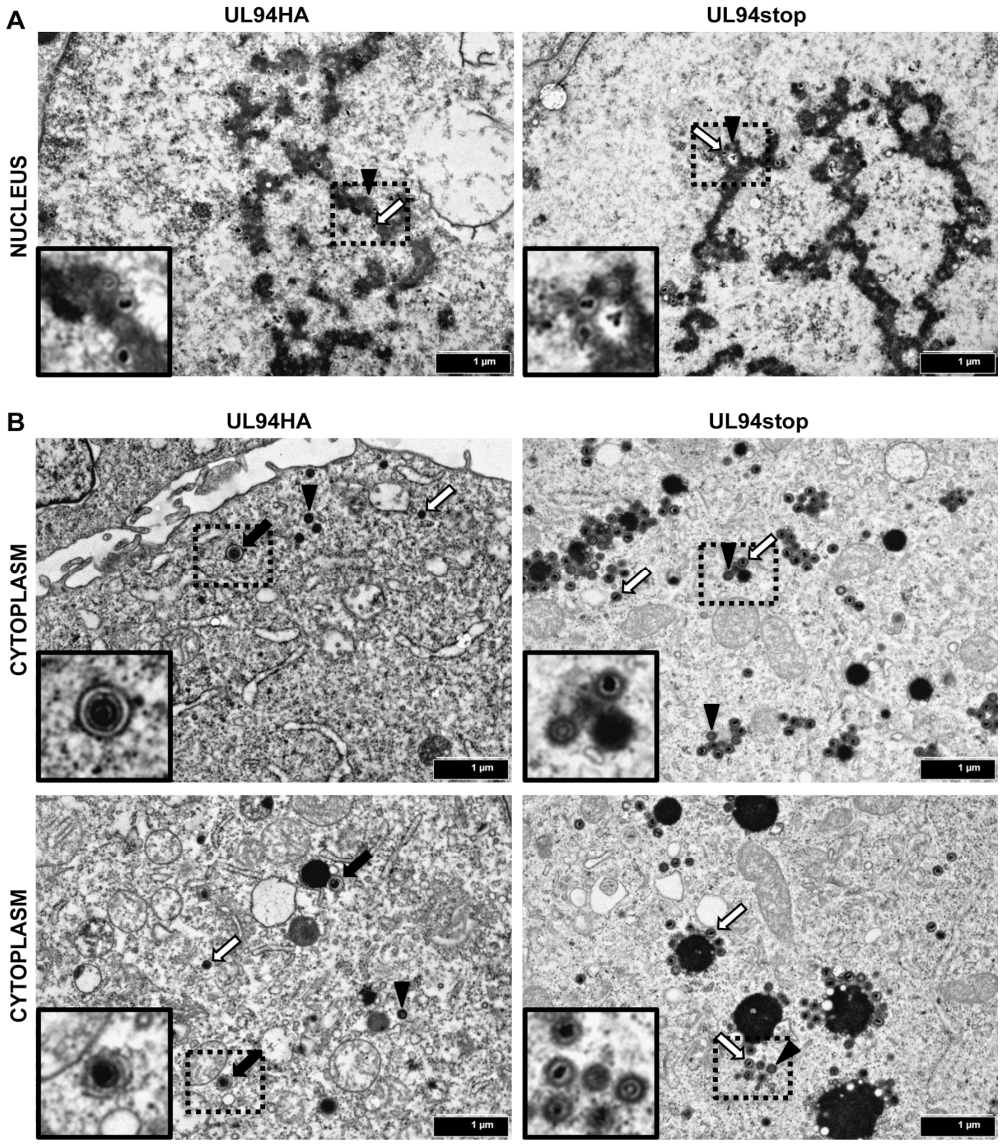

Figure 4-12. **UL94 is required for secondary envelopment.** HFF cells were infected with UL94HA or UL94stop virus at a multiplicity of 0.01 PFU/cell. Cells were fixed and processed for TEM 120 hours post-infection. Representative infected cell nuclear **(A)** or cytoplasmic **(B)** regions are shown. Black arrows indicate enveloped virions. White arrows indicate DNA-containing capsids. Black arrowheads indicate empty capsids. Images were taken at a final magnification of X20,000. Insets show magnified regions containing enveloped, empty, and DNA-containing capsids.

CHAPTER 5

THE INTERACTION BETWEEN UL94 AND UL99 IS ESSENTIAL FOR HCMV REPLICATION

Introduction

We and others have reported an interaction between the tegument proteins UL94 and UL99 (56, 75, 111). We demonstrated in Chapter 3 that this interaction occurs during infection as well as in the absence of other viral proteins. UL94 and UL99 are herpesvirus core genes that are conserved among all members of the herpesvirus family. In addition to their conservation at the genetic level, the interaction between UL94 and UL99 homologs also appears to be conserved (29, 114). This high level of evolutionary conservation suggests that the interaction between these tegument proteins plays an important role in viral replication. However, it should be noted that some UL94 and UL99 homologs are not essential for the replication of other herpesviruses in cell culture (7, 8, 85) whereas deletion of UL94 or UL99 results in a complete block in HCMV replication at the stage of secondary envelopment (76, 98). Therefore, it is likely that the function(s) of UL94 and UL99 are different or non-redundant during HCMV replication compared to their homologs in other herpesviruses.

UL99 is essential for final envelopment of virions in the cytoplasm. In the absence of UL99, early events of virus replication including viral gene expression and DNA replication proceed normally. However, late in infection, partially tegumented, non-enveloped, DNA-containing nucleocapsids accumulate in the cytoplasm (98). Thus a UL99-deletion mutant is incapable of producing infectious extracellular virus. We showed in Chapter 4 that the phenotype of a UL94-null virus is virtually identical to that of previously characterized UL99-deletion mutants (76).

In addition to the absence of enveloped virions in the cytoplasm, we also demonstrated that UL99 exhibits aberrant localization in the absence of UL94 expression (Figure 4-10). This observation is consistent with the results of a previous study showing that the proper localization of UL99 to the AC during infection requires the function of another viral late gene (96). Based on these

data, we hypothesize that the interaction between UL94 and UL99 is essential for the proper localization of UL99 to the AC and thus for HCMV replication.

To test this hypothesis, the amino acid residues of both UL94 and UL99 that are involved in their interaction were identified through mutagenesis of each protein. Mutations in either UL94 or UL99 that were found to abolish their interaction were then incorporated into the viral genome. The resulting mutant viruses were completely defective for replication. Further phenotypic analysis of these mutants indicated that both UL94 and UL99 exhibited aberrant localization and did not accumulate at the AC in the absence of their interaction. Taken together, these data suggest that the interaction between UL94 and UL99 is essential for the proper localization of UL94 and UL99 to the AC and for HCMV replication.

Results

***UL94 and UL99 alter each other's localization*.** We showed in Chapter 4 that like UL99, UL94 exhibits a different pattern of localization in infected cells when compared to the localization observed when UL94 is expressed in the absence of other viral proteins (Figure 4-4) (76, 89). We sought to determine whether UL94 and UL99 influence each other's subcellular localization in the absence of other viral proteins. HFF cells were transfected with plasmid vectors expressing HA-tagged UL94, UL99, or both. Cells were fixed and stained for immunofluorescence analysis 48 hours post-transfection. As shown in Fig. 5-1, when UL94 was expressed alone we observed a diffuse pattern of localization throughout both the nucleus and cytoplasm of the transfected cell as previously described (Fig. 5-1, top row) (76). When UL99 was transfected alone, UL99 protein was observed throughout the cytoplasm with an irregular punctate appearance, likely due to its association with cytoplasmic membranes of the endoplasmic reticulum-Golgi intermediate compartment (ERGIC) as previously described, (Fig. 5-1, middle row) (96). In contrast, when UL94 and UL99 were expressed together, the subcellular localization of UL94 and UL99 were

dramatically altered in that UL94 protein was largely excluded from the nucleus and both proteins displayed an identical perinuclear pattern of localization (Fig. 5-1, bottom row). These data demonstrate that UL94 and UL99 alter each other's localization in the absence of other viral proteins.

***UL94 protein is stabilized in the presence of UL99*.** In cells co-transfected with UL94 and UL99, we routinely observe a modest but reproducible increase in the levels of UL94 protein when compared to the levels of UL94 observed when transfected alone (Fig. 5-2 cell lysates, compare lanes 2 and 3). In contrast, UL99 is present in equal amounts regardless of the presence of UL94 (data not shown). This led us to hypothesize that UL99 stabilizes UL94.

To test this hypothesis, we first sought to determine whether UL99 expression leads to an increase in UL94 protein levels in a dose-dependent manner. Cells were co-transfected with a static amount of HAUL94 expression plasmid and increasing amounts of FLAGUL99 expression plasmid as indicated. Total protein was harvested 48 hours post-transfection and analyzed by Western blot. As shown in Fig. 5-3, we observed an increase in the levels of UL94 protein that positively correlates with the increasing amount of UL99 transfected. Tubulin is shown as a loading control to ensure that equal amounts of cell lysates were analyzed.

This increase in the levels of UL94 observed upon co-transfection with increasing amounts of UL99 led us to predict that the half-life of UL94 protein may be extended in the presence of UL99. To assess whether UL99 influences the half-life of UL94 protein, cells were co-transfected with equal amounts of HAUL94 and FLAGUL99 expression plasmid. Cycloheximide was added to the culture medium 48 hours post-transfection to inhibit new protein synthesis. Total protein was harvested at the indicated times post-cycloheximide treatment and analyzed by Western blot. We observed that in the absence of UL99, levels of UL94 protein were rapidly reduced upon the inhibition of new protein synthesis (Fig. 5-4, left). In contrast, in the presence of UL99, UL94 levels remained

constant and were significantly higher than those observed when UL94 is expressed alone (Fig. 5-4, right). Taken together, the data shown in Fig. 5-4 suggest that UL94 protein is stabilized by UL99.

Finally, to elucidate the mechanism by which UL94 degradation occurs in the absence of UL99, we investigated whether UL94 levels could be restored in the presence of cycloheximide by proteasome inhibition. Cells were transfected with HAUL94 and FLAGUL99 plasmids as indicated and treated with cycloheximide with or without the proteasome inhibitor MG132. Total protein was harvested 9 hours post-treatment and analyzed by Western blot. Inhibition of proteasome activity resulted in a restoration of UL94 levels to those observed in untreated cells (Fig. 5-5, compare lanes 1 and 3). Taken together, the data shown in Figure 5-5 suggest that UL94 protein is stabilized by UL99 in a proteasome-dependent manner.

Conserved cysteine residues of UL94 are involved in binding UL99**.** To investigate the functional significance of the interaction between UL94 and UL99, we first sought to identify the amino acids of both UL94 and UL99 that are required for their binding. We started by constructing a panel of UL94-truncation mutants through step-wise deletions from both the N and C-terminus of the 345 amino acid UL94 protein. These truncations were then tested for their ability to bind UL99 in a yeast two-hybrid assay. We found that all truncations of UL94 protein completely abolished the ability of UL94 to bind UL99 in the yeast two-hybrid assay (data not shown). Next we analyzed the expression of the UL94 truncation mutants in transfected cells to assess the expression levels of truncated forms of UL94 protein. We were unable to detect appreciable levels of any of the truncated forms of UL94 by Western blot analysis (data not shown). These results suggest that UL94 is sensitive to mutation in that the full length of UL94 protein may be required for the proper expression and stability of the

protein and are consistent with other reports attempting mutagenesis of UL94 or its HSV-1 homolog UL16 (37, 56, 123).

As a herpesvirus core gene, UL94 is conserved among all members of the herpesvirus family and alignment of UL94 with its homologs reveals the presence of several conserved amino acid residues in the C-terminus of the protein (119). We predicted that due to the conservation of the interaction between UL94 and UL99 homologs in other herpesviruses, the interaction between UL94 and UL99 may involve these conserved residues. Therefore, we mutated several cysteine residues that are conserved among UL94 homologs and have been shown to be important for binding of the HSV-1 homologs UL16 and UL11 (123). The amino acid sequence of UL94 that encompasses the conserved cysteine residues is shown in alignment with the sequence of selected UL94 homologs in Fig. 5-6A. The cysteines mutated for our mapping studies are highlighted. Each of the conserved cysteine residues was mutated to alanine using site-directed mutagenesis. As a control, we also mutated the cysteine residue at amino acid position 204 as it is not conserved among the UL94 homologs. We then tested these mutants for their ability to bind UL99 in the yeast two-hybrid assay (Fig. 5-7A). We found that all of the cysteine mutants retained their ability to bind UL99 with the exception of the C250A mutant. We also observed a moderate but reproducible decrease in the growth of yeast cells expressing the C252A mutant when plated on selective medium, suggesting that this mutation may cause a decrease in UL99 binding and thus a reduction in the activation of the *HIS3* reporter gene necessary for growth on plates lacking histidine.

To verify the results of the yeast two-hybrid assay, we analyzed the ability of the UL94 cysteine mutants to bind UL99 by co-immunoprecipitation from transfected cells. Due to the apparent sensitivity of UL94 to mutation, we first sought to determine whether the cysteine mutations affected the levels of UL94 expression. Cells were transfected with plasmids expressing wild type or mutant HAUL94 as indicated. Total protein was harvested 48 hours post-transfection for Western blot analysis. As shown in Fig. 5-6B, the mutation of the cysteines at

positions 200 and 204 had little effect on the levels of UL94 expression compared to wild type UL94 (Fig. 5-6B left, lanes 1-3). In contrast, the remaining cysteine mutations at amino acid positions 227, 250, 252, and 256 each resulted in a decrease in the level of UL94 expression compared to wild type (Fig. 5-6B left, lanes 4-7). We next asked whether the level of mutant forms of UL94 could be increased by co-transfection of UL99 as observed with wild type UL94. Cells were co-transfected with equal amounts of plasmids expressing wild type or mutant HAUL94 with FLAGUL99 and the levels of UL94 were determined by Western blot analysis 48 hours post-transfection. As shown in Fig. 5-6B, we observed a significant increase in the levels of the UL94 C227A and C256A mutants in the presence of UL99 (Fig. 5-6B, lanes 4 and 7 compare left and right panels). In contrast, we observed only a modest increase in the levels of UL94 in cells transfected with the UL94 C250A and C252A mutants in the presence of UL99 (Fig. 5-6B, lanes 5 and 6 compare left and right panels). Interestingly, the C227A and C256A mutants that appear to be stabilized by UL99 are those that also retained their ability to bind UL99 in the yeast two-hybrid assay. Conversely, the UL94 C250A and C252A mutants that exhibit little stabilization by UL99 also exhibit no or significantly reduced binding to UL99 in the yeast two-hybrid assay (Fig. 5-7A). These results suggest that stabilization of UL94 by UL99 requires their interaction and that mutant forms of UL94 that are unable to bind UL99 also show a defect in expression levels.

To confirm the results of the yeast two-hybrid assay, we assayed each of the UL94 cysteine mutants for its ability to bind UL99 by co-immunoprecipitation. As shown in the top panel of Fig. 5-7B, we observed significant levels of UL94 immunoprecipitation with UL99 in cells transfected with wild type, C200A, C204A, C227A, and C256A UL94. We were also able to detect UL94 in the immunoprecipitate of cells transfected with the C252A mutant, however the level was dramatically reduced compared to that of wild type UL94 (Fig. 5-7B, lane 7). We did not observe detectable levels of the UL94 C250A mutant in the

immunoprecipitate (Fig. 5-7B, lane 6), however the level of the C250A mutant present in the cell lysate was also reduced compared to wild type UL94.

To determine whether the absence of an interaction between UL94 C250A and UL99 resulted from the low level of UL94 expression, we treated transfected cells with MG132 to increase the levels of the UL94 C250A protein in the cell lysate. Co-immunoprecipitation was performed as described above and levels of UL94 C250A bound to UL99 were determined by Western blot analysis. We found that while UL94 C250A is stabilized under conditions of proteasome inhibition (Fig. 5-8, cell lysates, lane 4), we are still unable to detect appreciable amounts of UL94 C250A in the immunoprecipitate.

Taken together, these results are consistent with the results of the yeast two-hybrid analysis and demonstrate that the cysteine residues at amino acid position 250 and 252 of UL94 are likely involved in binding UL99. These results are also consistent with mutational analysis of HSV-1 UL16 that showed that these same cysteines are required for binding UL11 (123). Based on the combination of the yeast two-hybrid and co-immunoprecipitation results, we chose the UL94 C250A mutant for analysis of the interaction between UL94 and UL99 in the context of infection.

***UL99 amino acids 37-39 are required for binding UL94*.** In addition to identifying amino acids in UL94 that are required for the interaction with UL99, we also sought to map the interaction with respect to the amino acid residues of UL99 that are required for binding UL94. UL99 is a 190 amino acid myristoylated tegument protein. Several mutational analyses have been performed to identify the domains of UL99 that are necessary and sufficient for its essential function. Generation of C-terminal UL99 truncations in the context of the viral genome demonstrated that the N-terminal 57 amino acids of UL99 are necessary and sufficient for both wild type virus replication and incorporation of UL99 into virions (42, 96). Later studies confirmed these results and further defined an essential region of UL99 between amino acids 34 and 43. Mutant viruses lacking this

essential region are completely defective for replication and exhibit defects in the trafficking of UL99 to the AC and in its retention there. These defects ultimately result in the absence of virion envelopment and thus the production of infectious progeny (93, 95, 96).

Based on these previous studies, we began our mutational analysis of UL99 by assaying a panel of UL99 C-terminal truncation mutants for their ability to bind UL94 in the yeast two-hybrid assay. We generated constructs expressing the first 123, 90, 61, and 33 amino acids of UL99, as these mutants have been previously tested for their ability to support virus replication (96). In addition we tested two internal deletion mutants lacking amino acids 26-33 or 26-43 of UL99. As shown in Fig. 5-9A, the first 61 amino acids of UL99 were sufficient for binding UL94, whereas a truncation containing only the first 33 amino acids of UL99 did not bind UL94. In addition, while deletion of amino acids 26-33 did not affect the ability of UL99 to bind UL94, extending the deletion to encompass amino acids 26-43 completely abolished binding to UL94. The results obtained from the yeast two-hybrid analysis were confirmed by co-immunoprecipitation analysis from transfected cells (data not shown). Taken together these results suggest that the region of UL99 required for binding UL94 is located between amino acids 34-43 and support the hypothesis that the interaction between UL94 and UL99 is essential for virus replication, as mutant forms of UL99 that are incapable of supporting virus replication (UL99 1-33 and UL99 Δ26-43) are also defective for binding UL94.

We next wanted to confirm the yeast two-hybrid results as well as further define the amino acids of UL99 that are critical for binding UL94. We therefore constructed three additional internal deletions spanning the region from amino acids 34-43. We then analyzed the ability of these UL99 internal deletion mutants to bind UL94 by co-immunoprecipitation from transfected cells. As shown in the top panel of Fig. 5-9B, we were able to detect binding of UL99 Δ26-33 to UL94, similar to the levels observed with wild type UL99 (Fig. 5-9B, lanes 2 and 3). In contrast, we observed no binding between UL99 Δ26-43 and UL94 (Fig. 5-9B,

lane 4), confirming the results of the yeast two-hybrid assay. We also demonstrated that deletion of amino acids 37-39 completely abolished binding of UL99 to UL94, whereas deletion of the amino acids directly adjacent to these residues had no effect on binding (Fig. 5-9B, lanes 5-7). Analysis of the levels of UL94 in the lysates of cells co-transfected with these UL99 mutants further demonstrated that in the absence of the interaction between UL94 and UL99, there is a decrease in the level of UL94 expression (Fig. 5-9B, UL94 cell lysates, lanes 4 and 6). In contrast, UL99 Δ26-43 and UL99 Δ37-39 are expressed at levels equal to or greater than wild type UL99, suggesting that UL94 does not stabilize UL99.

These results demonstrate that amino acids 37-39 of UL99 are essential for the interaction between UL99 and UL94. We therefore chose the UL99 Δ37-39 mutation to further investigate the functional significance of the interaction between UL94 and UL99 in the context of infection.

***Mutations that abolish the interaction between UL94 and UL99 also prevent virus replication*.** The ultimate goal of our mapping studies was to identify mutations that abolish the interaction between UL94 and UL99 to then investigate the functional relevance of those mutations in the context of viral infection. To this end, we generated recombinant bacterial artificial chromosome (BAC) constructs incorporating the UL94 C250A mutation and the UL99 Δ37-39 mutations into the HCMV genome. In addition, we generated control constructs carrying the UL94 C204A and UL99 Δ40-43 mutations, neither of which has any effect on the interaction between UL94 and UL99. As additional controls, the UL94 C250A and UL99 Δ37-39 mutations were repaired to confirm the absence of secondary mutations elsewhere in the genome. The BAC constructs generated and the relative locations of the mutations inserted are depicted in Fig. 5-10A and 5-11A. Recombinant BACs were generated using the UL94HA ADCREGFP parental BAC (75) as described in materials and methods.

Generation of the desired recombinant BAC was verified by restriction digestion, PCR, and direct sequencing of BAC DNA (data not shown). To assess the production of replication competent virus, HFF cells were co-transfected with BAC DNA and pp71 expression plasmid. Generation of infectious virus was monitored by cytopathic effect and GFP expression from the viral genome.

Visual analysis of GFP expression in cells transfected with UL94 C250A BAC DNA showed the presence of single GFP-positive cells representing those that were initially transfected with BAC DNA, however we did not observe any subsequent spread of GFP expression to other cells in the culture. This result suggests that the UL94 C250A mutant is completely defective for viral growth. HFF cells transfected with the UL94 C204A control mutant and the UL94 C250A repair BAC exhibited significant CPE as well as spread of GFP expression indistinguishable from that observed in cells transfected with the UL94HA parental BAC (data not shown), suggesting that these constructs are competent for virus replication. Because the UL94 C250A mutation results in a block in virus replication, we used a previously described UL94 complementation system to generate stocks of this mutant for further analysis (76). UL94 C250A BAC DNA was transfected into HAUL94 complementing HFF cells. Virus was harvested when cells exhibited 100% cytopathic effect and then titered on complementing cells. The resulting UL94 C250A mutant virus grew slowly and to low titers (~10^4 PFU/ml), similar to the previously described UL94-null virus (76).

UL94HA (76), UL94 C204A, UL94 C250A, and UL94 C250A repair viruses were then used to infect HFF cells at a multiplicity of 0.01 PFU/cell to measure the levels of replication for each mutant. Total progeny virus from both cells and supernatant were harvested from infected cells 21 days post-infection and titered on HAUL94 complementing cells. Fig. 5-10B shows that while UL94HA, UL94 C204A, and UL94 C250A repair viruses replicated to similar titers by 21 days post-infection, the UL94 C250A mutant did not produce any infectious progeny virus. These results demonstrate that the cysteine residue at amino acid position 250 of UL94 is essential for virus replication.

Because the C250A mutation results in a decrease in UL94 expression levels in transfected cells, we also sought to determine the levels of UL94 expression in cells infected with the UL94 C250A mutant virus. HFF cells were infected at a multiplicity of 0.05 PFU/cell with either the UL94 C250A or UL94 C250A repair virus and total protein was harvested at 96 hours post-infection for Western blot analysis. As shown in Figure 5-10C, we observed comparable levels of both immediate early genes and UL99 in cells infected with the UL94 C250A mutant or the UL94 C250A repair virus, suggesting the C250A mutation does not affect the initiation of infection or the expression of viral late genes. Consistent with the results of our transfection studies, there is a decrease in the levels of UL94 C250A compared to wild type UL94, indicating that this mutation also affects the stability of UL94 in the context of infection. However, we are able to detect appreciable amounts of UL94 C250A protein, suggesting that the absolute growth defect observed with the UL94 C250A mutant virus is not likely due to a complete absence of UL94 expression.

We also generated several recombinant BAC constructs carrying mutations in the UL99 ORF to investigate the significance of the interaction between UL94 and UL99 during infection (Fig. 5-11). Transfection of HFF cells with the UL99 Δ37-39 mutant indicated that this mutation causes a complete inhibition of viral growth, as evidenced by the appearance of single GFP-positive cells with the absence of subsequent spread of infection. In contrast, cells transfected with the UL99 Δ40-43 or the UL99 Δ37-39 repair BAC produced infectious virus to levels similar to the parental UL94HA BAC (data not shown). Our ability to recover infectious virus from the UL99 mutant BAC transfected cells is summarized in Fig. 5-11B. Despite repeated attempts to complement the growth defect of the UL99 Δ37-39 mutant using HFF cells expressing wild type UL99 from a retroviral vector, we were unable to generate any infectious virus containing the UL99 Δ37-39 mutation for further analysis. Nonetheless, the results of our BAC transfections strongly suggest that amino acids 37-39 of UL99

are required for virus replication as well as for the interaction between UL94 and UL99.

***Proper localization of UL94 and UL99 during infection requires their interaction*.** We previously demonstrated that UL99 exhibits aberrant subcellular localization during infection in the absence of UL94 (76). Based on those results and the observation that UL94 and UL99 are capable of altering each other's localization in transfected cells, we hypothesized that the proper localization of both proteins during the course of infection is dependent on their ability to interact. To test this hypothesis, we sought to determine the subcellular localization of UL94 and UL99 in cells infected with viruses containing mutations that abolish their interaction.

Because we have a complementation system for propagating UL94 mutant viruses, we were able to assess the localization of UL94 and UL99 in the context of infection by directly infecting HFF cells with the virus generated from HAUL94 complementing cells. For immunofluorescence analysis of infected cells, HFF cells were infected with the UL94 C250A or control viruses at a multiplicity of 0.01 PFU/cell. These viruses were produced from the parental BAC ADCRE UL94HA, which does not express GFP, allowing for simultaneous immunofluorescent staining of both UL94 and UL99. Cells were fixed 96 hours post-infection and stained for UL94 and UL99 using α-HA and α-UL99 antibodies respectively. As shown in Fig. 5-12, during infection with the UL94HA virus, UL94 (green) and UL99 (red) both accumulated at the juxtanuclear AC as previously described (Fig. 5-12, top row) (76). Similar results were observed in cells infected with the UL94 C204A control mutant virus (Fig. 5-12, second row). In contrast, during infection with the UL94 C250A virus, both UL94 and UL99 exhibited largely diffuse localization throughout the cytoplasm and did not appear to accumulate to appreciable levels at the AC (Fig. 5-12, third row). When the UL94 C250A mutation was repaired, we observed a restoration of juxtanuclear localization for both UL94 and UL99 identical to that observed during infection

with the UL94HA virus (Fig. 5-12, bottom row). These results demonstrate that the cysteine residue at amino acid position 250 of UL94 is required for UL99 binding, virus replication, and the proper localization of both UL94 and UL99 to the AC during infection.

As mentioned previously, we were unable to complement the growth defect of the UL99 Δ37-39 mutant by providing UL99 *in trans*. We therefore assessed the localization of UL94 and UL99 in BAC transfected cells, a method that has been previously used to analyze the phenotype of mutants in the absence of sufficient complementation to generate virus stocks (4, 107, 117). UL99 mutations were inserted into the parental ADCRE UL94HA BAC that does not express GFP, allowing for simultaneous staining of UL94 and UL99 as described above. HFF cells were transfected with BAC DNA and fixed for immunofluorescence analysis 8 days post-transfection to allow for sufficient expression of viral late genes (4). Fixed cells were stained for UL94 and UL99 using α-HA and α-UL99 antibodies respectively.

In cells transfected with the UL94HA parental BAC, we observed the expected juxtanuclear localization of both UL94 and UL99 at the AC (Fig. 5-13, top row). A similar pattern of localization was observed in cells transfected with the UL99 Δ40-43 BAC (Fig. 5-13, second row) demonstrating that a mutation that does not affect the interaction between UL94 and UL99 also does not prevent their localization to the AC. In contrast, in cells transfected with the UL99 Δ37-39 BAC, both UL94 and UL99 exhibited diffuse cytoplasmic localization (Fig. 5-13, third row), suggesting that neither protein properly trafficked to the AC. Repairing the UL99 Δ37-39 mutation resulted in a restoration of the wild type pattern of localization for both UL94 and UL99 (Fig. 5-13, bottom row), demonstrating that the aberrant localization observed in cells transfected with the UL99 Δ37-39 BAC results specifically from the UL99 Δ37-39 mutation. These data suggest that amino acids 37-39 of UL99 are required for the interaction between UL94 and UL99, virus replication, and the proper localization of both UL94 and UL99 to the

AC in the context of infection. Taken together, the data presented here suggest that the interaction between UL94 and UL99 is required for HCMV replication, functioning at least in part by directing the proper localization of each protein to the AC.

Discussion

The mechanisms that facilitate the assembly of mature HCMV particles in the cytoplasm of infected cells are poorly understood. While the events that result in virion maturation remain largely undefined, many reports have demonstrated a crucial role for tegument proteins in virion assembly and morphogenesis. UL99 (pp28) is essential for secondary envelopment of virions in the cytoplasm. In the absence of UL99, partially tegumented but non-enveloped capsids accumulate in the cytoplasm of infected cells (98). Our previous characterization of the UL94-null mutant described in Chapter 4 demonstrated that the growth phenotype of HCMV in the absence of UL94 expression is virtually identical to that of a UL99-deletion mutant (76).

UL94 and UL99 physically interact in the absence of other viral proteins (56, 75, 111). We also demonstrated that this interaction occurs during late times in infection when progeny virus is being assembled and released from infected cells (Figure 3-5) (75). Further, the proper localization of UL99 to the AC in infected cells requires the expression of viral late genes (96). Based on these observations and the fact that deletion of either UL94 or UL99 results in an absolute defect in secondary envelopment, we hypothesized that the interaction between UL94 and UL99 is essential for HCMV replication at the stage of virion assembly.

Both UL94 and UL99 exhibit different patterns of localization in transfected cells compared to the localization observed during infection (76, 89). Therefore, we first investigated whether UL94 and UL99 are capable of altering each other's localization in the absence of other infected-cell proteins. Co-transfection of HFF cells with vectors expressing UL94 or UL99 demonstrated that the localization of

each protein was altered compared to that observed when both proteins are expressed together (Fig. 5-1). These results are consistent with the observation that UL99 exhibits aberrant localization in infected cells in the absence of UL94 (76), suggesting that the interaction between UL94 and UL99 is required for their proper localization during infection.

We repeatedly observed during the course of our immunoprecipitation analyses that the levels of UL94 detected by Western blot were reproducibly lower in the absence of UL99 expression (Fig. 5-2). We further demonstrate that UL99 is capable of effecting an increase in UL94 protein levels in a dose-dependent manner (Fig. 5-3), that the half-life of UL94 protein is extended in the presence of UL99 (Fig. 5-4), and that the degradation of UL94 in the absence of UL99 occurs in a proteasome-dependent manner (Fig. 5-5). In contrast, levels of UL99 remain unaffected by co-transfection with increasing amounts of UL94 (data not shown). Analysis of UL94 protein levels in cells transfected with mutant forms of either UL94 or UL99 that abolish their ability to interact demonstrates that this stabilization effect is dependent on their interaction (Fig. 5-6B and 5-7B). These results suggest that any mutation that disrupts the interaction between UL94 and UL99 will also result in a decrease in UL94 protein levels.

To assess the functional significance of the interaction between UL94 and UL99 during HCMV infection, we sought to identify the amino acids of each protein that are involved in their binding. Site-directed mutagenesis of conserved cysteine residues of UL94 demonstrated that the cysteine residue at amino acid position 250 is involved in UL99 binding (Fig. 5-6). Incorporation of this mutation into the viral genome revealed that C250 of UL94 is essential for virus replication as indicated by the complete inability of this mutant to generate infectious progeny (Fig. 58). Further, we observed that in cells infected with the UL94 C250A mutant virus, neither UL94 or UL99 appear to localize to the AC, and instead remain largely diffuse throughout the cytoplasm (Fig. 5-10). Taken together, these results suggest that amino acid C250 of UL94 is required for the interaction between UL94 and UL99, for the proper localization of each protein to

the AC, and for virus replication. In addition to disrupting the interaction between UL94 and UL99, mutation of UL94 C250 also resulted in a decrease in UL94 expression that could not be restored by co-expression of UL99 (Fig. 5-5B). Therefore, caution must be taken when interpreting the effect of the UL94 C250A mutation on virus replication. While our results with the UL94 C250A mutant are consistent with the hypothesis that the interaction between UL94 and UL99 is essential for virus replication, we cannot rule out the possibility that the growth defect observed is due to decreased levels of UL94 expression in cells infected with the UL94 C250A mutant. However, we were able to detect UL94 during infection with the UL94 C250A mutant virus by immunofluorescence and Western blot analysis (Fig. 5-10C and 5-12). Further, the observation that UL94 is stabilized in the presence of UL99 and that this stabilization requires their interaction, along with the results of the UL99 mapping studies, strongly suggest that the interaction between UL94 and UL99 is required for virus replication.

Our mapping studies also led to the identification of amino acids 37-39 of UL99 as the region involved in binding UL94 (Fig. 5-7). These amino acids are part of a region that has previously been demonstrated to be essential for UL99 function and thus for virus replication (96). Deletion of UL99 amino acids 37-39 in the context of the viral genome resulted in a complete inhibition of the production of infectious virus (Fig. 5-9). Further, immunofluorescence analysis of UL94 and UL99 in cells transfected with the UL99 Δ37-39 mutant genome demonstrated that both proteins are aberrantly localized compared to the pattern of localization observed in cells transfected with the UL94HA or control BAC (Fig. 5-11). Taken together, these data further support the hypothesis that the interaction between UL94 and UL99 is essential for HCMV replication.

A previous report demonstrated that UL99 multimerizes in both transfected and infected cells and is detected in a predominantly dimeric form by non-denaturing gel electrophoresis and sedimentation analysis (95). Mutagenesis carried out to map the amino acids required for the UL99 self-interaction showed that amino acids 34-43 of UL99 are important, but not

essential for its dimerization. Fluorescence resonance energy transfer (FRET) analysis was used to demonstrate that UL99 multimerization occurs only after its localization to the AC (95). Given the possibility of temporal differences in the association of UL99 with UL94 and with itself, essential roles for UL99 multimerization and for the interaction between UL94 and UL99 during infection are not mutually exclusive. For example, it is possible that the interaction between UL94 and UL99 occurs first and is responsible for trafficking UL99 to the AC. Once there, UL94 may dissociate from the region of UL99 encompassing amino acids 37-39, allowing for UL99 multimerization. Further studies would be necessary to elucidate the individual roles of the UL94-UL99 interaction and the multimerization of UL99 in the proper assembly of virions.

Based on our results, it appears that the interaction between UL94 and UL99 is required for each protein to traffic to the AC during infection. Analysis of the sequence requirements for trafficking of UL99 to the AC demonstrated that at steady-state late in infection (>6 days post-infection), only those forms of UL99 containing at least the first 50 amino acids were detected at the AC (96). Further, the localization of UL99 to the AC required a late viral gene product as evidenced by a defect in UL99 trafficking in the presence of a viral DNA-synthesis inhibitor (96). Phenotypic analysis of UL99 mutant viruses demonstrated that the localization of UL99 to the AC is required for secondary envelopment of virions (93). Therefore, we propose a model in which the interaction between UL94 and UL99 results in the localization of UL99 to the AC and in its retention there, likely through additional interactions of the UL94-UL99 complex with other yet to be identified proteins. Further studies are currently underway to identify additional binding partners of UL94 and UL99 and to elucidate the spatial and temporal relationships between viral and cellular protein interactions that are involved in the assembly and envelopment of infectious HCMV virions.

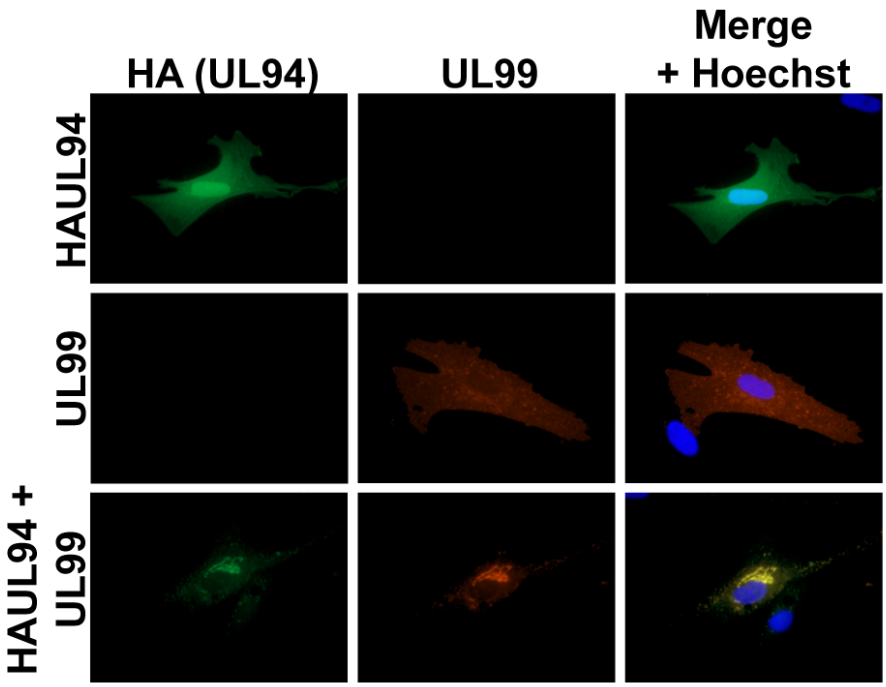

Figure 5-1. UL94 and UL99 alter each other's localization. HFF cells were transfected with plasmid DNA expressing HAUL94, UL99, or both. Cells were fixed and stained for immunofluorescence analysis 48 hours post-transfection. UL94 was detected with α-HA antibody (green). UL99 was detected with α-UL99 antibody (red). Nuclei are stained with Hoechst (blue).

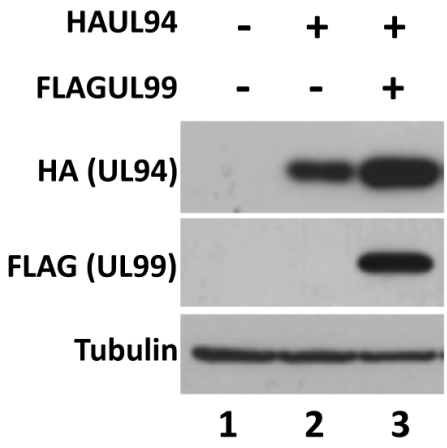

Figure 5-2. UL94 levels increase in the presence of UL99. 293T cells were transfected with 2 μg HAUL94 plasmid alone or with 2 μg FLAGUL99 plasmid as indicated. Total protein was harvested 48 hours post-transfection and Western blot was performed with α-HA or α-FLAG antibody to detect UL94 and UL99 respectively. Tubulin is shown as a loading control.

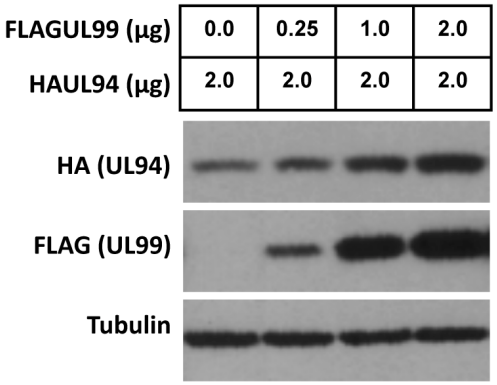

Figure 5-3. UL99 affects UL94 protein levels in a dose-dependent manner. 293T cells were co-transfected with the indicated amounts of plasmid DNA expressing HAUL94 and FLAGUL99 plasmids. Total protein was harvested 48 hours post-transfection and Western blot was performed with α-HA or α-FLAG antibody to detect UL94 and UL99 respectively. Tubulin is shown as a loading control.

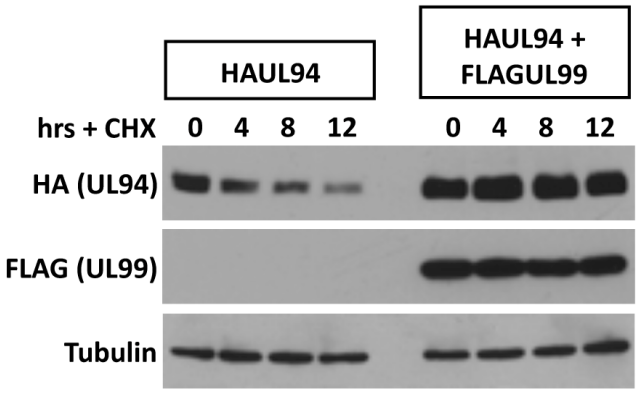

Figure 5-4. UL94 protein is stabilized in the presence of UL99. 293T cells were transfected with plasmid DNA expressing HAUL94 alone or co-transfected with FLAGUL99 as indicated. Cells were treated with cycloheximide (CHX) 48 hours post-transfection. Total protein was harvested at the indicated times after CHX treatment and Western blot was performed with α-HA or α-FLAG antibody to detect UL94 and UL99 respectively. Tubulin is shown as a loading control.

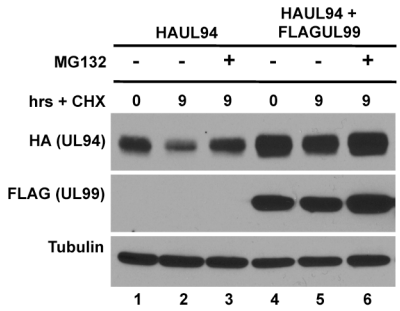

Figure 5-5. UL94 degradation is proteasome-dependent. 293T cells were transfected with plasmid DNA expressing HAUL94 alone or co-transfected with FLAGUL99 as indicated. Cells were treated with cycloheximide (CHX) 48 hours post-transfection with or without MG132 as indicated. Total protein was harvested at the indicated times after treatment and Western blot was performed with α-HA or α-FLAG antibody to detect UL94 and UL99 respectively. Tubulin is shown as a loading control.

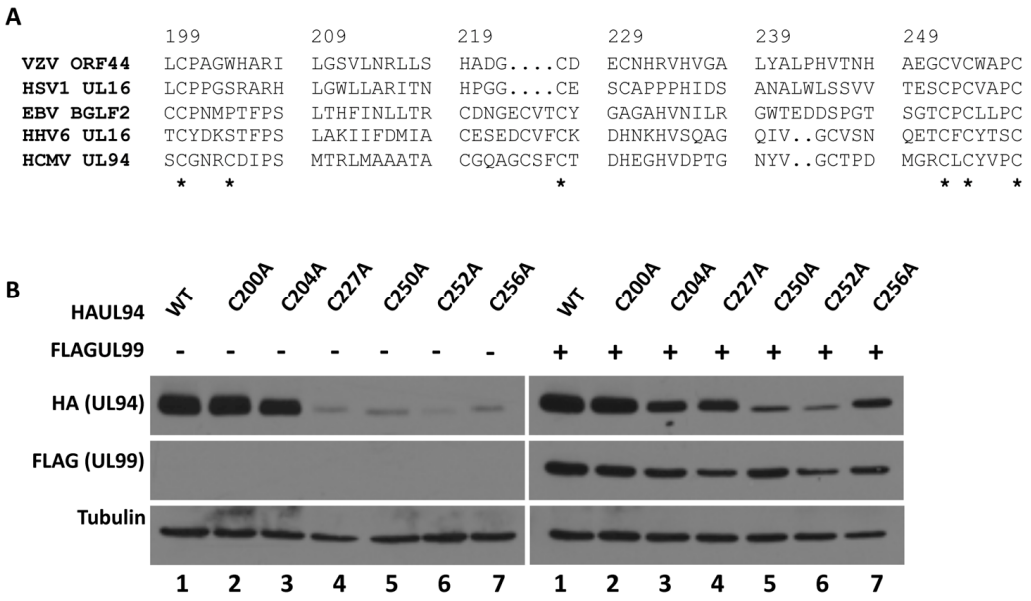

Figure 5-6. Generation of UL94 cysteine mutants. (A) Amino acid sequence alignment of residues 200-256 of HCMV UL94 with its homologs in varicella zoster (VZV), herpes simplex type-1 (HSV1), Epstein Barr virus (EBV), and human herpesvirus 6 (HHV6). Cysteine residues that were mutated to alanine for mapping studies are indicated with an asterisk. **(B)** 293T cells were transfected with plasmid DNA expressing the indicated HAUL94 alone (left) or with FLAGUL99 (right). Total protein was harvested 48 hours post-transfection and Western blot was performed with α-HA or α-FLAG antibody to detect UL94 and UL99 respectively. Tubulin is shown as a loading control.

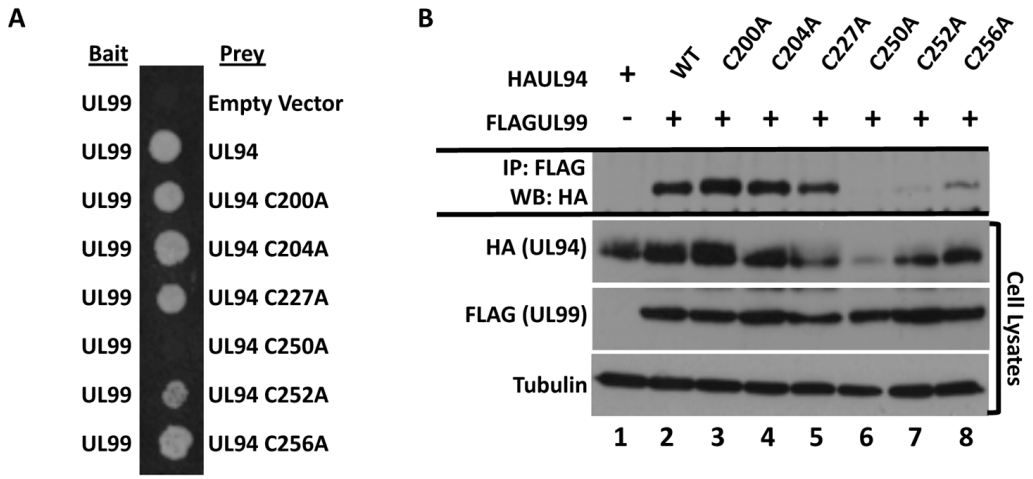

Figure 5-7. Mapping amino acids of UL94 involved in interaction with UL99. **(A)** MAV203 yeast cells were co-transformed with bait plasmid expressing wild type UL99 and prey plasmid expressing wild type UL94 or the indicated UL94 mutant. Interactions were assessed by growth of co-transformed cells on media lacking histidine. **(B)** 293T cells were co-transfected with plasmid DNA expressing the indicated HAUL94 and FLAGUL99. Total protein was harvested 48 hours post-transfection and immunoprecipitation was performed with α-FLAG antibody. Immune complexes were separated by SDS-PAGE and Western blot was performed with α-HA antibody.

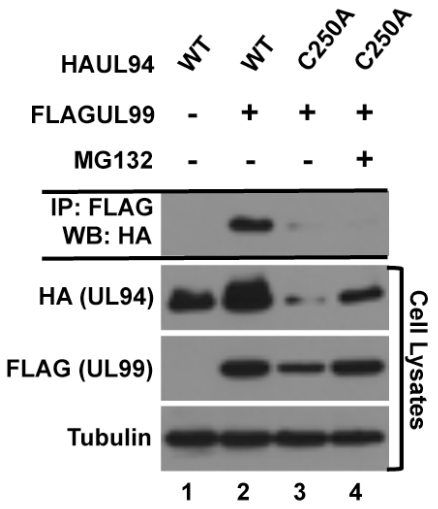

Figure 5-8. Amino acid C250 of UL94 is required for interaction with UL99. 293T cells were co-transfected with plasmid DNA expressing the indicated HAUL94 and FLAGUL99. Cells were treated with MG132 as indicated for 9 hours prior to protein harvest. Total protein was harvested 48 hours post-transfection and immunoprecipitation was performed with α-FLAG antibody. Immune complexes were separated by SDS-PAGE and Western blot was performed with α-HA antibody.

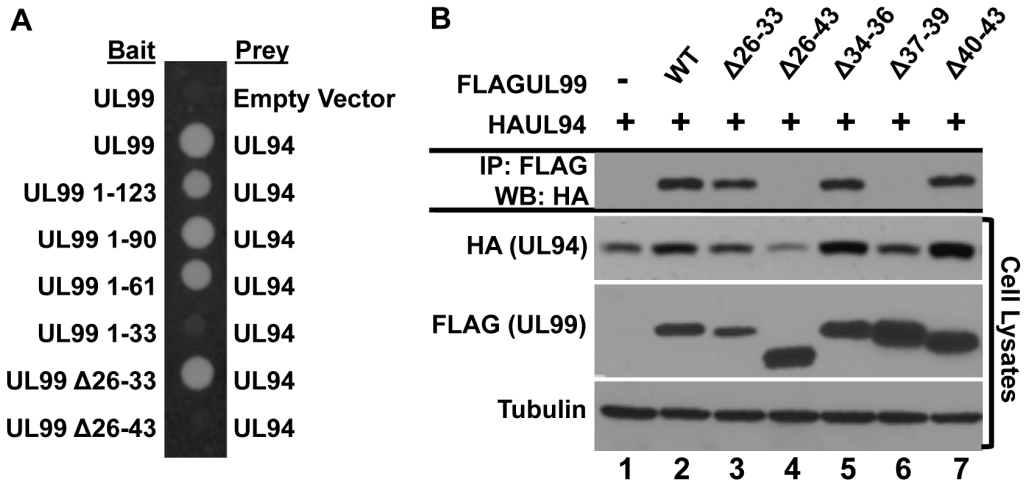

Figure 5-9. Mapping amino acids of UL99 involved in interaction with UL94. **(A)** MAV203 yeast cells were co-transformed with bait plasmid expressing wild type UL99 or the indicated UL99 mutant and prey plasmid expressing UL94. Interactions were assessed by growth of co-transformed cells on media lacking histidine. **(B)** 293T cells were co-transfected with plasmid DNA expressing HAUL94 and the indicated FLAGUL99. Total protein was harvested 48 hours post-transfection and immunoprecipitation was performed with α-FLAG antibody. Immune complexes were separated by SDS-PAGE and Western blot was performed with α-HA antibody.

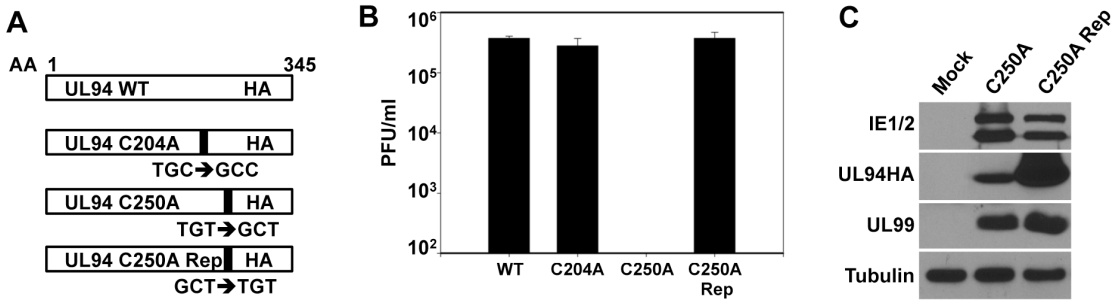

Figure 5-10. Generation of UL94 mutant viruses. (A) Nucleotide positions indicate the location of the UL94 ORF in the AD169 genome using GenBank accession number X17403. Nucleotide changes incorporated to change cysteine residues to alanine are indicated. **(B)** UL94 mutant virus stocks were generated from HAUL94 complementing HFF cells. Resulting virus was then used to infect non-complementing HFF cells at a multiplicity of 0.01 PFU/cell and total virus was harvested on day 21 post-infection. Progeny virus was titered on HAUL94 complementing cells. **(C)** HFF cells were infected at a multiplicity of 0.05 PFU/cell and total protein was harvested 120 hours post-infection. Levels of viral proteins were analyzed by Western blot.

A

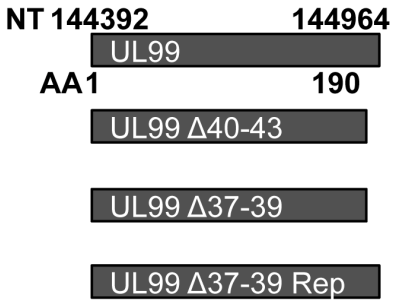

B

BAC	Virus Recovered
WT	+
UL99 Δ40-43	+
UL99 Δ37-39	-
UL99 Δ37-39 Rep	+

Figure 5-11. Generation of UL99 mutant viruses. (A) Nucleotide positions indicate the location of the UL99 ORF in the AD169 genome using GenBank accession number X17403. **(B)** UL99 mutant BAC were transfected into HFF cells and virus replication was monitored by cytopathic effect and GFP expression from the viral genome. Recovery of infectious virus from BAC transfected cells for each mutant is indicated.

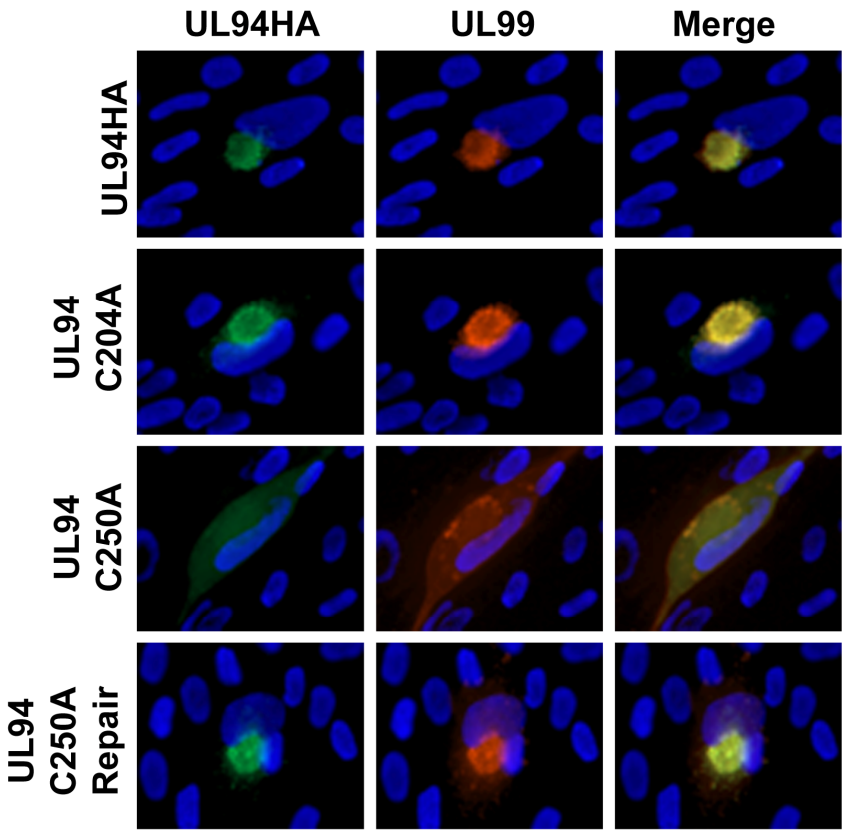

Figure 5-12. **Localization of UL94 and UL99 in infected cells.** HFF cells were infected with the indicated virus at a multiplicity of 0.01 PFU/cell. Cells were fixed 96 hours post-infection and immunofluorescence analysis was performed with the indicated antibodies to visualize viral proteins.

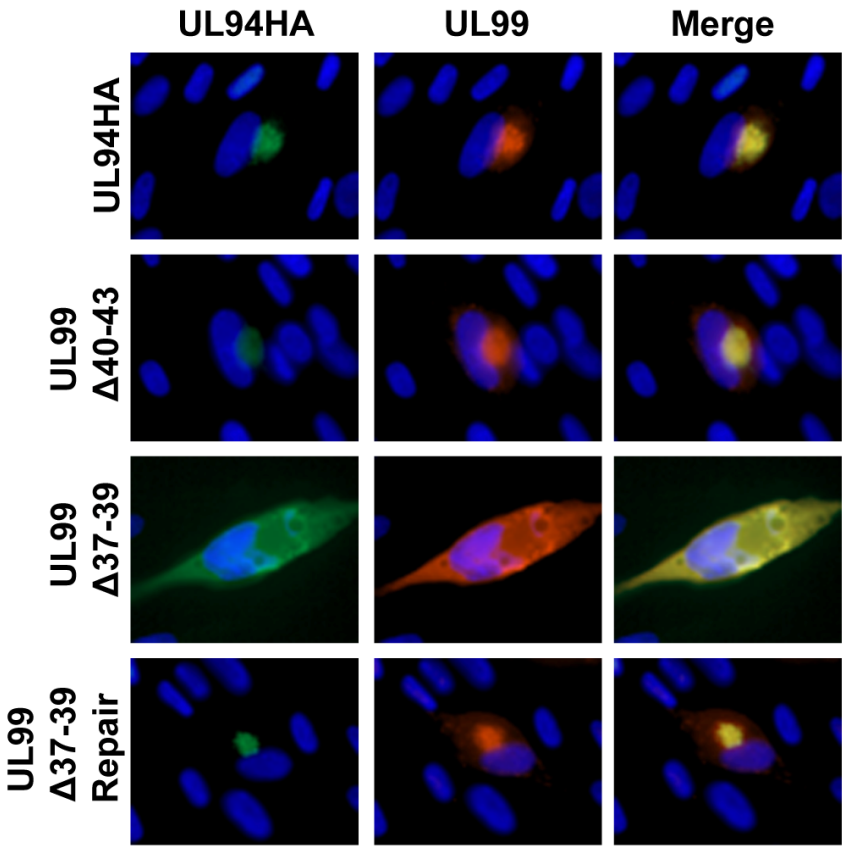

Figure 5-13. **Localization of UL94 and UL99 in BAC transfected cells.** HFF cells were transfected with the indicated BAC DNA. Cells were fixed 8 days post-transfection and immunofluorescence analysis was performed with the indicated antibodies to visualize viral proteins. UL94 was detected with α-HA antibody (green). UL99 was detected with α-UL99 antibody (red). Nuclei are stained with Hoechst (blue).

CHAPTER 6
SUMMARY AND FUTURE DIRECTIONS

Significance of protein interactions in virion assembly and structure

The overall goal of this work was to identify novel interactions among HCMV virion proteins and to investigate the functional significance of such interactions in the context of infection. This goal was based on the hypothesis that interactions between virion proteins are critical for viral replication and thus represent potential targets for novel antiviral therapeutics.

The first aim of this project was to identify candidate interactions between viral proteins for further investigation in the context of infection. To this end, we employed the yeast two-hybrid assay to identify binary interactions that occur among virally encoded proteins that are incorporated into the virus particle. We demonstrated several novel interactions among HCMV tegument proteins using both yeast two-hybrid and co-immunoprecipitation approaches. Importantly, we demonstrated that at least three of these novel interactions occur not only in transfected cells but also in the context of HCMV infection. Interactions that occur between viral proteins during infection may play important regulatory or structural roles in HCMV replication. Further, investigation of these interactions will likely provide important insight into tegument architecture or mechanisms of virion assembly, and allow us to make predictions about the potential functions of previously uncharacterized tegument proteins based on their interacting partners.

The herpesvirus tegument is thought to have an ordered structure with respect to the proteins that are closely associated with the nucleocapsid, whereas the outer tegument is largely amorphous (112, 127). Our screen did not reveal any interactions between HCMV tegument and capsid proteins. A comprehensive yeast two-hybrid screen performed for MCMV also failed to detect binary interactions between tegument and capsid proteins (29). However, we would predict that tegument acquisition begins through physical associations of tegument proteins with the capsid. Indeed, yeast two-hybrid analysis has been

used to demonstrate interactions between tegument and capsid proteins for α and γ-herpesviruses including HSV-1, Kaposi's sarcoma-associated herpesvirus (KSHV), and varicella-zoster virus (VZV) (52, 83, 100). While the failure to detect interactions between CMV capsid and tegument proteins using the yeast two-hybrid system may be explained by false negatives, the absence of such interactions may also point to fundamental differences in the architecture or mechanisms of assembly for β-herpesviruses compared to other herpesvirus family members. For example, it is possible that during HCMV infection, tegument proteins only interact with the capsid once it is fully assembled.

It is generally accepted that the majority of the HCMV tegument is acquired in the cytoplasm during virion assembly. However, electron microscopic analysis of HCMV infected cells shows that HCMV capsids appear to be coated with a thin layer of tegument upon nuclear egress (112). Immunofluorescence analysis and ^{35}S-methionine labeling of the abundant HCMV tegument protein UL32 (pp150) strongly suggest that this protein associates with capsids in the nucleus and remains bound to the capsid during nuclear egress and migration to the cytoplasmic site of assembly (39, 86). Cryoelectron microscopic analysis of simian CMV particles also predicts that the tegument proteins UL32 and UL82 (pp71) are closely associated with the capsid, based on their predicted molecular weights and molar abundance relative to the major capsid protein (112). This prediction is consistent with the results presented here and elsewhere demonstrating that an interaction exists between the UL32 and UL82 proteins (75, 90). Another study showed that UL32 and UL48 are the most capsid-proximal tegument proteins (127). Interestingly, UL32, which has been shown to be absolutely essential for cytoplasmic maturation of HCMV virions, is unique to the β-herpesviruses and is not conserved among the other herpesvirus subfamilies (4, 107). Taken together, these data support the prediction that the mechanisms of β-herpesvirus assembly differ markedly from those of α and γ-herpesviruses.

Due to the relatively large size of both UL32 and UL48 (150 kDa and 253 kDa respectively), it is possible that the early association of UL32 and/or UL48 with capsids in the nucleus precludes the direct association of the capsid with other tegument proteins. In fact, while cryoelectron microscopy analysis suggests that more than one species of tegument protein makes direct contact with the capsid, UL32 is the only CMV tegument protein that has been shown to directly bind the capsid (12). Also consistent with the absence of interactions between tegument and capsids proteins by yeast two-hybrid analysis is the observation that UL32 only binds fully assembled capsids isolated from intact virions and does not bind individual capsid proteins in a GST pull-down assay (33). Therefore, it is possible that HCMV tegument proteins may only bind the capsid in its fully assembled conformation and not to individual capsid subunits.

Tegument proteins are delivered directly to the host cell cytoplasm upon infection and can therefore function immediately upon entry, prior to the onset of viral gene expression. Therefore, there are two distinct populations of tegument proteins in infected cells, those that are delivered to the cell upon infection and those that are synthesized after initiation of viral gene expression. Whether these two populations have distinct and separable functions is largely unknown. The interactions identified in our screen may therefore occur at any stage of the viral life cycle. It remains to be determined whether these interactions are structural or regulatory in function. For example, minor virion components such as UL44, UL84, and UL112-113 are essential for viral DNA replication (71). These proteins are present in extremely low abundance in the virion compared to the major tegument proteins (113). Therefore, it is possible that the interactions between these proteins may play an important regulatory role in HCMV replication. In contrast, the abundant tegument components UL32 and UL99 have both been shown to play critical roles in virion maturation during the late phases of infection (4, 76). Therefore interactions involving these proteins may play roles in the proper assembly and structure of virus particles.

Our study and others have identified several tegument proteins such as UL25, UL45, and UL88 that are involved in several interactions with other tegument proteins. These proteins may serve as “hubs” for directing tegument assembly or for maintaining tegument architecture. Therefore, we hypothesize that these interactions are necessary for the proper incorporation of tegument proteins into the virion during assembly. This hypothesis can be tested by analyzing the protein composition of virions assembled in the absence of individual tegument proteins. While UL25, UL45, and UL88 all appear to be dispensable for HCMV replication *in vitro*, it is possible that the absence of these proteins *in vivo* would result in impaired replication due to reduced packaging of other tegument proteins that are essential for replication in the host (28, 125).

It also remains to be established whether these protein interactions are stable and maintained in the virus particle or occur transiently at some point during infection. While immunofluorescence analysis can be used to determine the subcellular localization of viral proteins, co-localization is not indicative of a physical interaction. A method such as FRET analysis over a time-course of viral infection would allow for determination of the spatial and temporal properties of protein-protein interactions throughout the viral life cycle. Further study of the kinetics, subcellular location, and functional significance of these interactions during infection will be necessary to characterize the potential contribution of each interaction to HCMV replication.

Potential functional roles of UL94 during HCMV infection

Based on the results of the yeast two-hybrid screen, we chose to further investigate the functional significance of the interaction between UL94 and UL99 in the context of HCMV infection. Prior to the work presented here, our understanding of the function(s) of UL94 during infection was limited. It was previously reported that UL94 may exist as a disulfide linked dimer in both infected and transfected cells (119). Further, it was shown that UL94 protein was found exclusively in the nuclear fraction of infected cells as well as in UL94-

expressing cell lines (118). Based on these observations as well as the presence of a conserved putative Cys_2His_2 zinc finger in the C-terminus of the UL94 protein, it was suggested that UL94 might play a role in the regulation of cellular or viral gene expression through direct DNA-binding.

Interestingly, we and others found that UL94 induces strong auto-activation of reporter genes when fused to the GAL4 DNA-binding domain in several yeast two-hybrid systems tested (75, 111)and unpublished observations. Auto-activation by the HSV-1 homolog UL16 in the yeast two-hybrid assay has also been observed (52, 111, 114). Auto-activation of reporter genes by the bait protein alone in the yeast two-hybrid assay may result from inherent transcriptional activity of the bait protein itself or through interaction of the bait protein with cellular factors that are capable of activating transcription. It is therefore tempting to speculate that UL94 itself is involved in transcriptional regulation. Although the evidence presented in this thesis work suggests that UL94 is essential for the assembly phase of viral replication, it is possible that the tegument portion of UL94 that is packaged into virions and delivered to the cytoplasm of the newly infected cell may localize to the nucleus and play a role in regulating gene expression. It would be interesting to determine the subcellular localization of UL94 immediately after infection, however these studies may prove technically challenging as UL94 is estimated to represent only 1% of the total protein content of the virion and thus may be difficult to detect by immunofluorescence, even in a high multiplicity infection (113). While our studies showed little effect of deletion of UL94 on viral gene expression, we tested only a small subset of all viral genes. It is possible that UL94 has an effect on the transcription of other viral genes not yet examined or on the expression of cellular genes.

Whether UL94 effects viral gene expression could be determined by comparative analysis of the viral transcriptome in cells infected with wild type virus compared to that of cells infected with the UL94stop mutant. Evidence for a role of UL94 in transcriptional regulation may also be provided by examining the

ability of UL94 to bind zinc or DNA. However, such assays would not provide information regarding specific genes that may be regulated by UL94. In addition to a role in transcriptional regulation, an ability of UL94 to bind DNA may suggest a role in the packaging of viral genomes into nuclear capsids. However, our data and other suggests that DNA-packaging proceeds normally in the absence of UL94 (64, 76).

While UL94 is a herpesvirus core gene, the only homolog of UL94 that has been extensively characterized is HSV-1 UL16. UL16 has been shown to associate with cytoplasmic but not extracellular capsids. This differential binding was found to be dependent on pH as well as free cysteines, suggesting that capsid binding involves disulfide bond formation as particles traffic through the secretory machinery to the extracellular space. UL16 also interacts with the UL99 homolog UL11, the capsid-associated tegument protein UL21, and with the cytoplasmic tail of glycoprotein E (gE). Based on this network of interactions and their dynamic properties, a model has been proposed in which the associations of UL16 with capsids, UL21, UL11, and gE act to aid in the proper assembly and structure of the HSV-1 virion. While the available data are consistent with this model, interestingly none of the four viral proteins involved in this proposed network are essential for HSV-1 replication (6-8, 122). This suggests that the formation of these complexes contributes to the efficient formation of infectious virus but that in their absence, redundant mechanisms may compensate for their loss. The absence of a known association between UL94 and HCMV capsids, as well as the absolute requirement of both UL94 and UL99 for viral replication further highlights important fundamental differences between the mechanisms of β and α-herpesvirus replication.

Model for functional significance of the interaction between UL94 and UL99

We have shown that UL94 and UL99 exhibit different subcellular localizations when expressed alone, together, or in the context of viral infection. We also demonstrated that in the absence of the interaction between UL94 and

UL99, both proteins exhibit aberrant localization during infection and do not appear to accumulate at the assembly complex. Taken together, these results suggest that the interaction between UL94 and UL99 results in the formation of a unique binding site for another not yet identified protein. Further, the data suggest that the unidentified binding partner is likely cellular, as a dramatic relocalization of both UL94 and UL99 occurs in the absence of infection. Therefore, we propose a model in which the interaction between UL94 and UL99 during infection functions to mediate an additional interaction with a cellular protein that is part of the viral assembly complex, thus resulting in the localization of both UL94 and UL99 to the site of virion assembly (Fig. 6-1).

UL99 is a myristoylated membrane-associated protein that co-localizes with markers of the endoplasmic reticulum-Golgi intermediate compartment (ERGIC) in the absence of infection (89). It would be interesting to determine whether myristoylation of UL99 is required for the relocalization observed in the presence of UL94. The myristoyl moiety at the N-terminus of UL99 is essential for its membrane association and mutation of the myristoylation signal results in the localization of UL99 to the nucleus in transfected cells (89). A simple transfection experiment with UL94 and a mutant form of UL99 that cannot be myristoylated would demonstrate whether UL99 still co-localizes with UL94 in the absence of its membrane association. If myristoylation mutants of UL99 exhibit the same pattern of localization as wild type UL99 in the presence of UL94, this would suggest that their localization is mediated by an interaction with a cellular protein, and not by insertion of UL99 in cytoplasmic membranes.

While the localization pattern of UL94 and UL99 when expressed together is consistent with the Golgi apparatus, further co-localization studies with cellular markers will be necessary to determine the identity of these structures. Co-localization of UL94 and UL99 with Golgi markers may implicate any number of Golgi-specific proteins as potential candidates for cellular binding partners associated with the UL94-UL99 complex.

Another potential candidate for a cellular protein that may alter the localization of UL94 and UL99 is the ER chaperone BiP/GRP78. BiP normally functions by binding sensors of the unfolded protein response, maintaining them in an inactive state in the absence of cellular stress. BiP function has been implicated in virion morphogenesis, as depletion of BiP in infected cells results in the accumulation of capsids in the nucleus and in the perinuclear space near the outer nuclear membrane (17). A subsequent study showed that BiP co-localizes with UL99 at the assembly complex and that UL99 immunoprecipitates in complex with BiP from infected cell lysates (16). Further, depletion of BiP resulted in the disruption of the assembly complex with respect to UL99 and gB localization (16). These authors did not perform additional binding assays to determine whether the association between UL99 and BiP is direct or if it only occurs in complex with other infected cell proteins. Therefore, it is tempting to speculate that UL94 may also be present in complex with UL99 and BiP at the assembly complex, and that the formation of this complex is required for the proper localization of both UL94 and UL99.

Additional candidates for binding partners of UL94 and UL99 are components of the endosomal sorting complex required for transport (ESCRT). Various ESCRT proteins localize to the assembly complex during HCMV infection and are required for efficient viral replication (106). Interestingly, UL99 traffics with markers of both trans-Golgi and ESCRT during the early phase of assembly (68). This is in contrast to the structural proteins gB and UL32, which traffic in separate vesicles that are endosomal or clathrin-associated, respectively. These independent vesicles then merge at late times in assembly into larger structures that presumably represent the site of final virion assembly and envelopment (68). Such compartmentalization of viral structural proteins during the early stages of assembly may represent a mechanism of spatial and temporal regulation that ensures that final tegumentation and envelopment are restricted to the correct subcellular site at which the full complement of virion components is present.

Our transfection studies demonstrate that UL94 and UL99 exhibit altered localization in the absence of infection, suggesting that the relocalization that is observed only when these proteins are expressed together does not require other viral factors. Further, ER and ERGIC components are not detected at the assembly complex during infection, whereas markers of trans-Golgi as well as early and late endosomes are consistently found both at the assembly complex and in the virion envelope (20, 89). Therefore, we hypothesize that the interaction between UL94 and UL99 functions to mediate additional interactions with cellular proteins that result in the association of UL94 and UL99 with distal components of the cellular secretory apparatus. These associations are likely critical for the proper formation of the assembly complex and thus for the production of enveloped virions.

While the data currently available are consistent with a model in which the interaction between UL94 and UL99 allows for the binding of a cellular protein that then directs their localization, we cannot rule out alternative mechanisms for the trafficking of these proteins to the assembly complex. HCMV induces a dramatic relocalization of the cellular secretory apparatus and the mechanisms by which this occurs are poorly understood (25, 26, 88). It is possible that upon binding UL94, UL99 remains associated with the ERGIC and that it is the interaction between these viral proteins that induces the morphological changes observed in these cellular membranes. Interaction with other viral proteins during infection may then be required for the association of UL94 and UL99 with components of the assembly complex. Identification of the membranes to which UL94 and UL99 localize in transfected cells would further define the mechanism of their relocalization.

It is also possible that the mechanisms responsible for the relocalization of UL94 and UL99 in transfected cells are completely different than those that result in their localization to the assembly complex in the environment of an infected cell. While we have demonstrated that the interaction between UL94 and UL99 is required for both proteins to traffic to the assembly complex, there may be other

viral proteins that are involved in this process. Identification of other proteins associated with UL94 and UL99 in both transfected and infected cells will allow us to further elucidate the mechanism by which UL94 and UL99 traffic to the assembly complex during infection.

Mechanisms of HCMV virion envelopment

It is clear that UL94 and UL99 are both required for secondary envelopment of virions in the cytoplasm based on the phenotypes of UL94 and UL99-deletion mutant viruses (76, 98). However, whether these proteins directly participate in the process of envelopment or whether their effect is indirect remains unknown. Because UL99 is a myristoylated protein that is membrane associated both during infection and in the absence of other viral proteins, it has been speculated that UL99 functions directly in driving envelope acquisition (93, 95, 98).

Several recent reports have expanded our knowledge of the viral and cellular proteins involved in formation of the assembly complex as well as those that are required for proper envelopment and egress. The viral kinase UL97 has long been known to function at many stages throughout the viral life cycle including regulation of viral gene expression, DNA replication, and nuclear egress of DNA-containing capsids (79). These functions are mediated by phosphorylation of both viral and cellular targets and thus require the kinase activity of UL97. More recently, UL97 function has been implicated in the proper formation of the assembly complex, requiring both kinase-dependent and independent functions of UL97 (5, 34). In the absence of UL97 or UL97 kinase activity, the nucleus fails to adopt the curved kidney shape that is a hallmark of HCMV infection. Further, there is a defect in the formation of a compact assembly complex and instead, viral structural proteins including UL99 remain diffusely perinuclear and co-localize with Golgi-derived proteins on the periphery of large vacuoles (5, 35). The result of this aberrant membrane organization is a defect in envelopment and thus in the release of extracellular infectious virus.

The tegument protein UL71 is also required for the proper formation of the assembly complex and for the completion of virion envelopment. In the absence of UL71, large acidified lysosomes form, similar to the enlarged vesicular structures observed in the absence of UL97. Also similar to the phenotype observed in cells infected with UL97 mutants, in cells infected with a UL71-null virus, UL99 accumulates at the periphery of these enlarged acidified structures. Interestingly, these structures are nearly identical in appearance to the large electron dense structures that we observe in cells infected with the UL94stop virus (Fig. 6-2). The formation of these lysosomes may represent an antiviral defense employed by the cell to target virus particles for degradation. It is possible that the virus has evolved to circumvent this antiviral response by preventing the formation of these lysosomes, and that in the absence of viral proteins that are involved in this process, virus particles are targeted for degradation thus resulting in the inhibition of virus release. There may also be differences in the kinetics of lysosome formation in cells infected with wild type virus such that wild type particles are able to efficiently assemble and be released from the cell prior to their degradation.

Identification of other binding partners of UL94 and UL99

Our model for the function of the interaction between UL94 and UL99 during infection predicts that the UL94-UL99 complex binds to at least one other not yet identified cellular protein. Based on this model, the next step in further defining the mechanism by which UL94 and UL99 traffic to the assembly complex is to identify cellular binding partners of the UL94-UL99 complex. Based on our model, ideal candidates for this unknown protein would bind UL94 and UL99 together but would not bind either protein alone.

One method for identifying proteins present in complex with UL94 and UL99 is to isolate these complexes from infected cells by immunoprecipitation. Precipitated complexes could then be separated by electrophoresis and individual proteins identified by mass spectrometry. Limitations to this approach

include identifying the appropriate lysis and immunoprecipitation conditions to ensure that the complex is isolated intact. Further, it may be technically challenging to obtain enough infected cell protein to yield sufficient material for this type of analysis. However, such analysis has been performed with a virus expressing a UL99-GFP fusion protein. Affinity purification of protein associated with the UL99-GFP fusion and subsequent identification of individual protein species by mass spectrometry identified ubiquitin in the isolated complexes (68). While ubiquitination is commonly associated with protein degradation, it also mediates the proper sorting of proteins, directing them from the ER/Golgi into the endosomal pathway. This process is carried out by the action of ESCRT components, many of which bind ubiquitinated proteins (97). The association of UL99 with ubiquitin in infected cells therefore led to the observation that UL99 traffics with ESCRT proteins during the assembly phase of infection. However, a direct interaction between UL99 and ESCRT proteins has not been demonstrated.

While these results provide information regarding the association of UL99 with other viral and cellular proteins during infection, our model predicts that UL94 and UL99 bind to a cellular protein that alters their localization in the absence of infection. Therefore, this protein of interest would be identified by isolation of complexes associated with UL94 and UL99 in transfected cells. The profile of cellular proteins associated with UL94 and UL99 together would then be compared to those obtained from cells expressing each protein alone. Candidate cellular proteins would be found in the immunoprecipitate from cells expressing both UL94 and UL99, but not either protein alone.

Another potential strategy for identifying cellular proteins associated with UL94 and UL99 would be to employ the yeast two-hybrid assay. Because UL94 exhibits strong auto-activation in the yeast two-hybrid assay, UL99 would be used as the bait protein. Identification of candidate cellular proteins would involve two independent screens. The first would identify cellular proteins that bind to UL99 alone. The second screen would be designed so that yeast cells express

the UL99 bait protein as well as UL94, potentially from the same construct, allowing for formation of the UL94-UL99 complex in these cells. Each screen would be performed with a library of prey constructs generated through fusion of cellular coding sequences with the appropriate transcriptional activation domain. Cellular proteins found to activate transcription of the reporter genes in the presence of UL94 and UL99 but not UL99 alone would represent candidates for cellular proteins capable of altering the subcellular localization of the UL94-UL99 complex.

Therapeutic implications

The efficacy and use of currently available antiviral drugs for treating HCMV infection are limited. While several drugs are effective in inhibiting HCMV replication, their use is limited by their significant toxicity. In addition, the development of drug-resistance is common. Due to the significant threat posed by HCMV to bone marrow and solid organ transplant recipients and the frequency with which infection of these patients occurs, the development of novel antiviral drugs is a high priority.

Currently, the first strategy for treating HCMV infection is ganciclovir, a guanosine analog that must be converted to its active form *in vivo*, in part through phosphorylation by the viral UL97 kinase (1). The active form of ganciclovir preferentially inhibits the synthesis of viral DNA by the viral DNA-polymerase UL54. Ganciclovir is associated with a variety of serious side effects and its oral bioavailability is poor, resulting in lower serum concentrations of the drug and thus an increased potential for the development of drug-resistant HCMV. The emergence of drug-resistance to ganciclovir is relatively common, especially in patients receiving kidney, pancreas, and lung transplants, nearly 20% of which become resistant to ganciclovir treatment (53). The most common basis for ganciclovir resistance is mutation in UL97, followed by mutation in UL54. The most highly resistant strains have developed mutations in both genes

and treatment of these strains poses a significant challenge due to the fact that other antivirals such as Foscarnet also target the viral DNA-polymerase (61).

Inhibition of essential interactions between viral proteins is an attractive strategy for the development of therapeutics. Inhibitors that specifically target an interaction between viral proteins may have lowered toxicity compared to drugs that target cellular processes. Further, the development of resistance against a drug that targets a protein-protein interaction may be significantly hampered compared to those that target an enzyme active site. Several such compounds have been identified for inhibiting a variety of protein-protein interactions that are essential for HIV-1 replication (128). Small molecule or peptide inhibitors that bind at the interface of the domains involved in the interaction between UL94 and UL99 may inhibit their interaction and thus prevent the assembly of HCMV virions. Although there is currently no structural data available for the binding interface between UL94 and UL99, our mapping data defines amino acids that are critical for this interaction and may provide useful information for designing inhibitors. For example, administration of a peptide containing amino acids 37-39 of UL99 may preferentially bind UL94, preventing its association with the full length UL99 protein.

Identification of molecules that specifically inhibit the interaction between UL94 and UL99 may be accomplished with interaction analysis technology such as surface plasmon resonance, which can be also be used to characterize the kinetics and affinity of the interaction (41). Inhibitors can be identified through screening libraries of natural or synthetic small molecules that prevent the binding of UL94 to UL99. Limitations to this strategy include potential challenges in producing enough purified protein for both UL94 and UL99 to conduct this analysis.

Summary Statement

The primary goals of this thesis work were two-fold. The first was to identify novel binary interactions between HCMV virion proteins. The second goal

of this work was to investigate the functional relevance of such interactions in the context of HCMV replication. To this end, we first identified binary interactions among HCMV virion proteins using a yeast two-hybrid approach. Using this strategy, we identified 24 interactions between virion proteins, 13 of which had not been previously reported. Several of these interactions were validated by co-immunoprecipitation both in transfected cells and in the context of viral infection.

We identified an interaction between the conserved tegument proteins UL94 and UL99 and this interaction was chosen for further investigation of its functional relevance during infection. Prior to this work, UL94 and its potential function during infection were largely uncharacterized. Therefore, we first sought to determine whether UL94 is essential for HCMV replication and to determine the stage of the viral life cycle at which UL94 is likely to function. We showed that UL94 is expressed with true-late kinetics and localizes to the viral assembly complex during infection. Further, using a UL94-deletion mutant we demonstrated that UL94 appears to function late in infection during the stage of virion assembly. In the absence of UL94 expression, UL99 does not localize to the assembly complex and there is a complete defect in secondary envelopment of virions in the cytoplasm.

Finally, we sought to determine whether the interaction between UL94 and UL99 is essential for viral replication. We showed that UL94 and UL99 are capable of altering each other's subcellular localization in the absence of other infected cells proteins. Further, we showed that UL99 stabilizes UL94 protein through a mechanism that requires their interaction. We then mapped amino acids of each protein that are involved their interaction. Mutation of these amino acids in the viral genome results in aberrant localization of both UL94 and UL99 and results in a complete block in virus replication. Taken together, these data show that the interaction between UL94 and UL99 is essential for HCMV replication.

This work contributes several novel findings to the field of HCMV replication and assembly. We have identified several novel interactions between

virion proteins, which may be important for viral replication or pathogenesis. We have also established that the UL94 tegument protein is essential for replication and this work represents the first report of a potential function for UL94 during infection. Finally, this work further defines the mechanism of UL99 trafficking to the assembly complex during infection, showing that its interaction with UL94 is required for this process. The requirement for the interaction between UL94 and UL99 for the production of progeny virus implicates this interaction as a potential target for novel antiviral therapeutics.

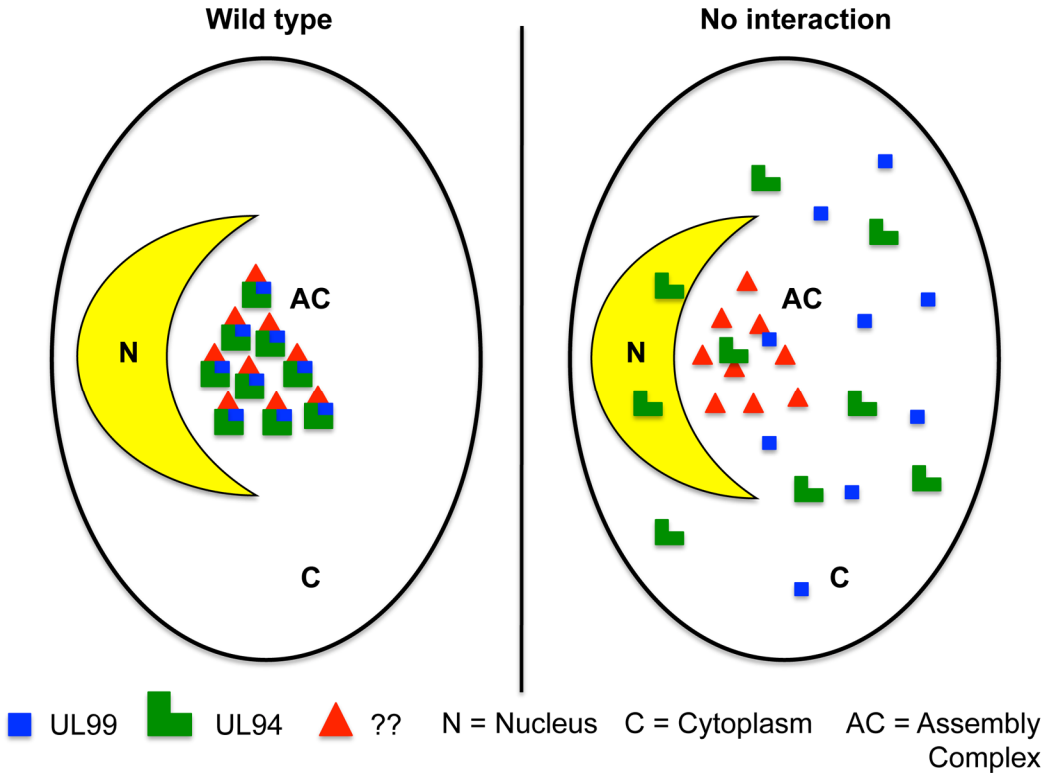

Figure 6-1. Model for the function of the interaction between UL94 and UL99 during infection. During wild type infection, interaction between UL94 and UL99 mediates additional interaction(s) with unidentified cellular protein(s) (left). In the absence of the interaction between UL94 and UL99, both UL94 and UL99 remain diffusely localized due to their inability to bind additional factors that are required for their localization to the assembly complex.

A

UL94HA

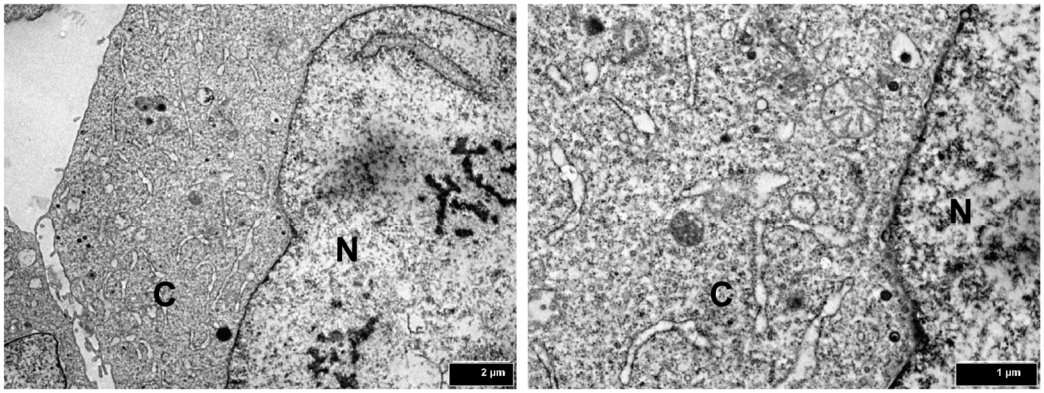

B

UL94stop

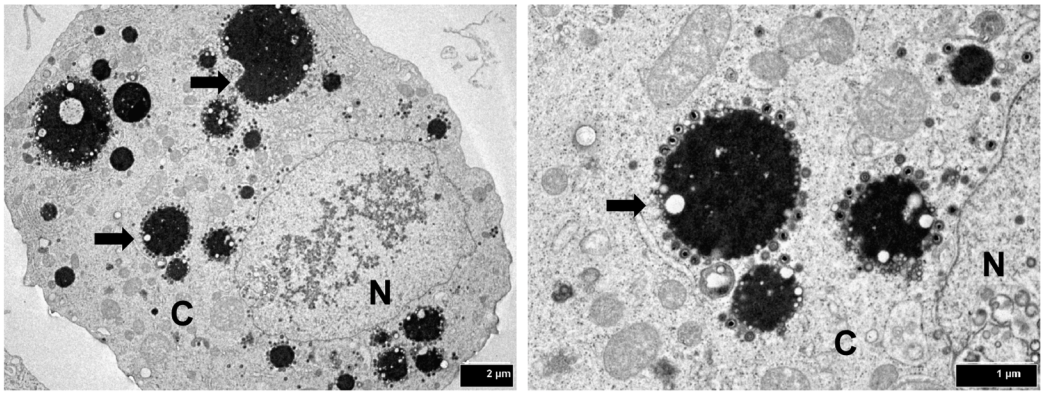

Figure 6-2. Large electron dense structures form in the cytoplasm of cells infected with the UL94stop mutant. HFF cells were infected with UL94HA **(A)** or UL94stop virus **(B)** at a multiplicity of 0.01 PFU/cell. Cells were fixed and processed for TEM 120 hours post-infection. Images represent X6000 (left) or X20,000 (right). N = nucleus, C = cytoplasm. Black arrows indicate enlarged electron dense structures around which virus particles accumulate in cells infected with the UL94stop mutant.

REFERENCES

1. **Andrei, G., E. De Clercq, and R. Snoeck.** 2009. Drug targets in cytomegalovirus infection. Infect Disord Drug Targets **9:**201-222.
2. **Appleton, B. A., A. Loregian, D. J. Filman, D. M. Coen, and J. M. Hogle.** 2004. The cytomegalovirus DNA polymerase subunit UL44 forms a C clamp-shaped dimer. Molecular Cell **15:**233-244.
3. **AuCoin, D. P., G. B. Smith, C. D. Meiering, and E. S. Mocarski.** 2006. Betaherpesvirus-conserved cytomegalovirus tegument protein ppUL32 (pp150) controls cytoplasmic events during virion maturation. Journal of Virology **80:**8199-8210.
4. **AuCoin, D. P., G. B. Smith, C. D. Meiering, and E. S. Mocarski.** 2006. Betaherpesvirus-conserved cytomegalovirus tegument protein ppUL32 (pp150) controls cytoplasmic events during virion maturation. J Virol **80:**8199-8210.
5. **Azzeh, M., A. Honigman, A. Taraboulos, A. Rouvinski, and D. G. Wolf.** 2006. Structural changes in human cytomegalovirus cytoplasmic assembly sites in the absence of UL97 kinase activity. Virology **354:**69-79.
6. **Baines, J. D., A. H. Koyama, T. Huang, and B. Roizman.** 1994. The UL21 gene products of herpes simplex virus 1 are dispensable for growth in cultured cells. J Virol **68:**2929-2936.
7. **Baines, J. D., and B. Roizman.** 1991. The open reading frames UL3, UL4, UL10, and UL16 are dispensable for the replication of herpes simplex virus 1 in cell culture. J Virol **65:**938-944.
8. **Baines, J. D., and B. Roizman.** 1992. The UL11 gene of herpes simplex virus 1 encodes a function that facilitates nucleocapsid envelopment and egress from cells. J Virol **66:**5168-5174.
9. **Baird, N. L., J. L. Starkey, D. J. Hughes, and J. W. Wills.** 2010. Myristylation and palmitylation of HSV-1 UL11 are not essential for its function. Virology **397:**80-88.
10. **Baldick, C. J., and T. Shenk.** 1996. Proteins associated with purified human cytomegalovirus particles. J Virol **70:**6097-6105.
11. **Battista, M. C., G. Bergamini, M. C. Boccuni, F. Campanini, A. Ripalti, and M. P. Landini.** 1999. Expression and characterization of a novel structural protein of human cytomegalovirus, pUL25. Journal of Virology **73:**3800-3809.
12. **Baxter, M. K., and W. Gibson.** 2001. Cytomegalovirus basic phosphoprotein (pUL32) binds to capsids in vitro through its amino one-third. Journal of Virology **75:**6865-6873.
13. **Bechtel, J. T., and T. Shenk.** 2002. Human cytomegalovirus UL47 tegument protein functions after entry and before immediate-early gene expression. Journal of Virology **76:**1043-1050.
14. **Bresnahan, W. A., and T. E. Shenk.** 2000. UL82 virion protein activates expression of immediate early viral genes in human cytomegalovirus-infected cells. Proceedings of the National Academy of Sciences of the United States of America **97:**14506-14511.

15. **Britt, W. J., and M. Mach.** 1996. Human cytomegalovirus glycoproteins. Intervirology **39:**401-412.
16. **Buchkovich, N. J., T. G. Maguire, A. W. Paton, J. C. Paton, and J. C. Alwine.** 2009. The Endoplasmic Reticulum Chaperone BiP/GRP78 Is Important in the Structure and Function of the Human Cytomegalovirus Assembly Compartment. Journal of Virology **83:**11421-11428.
17. **Buchkovich, N. J., T. G. Maguire, Y. Yu, A. W. Paton, J. C. Paton, and J. C. Alwine.** 2008. Human cytomegalovirus specifically controls the levels of the endoplasmic reticulum chaperone BiP/GRP78, which is required for virion assembly. J Virol **82:**31-39.
18. **Butcher, S. J., J. Aitken, J. Mitchell, B. Gowen, and D. J. Dargan.** 1998. Structure of the human cytomegalovirus B capsid by electron cryomicroscopy and image reconstruction. J Struct Biol **124:**70-76.
19. **Cantrell, S. R., and W. A. Bresnahan.** 2005. Interaction between the human cytomegalovirus UL82 gene product (pp71) and hDaxx regulates immediate-early gene expression and viral replication. Journal of Virology **79:**7792-7802.
20. **Cepeda, V., M. Esteban, and A. Fraile-Ramos.** 2010. Human cytomegalovirus final envelopment on membranes containing both trans-Golgi network and endosomal markers. Cellular Microbiology **12:**386-404.
21. **Chevillotte, M., S. Landwehr, L. Linta, G. Frascaroli, A. Luske, C. Buser, T. Mertens, and J. von Einem.** 2009. Major Tegument Protein pp65 of Human Cytomegalovirus Is Required for the Incorporation of pUL69 and pUL97 into the Virus Particle and for Viral Growth in Macrophages. Journal of Virology **83:**2480-2490.
22. **Child, S. J., M. Hakki, K. L. De Niro, and A. P. Geballe.** 2004. Evasion of cellular antiviral responses by human cytomegalovirus TRS1 and IRS1. Journal of Virology **78:**197-205.
23. **Colberg-Poley, A. M.** 1996. Functional roles of immediate early proteins encoded by the human cytomegalovirus UL36-38, UL115-119, TRS1/IRS1 and US3 loci. Intervirology **39:**350-360.
24. **Compton, T.** 2004. Receptors and immune sensors: the complex entry path of human cytomegalovirus. Trends Cell Biol **14:**5-8.
25. **Das, S., and P. E. Pellett.** 2011. Spatial relationships between markers for secretory and endosomal machinery in human cytomegalovirus-infected cells versus those in uninfected cells. J Virol **85:**5864-5879.
26. **Das, S., A. Vasanji, and P. E. Pellettl.** 2007. Three-dimensional structure of the human cytomegalovirus cytoplasmic virion assembly complex includes a reoriented secretory apparatus. Journal of Virology **81:**11861-11869.
27. **Demmler, G. J.** 1996. Congenital cytomegalovirus infection and disease. Adv Pediatr Infect Dis **11:**135-162.
28. **Dunn, W., C. Chou, H. Li, R. Hai, D. Patterson, V. Stolc, H. Zhu, and F. Y. Liu.** 2003. Functional profiling of a human cytomegalovirus genome. Proceedings of the National Academy of Sciences of the United States of America **100:**14223-14228.

29. **Fossum, E., C. C. Friedel, S. V. Rajagopala, B. Titz, A. Baiker, T. Schmidt, T. Kraus, T. Stellberger, C. Rutenberg, S. Suthram, S. Bandyopadhyay, D. Rose, A. von Brunn, M. Uhlmann, C. Zeretzke, Y. A. Dong, H. Boulet, M. Koegl, S. M. Bailer, U. Koszinowski, T. Ideker, P. Uetz, R. Zimmer, and J. Haas.** 2009. Evolutionarily Conserved Herpesviral Protein Interaction Networks. Plos Pathogens **5**.
30. **Gao, Y., K. Colletti, and G. S. Pari.** 2008. Identification of human cytomegalovirus UL84 virus- and cell-encoded binding partners by using proteomics analysis. Journal of Virology **82:**96-104.
31. **Gibson, W.** 1996. Structure and assembly of the virion. Intervirology **39:**389-400.
32. **Gibson, W.** 2008. Structure and formation of the cytomegalovirus virion, p. 187-204, Human Cytomegalovirus, vol. 325.
33. **Gibson, W., M. K. Baxter, and K. S. Clopper.** 1996. Cytomegalovirus "missing" capsid protein identified as heat-aggregable product of human cytomegalovirus UL46. Journal of Virology **70:**7454-7461.
34. **Goldberg, M. D., A. Honigman, J. Weinstein, S. Chou, A. Taraboulos, A. Rouvinski, V. Shinder, and D. G. Wolf.** 2011. Human cytomegalovirus UL97 kinase and nonkinase functions mediate viral cytoplasmic secondary envelopment. J Virol **85:**3375-3384.
35. **Goldberg, M. D., A. Honigman, J. Weinstein, S. W. Chou, A. Taraboulos, A. Rouvinski, V. Shinder, and D. G. Wolf.** 2011. Human Cytomegalovirus UL97 Kinase and Nonkinase Functions Mediate Viral Cytoplasmic Secondary Envelopment. Journal of Virology **85:**3375-3384.
36. **Hahn, G., H. Khan, F. Baldanti, U. H. Koszinowski, M. G. Revello, and G. Gerna.** 2002. The human cytomegalovirus ribonucleotide reductase homolog UL45 is dispensable for growth in endothelial cells, as determined by a BAC-cloned clinical isolate of human cytomegalovirus with preserved wild-type characteristics. Journal of Virology **76:**9551-9555.
37. **Harper, A. L., D. G. Meckes, J. A. Marsh, M. D. Ward, P. C. Yeh, N. L. Baird, C. B. Wilson, O. J. Semmes, and J. W. Wills.** 2010. Interaction domains of the UL16 and UL21 tegument proteins of herpes simplex virus. J Virol **84:**2963-2971.
38. **Hensel, G., H. Meyer, S. Gartner, G. Brand, and H. F. Kern.** 1995. NUCLEAR-LOCALIZATION OF THE HUMAN CYTOMEGALOVIRUS TEGUMENT PROTEIN PP150 (PPUL32). Journal of General Virology **76:**1591-1601.
39. **Hensel, G., H. Meyer, S. Gärtner, G. Brand, and H. F. Kern.** 1995. Nuclear localization of the human cytomegalovirus tegument protein pp150 (ppUL32). J Gen Virol **76 (Pt 7):**1591-1601.
40. **Isaacson, M. K., A. L. Feire, and T. Compton.** 2007. Epidermal growth factor receptor is not required for human cytomegalovirus entry or signaling. J Virol **81:**6241-6247.

41. **Jason-Moller, L., M. Murphy, and J. Bruno.** 2006. Overview of Biacore systems and their applications. Curr Protoc Protein Sci **Chapter 19:**Unit 19.13.
42. **Jones, T. R., and S. W. Lee.** 2004. An acidic cluster of human cytomegalovirus UL99 tegument protein is required for trafficking and function. J Virol **78:**1488-1502.
43. **Kalejta, R. F.** 2008. Tegument proteins of human cytomegalovirus. Microbiology and Molecular Biology Reviews **72:**249-265.
44. **Kalejta, R. F.** 2008. Tegument proteins of human cytomegalovirus. Microbiol Mol Biol Rev **72:**249-265, table of contents.
45. **Kamil, J. P., and D. M. Coen.** 2007. Human cytomegalovirus protein kinase UL97 forms a complex with the tegument phosphoprotein pp65 (vol 81, pg 10659, 2007). Journal of Virology **81:**13277-13277.
46. **Kim, E. T., S. E. Oh, Y.-O. Lee, W. Gibson, and J.-H. Ahn.** 2009. Cleavage Specificity of the UL48 Deubiquitinating Protease Activity of Human Cytomegalovirus and the Growth of an Active-Site Mutant Virus in Cultured Cells. Journal of Virology **83**.
47. **Kim, Y. E., and J. H. Ahn.** 2010. Role of the specific interaction of UL112-113 p84 with UL44 DNA polymerase processivity factor in promoting DNA replication of human cytomegalovirus. Journal of Virology.
48. **Kotton, C. N.** 2010. Management of cytomegalovirus infection in solid organ transplantation. Nat Rev Nephrol **6:**711-721.
49. **Krosky, P. M., M. C. Baek, and D. M. Coen.** 2003. The human cytomegalovirus UL97 protein kinase, an antiviral drug target, is required at the stage of nuclear egress. Journal of Virology **77:**905-914.
50. **Krzyzaniak, M. A., M. Mach, and W. J. Britt.** 2009. HCMV-encoded glycoprotein M (UL100) interacts with Rab11 effector protein FIP4. Traffic **10:**1439-1457.
51. **Lai, L. L., and W. J. Britt.** 2003. The interaction between the major capsid protein and the smallest capsid protein of human cytomegalovirus is dependent on two linear sequences in the smallest capsid protein. Journal of Virology **77:**2730-2735.
52. **Lee, J. H., V. Vittone, E. Diefenbach, A. L. Cunningham, and R. J. Diefenbach.** 2008. Identification of structural protein-protein interactions of herpes simplex virus type 1. Virology **378:**347-354.
53. **Limaye, A. P.** 2002. Ganciclovir-resistant cytomegalovirus in organ transplant recipients. Clin Infect Dis **35:**866-872.
54. **Lischka, P., M. Thomas, Z. Toth, R. Mueller, and T. Stamminger.** 2007. Multimerization of human cytomegalovirus regulatory protein UL69 via a domain that is conserved within its herpesvirus homologues. Journal of General Virology **88:**405-410.
55. **Liu, Y., Z. Zhang, X. Zhao, H. Wei, J. Deng, Z. Cui, and X. E. Zhang.** 2012. Human cytomegalovirus UL94 is a nucleocytoplasmic shuttling protein containing two NLSs and one NES. Virus Res.

56. **Liu, Y. L., Z. Q. Cui, Z. P. Zhang, H. P. Wei, Y. F. Zhou, M. L. Wang, and X. E. Zhang.** 2009. The tegument protein UL94 of human cytomegalovirus as a binding partner for tegument protein pp28 identified by intracellular imaging. Virology **388:**68-77.
57. **Loomis, J. S., J. B. Bowzard, R. J. Courtney, and J. W. Wills.** 2001. Intracellular trafficking of the UL11 tegument protein of herpes simplex virus type 1. J Virol **75:**12209-12219.
58. **Loomis, J. S., R. J. Courtney, and J. W. Wills.** 2003. Binding partners for the UL11 tegument protein of herpes simplex virus type 1. Journal of Virology **77:**11417-11424.
59. **Loveland, A. N., N. L. Nguyen, E. J. Brignole, and W. Gibson.** 2007. The amino-conserved domain of human cytomegalovirus UL80a proteins is required for key interactions during early stages of capsid formation and virus production. Journal of Virology **81:**620-628.
60. **Loveland, A. N., N. L. Nguyen, E. J. Brignole, and W. Gibson.** 2007. The amino-conserved domain of human cytomegalovirus UL80a proteins is required for key interactions during early stages of capsid formation and virus production. J Virol **81:**620-628.
61. **Lurain, N. S., and S. Chou.** 2010. Antiviral drug resistance of human cytomegalovirus. Clin Microbiol Rev **23:**689-712.
62. **MacLean, C. A., B. Clark, and D. J. McGeoch.** 1989. Gene UL11 of herpes simplex virus type 1 encodes a virion protein which is myristylated. J Gen Virol **70 (Pt 12):**3147-3157.
63. **MacLean, C. A., A. Dolan, F. E. Jamieson, and D. J. McGeoch.** 1992. The myristylated virion proteins of herpes simplex virus type 1: investigation of their role in the virus life cycle. J Gen Virol **73 (Pt 3):**539-547.
64. **Maninger, S., J. B. Bosse, F. Lemnitzer, M. Pogoda, C. A. Mohr, J. von Einem, P. Walther, U. H. Koszinowski, and Z. Ruzsics.** 2011. M94 is essential for the secondary envelopment of murine cytomegalovirus. J Virol **85:**9254-9267.
65. **Marschall, M., M. Freitag, P. Suchy, D. Romaker, R. Kupfer, M. Hanke, and T. Stamminger.** 2003. The protein kinase pUL97 of human cytomegalovirus interacts with and phosphorylates the DNA polymerase processivity factor pUL44. Virology **311:**60-71.
66. **Meckes, D. G., and J. W. Wills.** 2007. Dynamic interactions of the UL16 tegument protein with the capsid of herpes simplex virus. J Virol **81:**13028-13036.
67. **Mocarski, E. S., Jr., and C. Tan Courcelle.** 2001. Cytomegaloviruses and Their Replication, Fourth ed, vol. 2. Lippincott, Williams, & Wilkins, Philadelphia, PA.
68. **Moorman, N. J., R. Sharon-Friling, T. Shenk, and I. M. Cristea.** 2010. A targeted spatial-temporal proteomics approach implicates multiple cellular trafficking pathways in human cytomegalovirus virion maturation. Mol Cell Proteomics **9:**851-860.

69. **Murphy, E., I. Rigoutsos, T. Shibuya, and T. E. Shenk.** 2003. Reevaluation of human cytomegalovirus coding potential. Proceedings of the National Academy of Sciences of the United States of America **100:**13585-13590.
70. **Murphy, E., D. Yu, J. Grimwood, J. Schmutz, M. Dickson, M. A. Jarvis, G. Hahn, J. A. Nelson, R. M. Myers, and T. E. Shenk.** 2003. Coding potential of laboratory and clinical strains of human cytomegalovirus. Proceedings of the National Academy of Sciences of the United States of America **100:**14976-14981.
71. **Pari, G. S.** 2008. Nuts and bolts of human cytomegalovirus lytic DNA replication. Curr Top Microbiol Immunol **325:**153-166.
72. **Park, M. Y., Y. E. Kim, M. R. Seo, J. R. Lee, C. H. Lee, and J. H. Ahn.** 2006. Interactions among four proteins encoded by the human cytomegalovirus UL112-113 region regulate their intranuclear targeting and the recruitment of UL44 to prereplication foci. Journal of Virology **80:**2718-2727.
73. **Pass, R. F.** 2001. Cytomegalovirus, p. 2675-2706. *In* D. M. K. a. P. M. H. (ed.) (ed.), Fields Virology, 4th ed, vol. 2. Lippincott, Williams, & Williams, Philadelphia, PA.
74. **Patrone, M., E. Percivalle, M. Secchi, L. Fiorina, G. Pedrali-Noy, M. Zoppe, F. Baldanti, G. Hahn, U. H. Koszinowski, G. Milanesi, and A. Gallina.** 2003. The human cytomegalovirus UL45 gene product is a late, virion-associated protein and influences virus growth at low multiplicities of infection. Journal of General Virology **84:**3359-3370.
75. **Phillips, S. L., and W. A. Bresnahan.** 2011. Identification of binary interactions between human cytomegalovirus virion proteins. J Virol **85:**440-447.
76. **Phillips, S. L., and W. A. Bresnahan.** 2012. The Human Cytomegalovirus (HCMV) Tegument Protein UL94 Is Essential for Secondary Envelopment of HCMV Virions. J Virol **86:**2523-2532.
77. **Pietropaolo, R., and T. Compton.** 1999. Interference with annexin II has no effect on entry of human cytomegalovirus into fibroblast cells. J Gen Virol **80 (Pt 7):**1807-1816.
78. **Pietropaolo, R. L., and T. Compton.** 1997. Direct interaction between human cytomegalovirus glycoprotein B and cellular annexin II. J Virol **71:**9803-9807.
79. **Prichard, M. N.** 2009. Function of human cytomegalovirus UL97 kinase in viral infection and its inhibition by maribavir. Rev Med Virol **19:**215-229.
80. **Qian, Z. K., B. Q. Xuan, T. T. Hong, and D. Yu.** 2008. The full-length protein encoded by human cytomegalovirus gene UL117 is required for the proper maturation of viral replication compartments. Journal of Virology **82:**3452-3465.
81. **Re, M. C., M. P. Landini, P. Coppolecchia, G. Furlini, and M. Laplaca.** 1985. A 28000 MOLECULAR-WEIGHT HUMAN CYTOMEGALO-VIRUS STRUCTURAL POLYPEPTIDE STUDIED BY MEANS OF A SPECIFIC MONOCLONAL-ANTIBODY. Journal of General Virology **66:**2507-2511.
82. **Romanowski, M. J., and T. Shenk.** 1997. Characterization of the human cytomegalovirus irs1 and trs1 genes: A second immediate-early transcription unit within irs1 whose product antagonizes transcriptional activation. Journal of Virology **71:**1485-1496.

83. **Rozen, R., N. Sathish, Y. Li, and Y. Yuan.** 2008. Virion-wide protein interactions of Kaposi's sarcoma-associated herpesvirus. Journal of Virology **82:**4742-4750.
84. **Ryckman, B. J., B. L. Rainish, M. C. Chase, J. A. Borton, J. A. Nelson, M. A. Jarvis, and D. C. Johnson.** 2008. Characterization of the human cytomegalovirus gH/gL/UL128-131 complex that mediates entry into epithelial and endothelial cells. J Virol **82:**60-70.
85. **Sadaoka, T., H. Yoshii, T. Imazawa, K. Yamanishi, and Y. Mori.** 2007. Deletion in open reading frame 49 of varicella-zoster virus reduces virus growth in human malignant melanoma cells but not in human embryonic fibroblasts. J Virol **81:**12654-12665.
86. **Sampaio, K. L., Y. Cavignac, Y. D. Stierhof, and C. Sinzger.** 2005. Human cytomegalovirus labeled with green fluorescent protein for live analysis of intracellular particle movements. Journal of Virology **79:**2754-2767.
87. **Sampaio, K. L., Y. Cavignac, Y. D. Stierhof, and C. Sinzger.** 2005. Human cytomegalovirus labeled with green fluorescent protein for live analysis of intracellular particle movements. J Virol **79:**2754-2767.
88. **Sanchez, V., K. D. Greis, E. Sztul, and W. J. Britt.** 2000. Accumulation of virion tegument and envelope proteins in a stable cytoplasmic compartment during human cytomegalovirus replication: Characterization of a potential site of virus assembly. Journal of Virology **74:**975-986.
89. **Sanchez, V., E. Sztul, and W. J. Britt.** 2000. Human cytomegalovirus pp28 (UL99) localizes to a cytoplasmic compartment which overlaps the endoplasmic reticulum-Golgi-intermediate compartment. Journal of Virology **74:**3842-3851.
90. **Schierling, K., T. Stamminger, T. Mertens, and M. Winkler.** 2004. Human cytomegalovirus tegument proteins ppUL82 (pp71) and ppUL35 interact and cooperatively activate the major immediate-early enhancer. Journal of Virology **78:**9512-9523.
91. **Schleiss, M. R.** 2008. Cytomegalovirus vaccine development. Curr Top Microbiol Immunol **325:**361-382.
92. **Schregel, V., S. Auerochs, R. Jochmann, K. Maurer, T. Stamminger, and M. Marschall.** 2007. Mapping of a self-interaction domain of the cytomegalovirus protein kinase pUL97. Journal of General Virology **88:**395-404.
93. **Seo, J. Y., and W. J. Britt.** 2007. Cytoplasmic envelopment of human cytomegalovirus requires the postlocalization function of tegument protein pp28 within the assembly compartment. J Virol **81:**6536-6547.
94. **Seo, J. Y., and W. J. Britt.** 2008. Multimerization of tegument protein pp28 within the assembly compartment is required for cytoplasmic envelopment of human cytomegalovirus. Journal of Virology **82:**6272-6287.
95. **Seo, J. Y., and W. J. Britt.** 2008. Multimerization of tegument protein pp28 within the assembly compartment is required for cytoplasmic envelopment of human cytomegalovirus. J Virol **82:**6272-6287.

96. **Seo, J. Y., and W. J. Britt.** 2006. Sequence requirements for localization of human cytomegalovirus tegument protein pp28 to the virus assembly compartment and for assembly of infectious virus. J Virol **80:**5611-5626.
97. **Shields, S. B., and R. C. Piper.** 2011. How ubiquitin functions with ESCRTs. Traffic **12:**1306-1317.
98. **Silva, M. C., Q. C. Yu, L. Enquist, and T. Shenk.** 2003. Human cytomegalovirus UL99-encoded pp28 is required for the cytoplasmic envelopment of tegument-associated capsids. Journal of Virology **77:**10594-10605.
99. **Stagno, S., R. F. Pass, G. Cloud, W. J. Britt, R. E. Henderson, P. D. Walton, D. A. Veren, F. Page, and C. A. Alford.** 1986. Primary cytomegalovirus infection in pregnancy. Incidence, transmission to fetus, and clinical outcome. JAMA **256:**1904-1908.
100. **Stellberger, T., R. Hauser, A. Baiker, V. R. Pothineni, J. Haas, and P. Uetz.** 2010. Improving the yeast two-hybrid system with permutated fusion proteins: the Varicella Zoster Virus interactome. Proteome Science **8:**9.
101. **Stinski, M. F., and D. T. Petrik.** 2008. Functional roles of the human cytomegalovirus essential IE86 protein. Curr Top Microbiol Immunol **325:**133-152.
102. **Strang, B. L., A. P. Geballe, and D. M. Coen.** 2010. Association of human cytomegalovirus proteins IRS1 and TRS1 with the viral DNA polymerase accessory subunit UL44. Journal of Virology.
103. **Strang, B. L., E. Sinigalia, L. A. Silva, D. M. Coen, and A. Loregian.** 2009. Analysis of the Association of the Human Cytomegalovirus DNA Polymerase Subunit UL44 with the Viral DNA Replication Factor UL84. Journal of Virology **83:**7581-7589.
104. **Sung, H., and M. R. Schleiss.** 2010. Update on the current status of cytomegalovirus vaccines. Expert Rev Vaccines **9:**1303-1314.
105. **Syggelou, A., N. Iacovidou, S. Kloudas, Z. Christoni, and V. Papaevangelou.** 2010. Congenital cytomegalovirus infection. Ann N Y Acad Sci **1205:**144-147.
106. **Tandon, R., D. P. AuCoin, and E. S. Mocarski.** 2009. Human Cytomegalovirus Exploits ESCRT Machinery in the Process of Virion Maturation. Journal of Virology **83**.
107. **Tandon, R., and E. S. Mocarski.** 2008. Control of cytoplasmic maturation events by cytomegalovirus tegument protein pp150. J Virol **82:**9433-9444.
108. **Tandon, R., and E. S. Mocarski.** 2011. Cytomegalovirus pUL96 Is Critical for the Stability of pp150-Associated Nucleocapsids. J Virol **85:**7129-7141.
109. **Thomas, M., S. Rechter, J. Milbradt, S. Auerochs, R. Muller, T. Stamminger, and M. Marschall.** 2009. Cytomegaloviral protein kinase pUL97 interacts with the nuclear mRNA export factor pUL69 to modulate its intranuclear localization and activity. Journal of General Virology **90:**567-578.
110. **Tischer, B. K., J. von Einem, B. Kaufer, and N. Osterrieder.** 2006. Two-step red-mediated recombination for versatile high-efficiency markerless DNA manipulation in Escherichia coli. Biotechniques **40:**191-197.

111. **To, A., Y. Bai, A. Shen, H. Gong, S. Umamoto, S. Lu, and F. Liu.** 2011. Yeast two hybrid analyses reveal novel binary interactions between human cytomegalovirus-encoded virion proteins. PLoS One **6:**e17796.
112. **Trus, B. L., W. Gibson, N. Q. Cheng, and A. C. Steven.** 1999. Capsid structure of simian cytomegalovirus from cryoelectron microscopy: Evidence for tegument attachment sites. Journal of Virology **73:**2181-2192.
113. **Varnum, S. M., D. N. Streblow, M. E. Monroe, P. Smith, K. J. Auberry, L. Pasa-Tolic, D. Wang, D. G. Camp, K. Rodland, S. Wiley, W. Britt, T. Shenk, R. D. Smith, and J. A. Nelson.** 2004. Identification of proteins in human cytomegalovirus (HCMV) particles: the HCMV proteome (vol 78, pg 10960, 2004). Journal of Virology **78:**13395-13395.
114. **Vittone, V., E. Diefenbach, D. Triffett, M. W. Douglas, A. L. Cunningham, and R. J. Diefenbach.** 2005. Determination of interactions between tegument proteins of herpes simplex virus type 1. Journal of Virology **79:**9566-9571.
115. **Wang, X., S. M. Huong, M. L. Chiu, N. Raab-Traub, and E. S. Huang.** 2003. Epidermal growth factor receptor is a cellular receptor for human cytomegalovirus. Nature **424:**456-461.
116. **Warming, S., N. Costantino, D. L. Court, N. A. Jenkins, and N. G. Copeland.** 2005. Simple and highly efficient BAC recombineering using gaIK selection. Nucleic Acids Research **33**.
117. **White, E. A., C. L. Clark, V. Sanchez, and D. H. Spector.** 2004. Small internal deletions in the human cytomegalovirus IE2 gene result in nonviable recombinant viruses with differential defects in viral gene expression. J Virol **78:**1817-1830.
118. **Wing, B. A., and E. S. Huang.** 1995. Analysis and mapping of a family of 3'-coterminal transcripts containing coding sequences for human cytomegalovirus open reading frames UL93 through UL99. J Virol **69:**1521-1531.
119. **Wing, B. A., G. C. Y. Lee, and E. S. Huang.** 1996. The human cytomegalovirus UL94 open reading frame encodes a conserved herpesvirus capsid/tegument-associated virion protein that is expressed with true late kinetics. Journal of Virology **70:**3339-3345.
120. **Winkler, M., S. A. Rice, and T. Stamminger.** 1994. UL69 OF HUMAN CYTOMEGALOVIRUS, AN OPEN READING FRAME WITH HOMOLOGY TO ICP27 OF HERPES-SIMPLEX VIRUS, ENCODES A TRANSACTIVATOR OF GENE-EXPRESSION. Journal of Virology **68:**3943-3954.
121. **Wood, L. J., M. K. Baxter, S. M. Plafker, and W. Gibson.** 1997. Human cytomegalovirus capsid assembly protein precursor (pUL80.5) interacts with itself and with the major capsid protein (pU86) through two different domains. Journal of Virology **71:**179-190.
122. **Yeh, P. C., J. Han, P. Chadha, D. G. Meckes, M. D. Ward, O. J. Semmes, and J. W. Wills.** 2011. Direct and specific binding of the UL16 tegument protein of herpes simplex virus to the cytoplasmic tail of glycoprotein E. J Virol **85:**9425-9436.

123. **Yeh, P. C., D. G. Meckes, and J. W. Wills.** 2008. Analysis of the interaction between the UL11 and UL16 tegument proteins of herpes simplex virus. J Virol **82:**10693-10700.
124. **Yinon, Y., D. Farine, and M. H. Yudin.** 2010. Screening, diagnosis, and management of cytomegalovirus infection in pregnancy. Obstet Gynecol Surv **65:**736-743.
125. **Yu, D., M. C. Silva, and T. Shenk.** 2003. Functional map of human cytomegalovirus AD169 defined by global mutational analysis. Proceedings of the National Academy of Sciences of the United States of America **100:**12396-12401.
126. **Yu, D., G. A. Smith, L. W. Enquist, and T. Shenk.** 2002. Construction of a self-excisable bacterial artificial chromosome containing the human cytomegalovirus genome and mutagenesis of the diploid TRL/IRL13 gene. J Virol **76:**2316-2328.
127. **Yu, X., S. Shah, M. Lee, W. Dai, P. Lo, W. Britt, H. Zhu, F. Liu, and Z. H. Zhou.** 2011. Biochemical and structural characterization of the capsid-bound tegument proteins of human cytomegalovirus. J Struct Biol **174:**451-460.
128. **Zhan, P., W. Li, H. Chen, and X. Liu.** 2010. Targeting protein-protein interactions: a promising avenue of anti-HIV drug discovery. Curr Med Chem **17:**3393-3409.